# Algebra and Dynamics of Reaction Network Models

By

**Polly Wing Yan Yu**

A dissertation submitted in partial fulfillment

of the requirements for the degree of

Doctor of Philosophy

(Mathematics)

at the

**UNIVERSITY OF WISCONSIN–MADISON**

2021

Date of final oral examination: June 10, 2020

The dissertation is approved by the following members of the Final Oral Committee:

G. Craciun, Professor, Mathematics and Biomolecular Chemistry

D.F. Anderson, Vilas Distinguished Achievement Professor, Mathematics

B. Boros, Visiting Assistant Professor, Mathematics

D. Erman, Associate Professor, Mathematics

# Abstract

Reaction networks, or interaction networks, encapsulate rules how entities, be it chemical species or organisms, may interact with one another. The dynamics of such interactions may be difficult to analyze, given the intricate connections. At times, however, network structure dictates the possible behaviours of the system. Detailed-balanced and complex-balanced mass-action systems are good examples; they enjoy a variety of algebraic and stability properties. However, they also typically describe ideal systems, which are rare in biochemistry and biology. In this thesis, we extend properties of detailed-balanced and complex-balanced systems to models that approximate them in certain senses. These include: mass-action systems that are *dynamically equivalent* to complex-balanced ones, and perturbing the rate constants of *robustly permanent* complex-balanced systems while maintaining global stability. We also consider *vertex-balanced steady states*, the analog of complex-balanced ones, for generalized mass-action systems, where the rate functions do not match the stoichiometric coefficients. Finally, for mass-action kinetics with delay, we study *delay stability* (asymptotic stability independent of rate constants and delay parameters.

# Acknowledgements

This document exists thanks to many people, including my many co-authors. Sections 2.1 and 2.2, based on [39,40], are results of joint work with Gheorghe Craciun and Jiaxin Jin, while Section 2.3 is joint work with Gheorghe Craciun. Chapter 3 was based on [44], completed with Gheorghe Craciun, Stefan Müller, and Casian Pantea. Finally, Chapter 4, based on [42, 43], is joint work with Gheorghe Craciun, Maya Mincheva, and Casian Pantea.

First, I would like to thank my advisor, Gheorghe Craciun, for his support since the beginning. You have been incredibly patient with me, and you never stop surprising me with new ideas. Also thank you for introducing me to this research community. To the people I have met, from conferences or as collaborators, thank you for welcoming me into your midst. I would also like to thank my mentors, especially Eric Cytrynbaum, Fok-Shuen Leung, Laurent Marcoux, and Daniel Erman, for their encouragements when I felt uncertain and confused.

I have been blessed with too many friends to do them justice. Among those from the department, Geoff Bentsen and Ying Li deserve a special shout out for the shared moments of frustrations, and silly laughter. My brothers and sisters from GCF, thank you for being the inspiring examples, and also for your honesty with your struggles. A special thanks to those I served alongside with on exec; you made this community all the more meaningful. Of course, thanks you, Jon Dahl, for your wisdom and guidance. Thank you, Tim Wai, for being like a father to me; no words can express my gratitude.

I would also like to thank my parents for letting me go on this unexpected journey. To my brother, thanks for shouldering extra responsibilities while I am away. Thank you, Benjamin Mak, for speaking reason and love into a stubborn and sometimes unreasonable heart; thanks for being my anchor.

Above all, thank you my Lord and Saviour.

# List of Figures

# Notations and Symbols

## Mathematical

| | |
|---|---|
| $\mathbb{R}_{\geq}$ | set of non-negative real numbers |
| $\mathbb{R}^n_{\geq}$ | set of vectors with components in $\mathbb{R}_{\geq}$ |
| $\mathbb{R}^X$ | set of vectors indexed by $X$ |

Similarly defined are $\mathbb{R}_{>}$, $\mathbb{R}^n_{>}$, $\mathbb{Z}_{\geq}$, $\mathbb{Z}^n_{\geq}$, etc.

| | |
|---|---|
| $\boldsymbol{x}$ | (italic bold) vector |
| $\boldsymbol{x} > 0$ | $\boldsymbol{x} \in \mathbb{R}^n_{>}$ (similarly, $\boldsymbol{x} \geq 0$ whenever $\boldsymbol{x} \in \mathbb{R}^n_{\geq}$) |
| $\mathbf{A}$ | (uppercase upright bold) matrix |
| $\langle \cdot\ ,\ \cdot \rangle$ | dot product |
| $\boldsymbol{x}^{\boldsymbol{y}}$ | $(x_1^{y_1}, x_2^{y_2}, \ldots, x_n^{y_n})^\top$ |
| $\boldsymbol{x}^{\mathbf{Y}}$ | $(\boldsymbol{x}^{\boldsymbol{y}_1}, \boldsymbol{x}^{\boldsymbol{y}_2}, \ldots, \boldsymbol{x}^{\boldsymbol{y}_m})^\top$ where $\mathbf{Y} = \big(\boldsymbol{y}_1, \boldsymbol{y}_2, \ldots, \boldsymbol{y}_m\big) \in \mathbb{R}^{n\times m}$ |
| $\boldsymbol{x} \circ \boldsymbol{y}$ | $(x_1 y_1, x_2 y_2, \ldots, x_n y_n)^\top$ |
| $\frac{\boldsymbol{x}}{\boldsymbol{y}}$ | $\left(\frac{x_1}{y_1}, \frac{x_2}{y_2}, \ldots, \frac{x_n}{y_n}\right)^\top$ |
| $\exp(\boldsymbol{x})$ | $(e^{x_1}, e^{x_2}, \ldots, e^{x_n})^\top$ |
| $\log(\boldsymbol{x})$ | $(\log x_1, \log x_2, \ldots, \log x_n)^\top$ |
| $\operatorname{supp}(\boldsymbol{x})$ | $\{i \in n \ \ : \ \ x_i \neq 0\}$ |

The above vector operations, when applied to a set, are applied to elements of the set.

| | |
|---|---|
| $\partial X$ | boundary of the set $X$ |
| $\dot{\boldsymbol{x}}$ | $\frac{d\boldsymbol{x}}{dt}$ |

## Reaction network

| | |
|---|---|
| $\mathsf{X}_i$, $\mathsf{X}$, $\mathsf{Y}$, ... | (uppercase sans-serif) species |
| $n$ | number of species |
| $m$ | number of complexes or vertices |
| $\boldsymbol{y}_i \to \boldsymbol{y}_j$ | reaction from complex $\boldsymbol{y}_i$ to complex $\boldsymbol{y}_j$ |
| $\boldsymbol{y}_i \rightleftharpoons \boldsymbol{y}_j$ | $\boldsymbol{y}_i \to \boldsymbol{y}_j$ and $\boldsymbol{y}_j \to \boldsymbol{y}_i$ |

# Contents

# Chapter 1

# Introduction

In applications ranging from chemistry, biochemistry, to population dynamics, different entities interact according to preset rules. Different molecules may chemically react while others are inert; proteins and genes interact in certain ways; predators prey on specific animals; diseases may spread upon contacts. These rules of interactions can be summarized by a network, and one can use mathematical tools to analyze the dynamics. The models can be deterministic or stochastic; continuous or discrete; homogeneous or spatially distributed. These typically high-dimensional and non-linear models can be approached numerically or analytically, or a combination thereof.

Different assumptions behind biological models lead to different mathematical techniques being employed [47, 51, 54, 125]. These could involve continuous state spaces, e.g., ordinary differential equations (ODEs), partial differential equations (PDEs), delay differential equations (DDEs). But they could also involve discrete state spaces, such as in continuous-time Markov chains and Boolean networks.

One could argue that among the different models, the simplest of which are ODE deterministic models. However, even here, the diversity of possible dynamics is staggering. For example, the three networks in Figure 1.1 generate wildly different dynamics under *mass-action kinetics*. Mass-action systems, whose systems of ODEs have polynomial right-hand sides, can exhibit global stability (Figure 1.1(a)), bistability (Figure 1.1(b)), and oscillation (Figure 1.1(c)). The network in Figure 1.1(c) is a version of Sel'kov's model of glycolysis [120]. In higher dimensions, it is even possible for a mass-action system to exhibit chaotic dynamics.

We defer a detailed discussion of *mass-action kinetics*, the focus of this thesis, until Section 1.3. It suffices to say that ODE models have had a long history, dating back to Thomas Malthus' exponential growth model for human populations in 1978 [100], and Pierre-François Verhulst's first logistic model in 1838 [130].

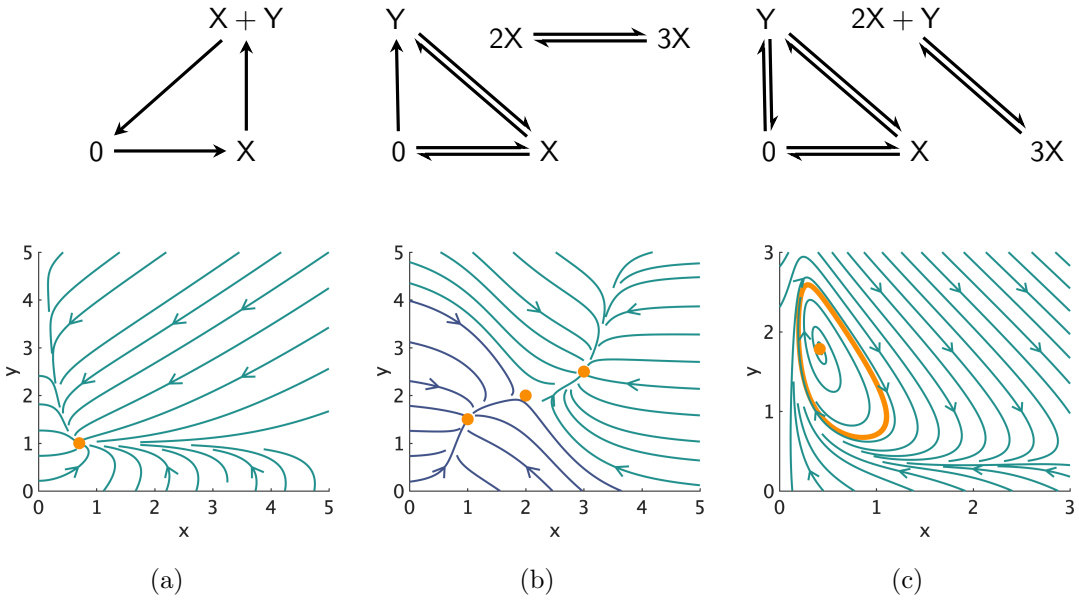


Figure 1.1: Possible dynamics under mass-action kinetics: (a) network with a globally stable equilibrium, (b) one that exhibits bistability, and (c) one with a stable limit cycle.

ODE models, unlike those using PDEs, assume the system is spatially homogeneous, i.e., they contain no spatial information. Within the cell, however, not only are there physical boundaries (e.g., cell membranes), but there are processes that crucially rely on chemical gradients. Two examples are ion gradients, used to generate electric potential across membranes, and proton gradient, involved in the production of ATP, the energy currency of living organisms. In other scenarios, diffusion or transport play important roles [99]. In cases where spatial information is consequential, PDEs models, keeping track of concentrations or population sizes as functions of time and space, are more appropriate.

Where diffusion influences the dynamics, one could use *reaction-diffusion equations*. This is one of the most studied mathematical model for macroscopic patterns or markings in

organisms [90]. Figure 1.2 hints at how the reaction-diffusion equation is a candidate for the theoretical underpinning of pattern formation in biology.

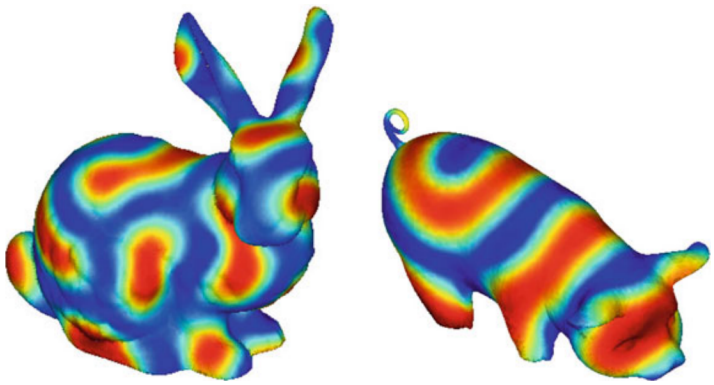

Figure 1.2: Examples of Turing patterns on surfaces from [135].

Delay models incorporate a delay time between initiation of a chemical reaction and its termination. The time lag could also come from simplifying an existing model, say, by combining several reaction steps into one. Delay models form the topic of Chapter 4.

When the number of biomolecules is so low that "concentration" cannot be defined, stochastic models are better suited for the job. Instead of keeping track of concentrations, one instead keeps track of the exact number of each type of molecules as a function of time. At randomly determined times, a reaction may fire; which reaction fires is also randomly determined. The molecular count $\boldsymbol{X}(t) \in \mathbb{Z}^n_{\geq}$ is a continuous-time Markov chain. See [5, 134] for introductions.

A different discrete model is that of Boolean networks [89, Chapter 5]. The state space of a Boolean model is simply $\{0,1\}^n$, with 0 representing the "off" state and 1 representing the "on" state. In the context of gene regulatory networks, a Boolean network can be used to model when genes are switched on or off based on current understanding of how genes and their downstream proteins interact.

The models described above only represent a fraction of the possibilities. For example, stochastic differential equations were not even mentioned, but can be used to include a noise

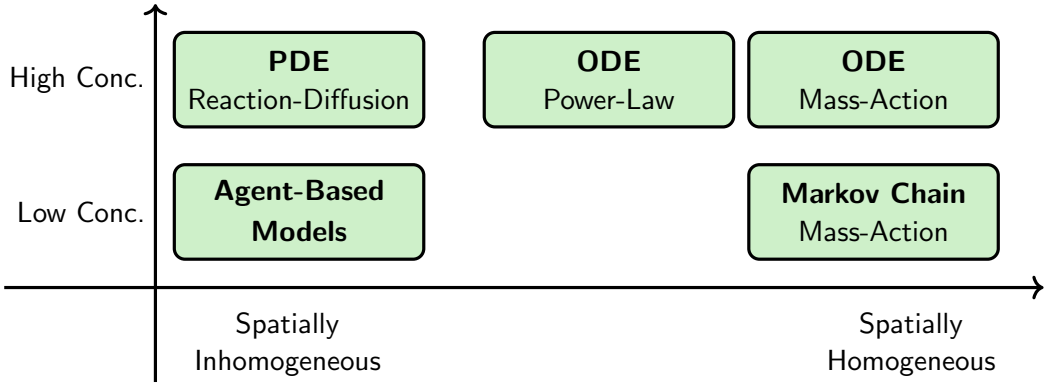


Figure 1.3: Several mathematical models for biochemical systems and their applicability with respect to spatial homogeneity and molecular counts.

on the average system behaviour, or when there is low molecular count alongside spatial inhomogeneity [1]. Moreover, the above assumptions can be combined in many different ways, and each model has its place, depending on the biological questions of interest.

The lengthy discussion thus far only speaks to biological *dynamics*. Researchers are also working on fitting experimental data, identifying parameters, extrapolating relations from high-throughput data; this is in addition to designing and controlling system dynamics. The application of mathematics and quantitative methods to biology can be and should be approached from many different fronts.

## 1.1 Overview

The starting point of modelling a system's dynamics is a network that describes the interactions of all relevant participants. The remainder of this introductory chapter defines reaction networks, mass-action systems, and notions that are relevant to this thesis. In particular, Section 1.4 reviews what is known about detailed-balanced and complex-balanced systems, collectively called toric systems in this thesis. Their algebraic and dynamical properties are reviewed in Sections 1.4.1 and 1.4.2, respectively.

Chapter 2 extends toric systems' global stability[1] to other mass-action systems. In Section 2.2, we characterize when *single-target models*, a family of mass-action systems that are not weakly reversible, are essentially detailed-balanced via *dynamical equivalence*. In Section 2.3, we prove that under the Permanence Conjecture, mass-action systems that came from perturbing the rate constants in a complex-balanced system, are globally stable.

In Chapter 3, complex-balancing is extended to power-law kinetics within the framework of *generalized mass-action systems*. We study the existence and uniqueness of vertex-balanced steady states in every invariant polytope generated by mass conservation relations. Essentially, we extend Birch's Theorem (Theorem 1.4.4), which states that for a fixed vector subspace $S \subseteq \mathbb{R}^n$, the intersection $(\boldsymbol{x}_0 + S) \cap (\boldsymbol{x}^* \circ \exp S^\perp)$ consists of exactly one point for any $\boldsymbol{x}_0$, $\boldsymbol{x}^* \in \mathbb{R}^n_>$. Our generalization provides conditions for when $(\boldsymbol{x}_0 + S) \cap (\boldsymbol{x}^* \circ \exp \tilde{S}^\perp)$ consists of exactly one point for any $\boldsymbol{x}_0$, $\boldsymbol{x}^* \in \mathbb{R}^n_>$, where $S$ and $\tilde{S} \subseteq \mathbb{R}^n$ are vector subspaces.

Finally, in Chapter 4, we look at mass-action systems with delay. We provide an algebraic condition in Section 4.2 for when any positive steady state is asymptotically stable, independent of the delay parameters, i.e., *absolutely stable*. The rest of the chapter introduces the *directed species-reaction graph* and provides a graph-theoretic condition for asymptotic stability independent of delay parameters and rate constants. That is the content of Section 4.5.

## 1.2 Reaction networks

In this section, we introduce ***reaction network*** as a mathematical object and two representations of it. One of these has its roots in *Chemical Reaction Network Theory* [59, 73, 78, 136] and is more readily recognizable by biologists and chemists. The other, more recent and geometric, representation is especially useful when studying mass-action kinetics in relation to its network structure. This latter perspective is important to our work. The notations established in this section are used throughout this thesis.

[1] Global stability is conjectured for toric systems in general, with some cases proven. We will only consider those that are known to be globally stable.

Although called a reaction network, it should be thought of more as an *interaction network*, as the population model in Example 1.2.2 shows. Nonetheless, we retain the historical terminology while acknowledging that the theory discussed in this chapter has wider application than to chemical reactions.

**Example 1.2.1.** Leonor Michaelis and Maud Menten [81, 102] investigated the enzymatic mechanism

$$\mathsf{E} + \mathsf{S} \rightleftharpoons \mathsf{ES} \longrightarrow \mathsf{E} + \mathsf{P}$$

whereby a substrate $\mathsf{S}$ is converted to a product $\mathsf{P}$ by an enzyme $\mathsf{E}$, via an intermediate $\mathsf{ES}$. In the language of Chemical Reaction Network Theory, the chemical *species* are $\mathsf{S}$, $\mathsf{P}$, $\mathsf{E}$, and $\mathsf{ES}$; these are the entities whose concentrations we are interested in.

The Michaelis–Menten equation for enzyme kinetics

$$\frac{d[\mathsf{P}]}{dt} = \frac{V_{\max}[\mathsf{S}]}{K_M + [\mathsf{S}]}$$

describes the initial reaction rate as a function of substrate concentration $[\mathsf{S}]$. In a biochemistry textbook, this equation might be derived from mass-action kinetics under the *quasi-steady state approximation*, i.e., that the concentration of the intermediate $[\mathsf{ES}]$ is approximately constant. Related but more restrictive is the *rapid equilibrium assumption*, where one assumes that the reaction $\mathsf{ES} \to \mathsf{E} + \mathsf{S}$ proceeds much faster than $\mathsf{ES} \to \mathsf{E} + \mathsf{P}$, and that $[\mathsf{ES}] + [\mathsf{E}] \ll [\mathsf{S}]$. The same Michaelis–Menten equation follows [79]. Michaelis and Menten in [102] applied the rapid equilibrium assumption, and the quasi-steady state approximation was proposed by Briggs and Haldane in 1925 [118].

The mechanism consists of three *elementary reactions*. One such reaction is the binding of $\mathsf{E}$ to $\mathsf{S}$ in order to produce the intermediate $\mathsf{ES}$. One typically assumes that the reaction proceeds at some prescribed rate, mass-action kinetics being an extremely common assumption.

Finally, the non-negative combinations of species appearing as either the source (or

*reactant*) or target (or *product*) of reactions are called ***complexes***. The mechanism above has three complexes: $\mathsf{E}+\mathsf{S}$, $\mathsf{ES}$, and $\mathsf{E}+\mathsf{P}$. The coefficients of the species in each complex are its ***stoichiometric coefficients***.

**Example 1.2.2.** Consider the Lotka–Volterra predator-prey model [10, 97, 98, 132], where a prey $\mathsf{X}$, say a snowshoe hare, is hunted by a predator $\mathsf{Y}$, e.g., a Canadian lynx. Also assume that the hares are reproducing and lynxes die over time naturally. Together, these interactions can be represented by the (interaction) network

$$\mathsf{X} \longrightarrow 2\mathsf{X} \qquad \mathsf{X}+\mathsf{Y} \longrightarrow 2\mathsf{Y} \qquad \mathsf{Y} \longrightarrow 0$$

with two species ($\mathsf{X}$ and $\mathsf{Y}$), three reactions, and six complexes ($\mathsf{X}$, $2\mathsf{X}$, $\mathsf{X}+\mathsf{Y}$, $\mathsf{Y}$, $2\mathsf{Y}$, and $0$). In the interaction $\mathsf{X}+\mathsf{Y} \to 2\mathsf{Y}$, the reactant complex is $\mathsf{X}+\mathsf{Y}$, while the product complex is $2\mathsf{Y}$; the stoichiometric coefficients of the reactant species $\mathsf{X}$ and $\mathsf{Y}$ are 1 and 1 respectively, while the stoichiometric coefficients of the product species $\mathsf{Y}$ is 2.

Historically, a *chemical reaction network* is the triple $\mathcal{N} = (\mathcal{S}, \mathcal{C}, \mathcal{R})$, where $\mathcal{S} = \{\mathsf{X}_1, \mathsf{X}_2, \ldots, \mathsf{X}_n\}$ is the set of *species*, $\mathcal{C}$ is the set of *complexes*, and $\mathcal{R}$ is the set of *reactions* [59]. The concentration of the species $\mathsf{X}_i$ is denoted $x_i$, and the vector of concentrations is an element of $\mathbb{R}^{\mathcal{S}}_{\geq}$. The whole framework was designed to avoid imposing an order on the chemical species. However, practicality wins; when building a model for $n$ species, we often impose an (arbitrary) order on the species and identify the space $\mathbb{R}^{\mathcal{S}}$ with $\mathbb{R}^n$. With this ordering of the species, each complex is naturally associated to a vector whose components are its stoichiometric coefficients. Edges between the distinct complexes are reactions. A reaction network is fundamentally a directed graph.

In Example 1.2.2, let $\mathsf{X}$ be the first species and $\mathsf{Y}$ be the second. Then we have a graph with three edges:

$$\begin{pmatrix}1\\0\end{pmatrix} \to \begin{pmatrix}2\\0\end{pmatrix}, \quad \begin{pmatrix}1\\1\end{pmatrix} \to \begin{pmatrix}0\\2\end{pmatrix}, \quad \text{and} \quad \begin{pmatrix}0\\1\end{pmatrix} \to \begin{pmatrix}0\\0\end{pmatrix}.$$

**Definition 1.2.3.** A ***reaction network*** is a finite directed graph $G = (V, E)$ whose vertices are vectors in $\mathbb{R}^n_{\geq}$[2]. We assume that the graph $G$ has no self-loops and no vertices are isolated[3]. A vertex is also called a ***complex***. An edge $(\boldsymbol{y}_i, \boldsymbol{y}_j)$, also denoted $\boldsymbol{y}_i \to \boldsymbol{y}_j$ or $(i, j)$, is called a ***reaction***. If $\boldsymbol{y}_i \to \boldsymbol{y}_j$ and $\boldsymbol{y}_j \to \boldsymbol{y}_i$ are edges in $E$, we denote the reaction pair as $\boldsymbol{y}_i \rightleftharpoons \boldsymbol{y}_j$. Finally, the vector $\boldsymbol{y}_j - \boldsymbol{y}_i$ is the ***reaction vector*** of the edge $\boldsymbol{y}_i \to \boldsymbol{y}_j$.

The reader might have noticed a jump from a complex being associated to a vector, to a complex being *de facto* a vector. In the literature, a reaction network whose vertices are vectors in $\mathbb{R}^n$ is sometimes more explicitly called a ***Euclidean embedded graph*** or ***E-graph*** [31]. In this view, a reaction is a *bona fide* vector originating from its source complex. For example, the Euclidean embedded graph of the Lotka–Volterra model of Example 1.2.2 is in Figure 1.4(a). The labels of the complexes, which can be read from the coordinates of the vertices, are extraneous but provided here for the reader's convenience. From this point on, we do not distinguish between the more geometric representation of the Euclidean embedded graph (Figure 1.4(a)) and the more traditional representation writing out the source and product complexes (Example 1.2.2). We use either representation as needed.

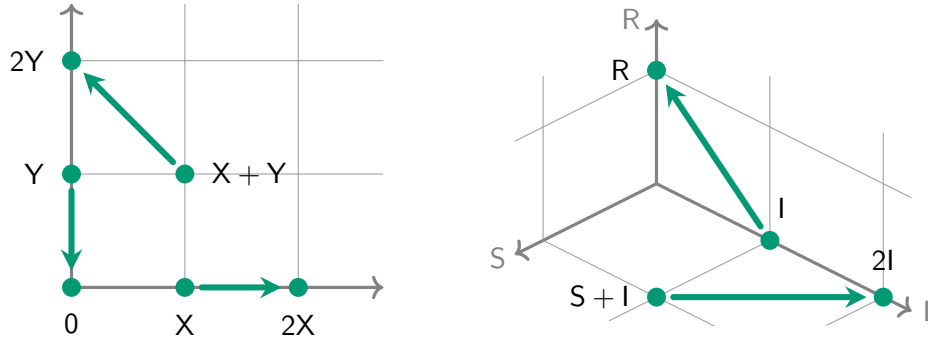


(a) (b)

Figure 1.4: The Euclidean embedded graphs of (a) the Lotka–Volterra model in Example 1.2.2 and (b) the SIR model for infectious disease Example 1.3.2.

[2]Traditionally, vertices, whose coefficients represent the stoichiometry in a reaction, are restricted to $\mathbb{Z}^n_{\geq}$. The most general setting, allowing vertices to be any vectors in $\mathbb{R}^n$, has some dynamical implications for mass-action kinetics. These will be remarked on in due course.

[3]These assumptions will have no effect on any dynamics that we will consider. They present minor annoyances when defining the Laplacian matrix in Equation (1.6).

Two graph-theoretic properties of reaction networks are related to special classes of equilibria in mass-action systems.

**Definition 1.2.4.** Let $G = (V, E)$ be a reaction network.

(a) We say $G$ is ***reversible*** if whenever $\boldsymbol{y}_i \to \boldsymbol{y}_j \in E$, then $\boldsymbol{y}_j \to \boldsymbol{y}_i \in E$. In other words, the set of reactions can be written as the set of reaction pairs.

(b) We say $G$ is ***weakly reversible*** if every edge is part of an oriented cycle. Equivalently, whenever there is a directed path from $\boldsymbol{y}_i$ to $\boldsymbol{y}_j$, then there exists a directed path from $\boldsymbol{y}_j$ to $\boldsymbol{y}_i$.

For example, all three networks in Figure 1.1 are weakly reversible, but the network in Figure 1.1(c) is also reversible. The networks of the Lotka–Volterra model and the SIR model for infectious disease in Figure 1.4 are neither weakly reversible nor reversible. Clearly, a reversible network is weakly reversible.

## 1.3 Kinetic models

In this section, we consider how to construct a deterministic ODE model for the time evolution of concentrations. This is accomplished by choosing a *kinetics*, an assumption on how fast each reaction proceeds.

Although we use the language of chemistry and biochemistry (e.g., concentrations), the framework is applicable in other contexts, such as populations dynamics in the Lotka–Volterra predatory-prey model of Example 1.2.2. In population models, the analogue of concentration is either number of individuals, or population density.

We now discuss assumptions common to many deterministic ODE models. First, determinism implies that if the system starts from the same state[4], the dynamics will be exactly the same. Systems at a macro level tend to be deterministic in nature, in the sense

[4]For non-autonomous systems that involve external influences dependent on time, it is assumed that these influences also remain the same at the appropriate time.

that in all observable ways they behave the same. This reflects the averaging that occurs when measuring macroscopic properties.

Second, the system is assumed to be spatially homogeneous, i.e., the concentration at one corner of the container is the same as at another location. Also known as the *well-mixed* assumption, this is frequently accomplished by mechanical stirring in the reaction vessel. Spatial homogeneity is approximately true if the timescales of the reactions are much slower than the timescale of diffusion.

Finally, it is assumed that all the actions associated to a reaction happens instantaneously. Reactant species are consumed at the same time product species become available. Again, at a molecular scale this is simply untrue; reactions go through transition states. But if the timescales of the transitions are much faster than that of the reactions, then this approximation holds. In Chapter 4, we drop this assumption when discussing delay models.

Under the assumptions discussed above, we model the time evolution of the state variables as governed by the reaction network $G = (V, E)$, using the system of ordinary differential equations

$$\frac{d\boldsymbol{x}}{dt} = \sum_{(i,j)\in E} \nu_{ij}(\boldsymbol{x}, t)\left(\boldsymbol{y}_j - \boldsymbol{y}_i\right), \tag{1.1}$$

where a choice of kinetics determines the rate functions $\nu_{ij} \colon \mathbb{R}^n_{\geq} \times \mathbb{R} \to \mathbb{R}_{\geq}$. For example, *Michaelis–Menten kinetics* assumes that the initial rate of the reaction $\mathsf{S} \to \mathsf{P}$, catalyzed by an enzyme $\mathsf{E}$ is modelled by

$$\nu([\mathsf{S}], [\mathsf{P}], t; [\mathsf{E}]_0) = \frac{V_{\max}[\mathsf{S}]}{K_M + [\mathsf{S}]},$$

where the total concentration of enzyme $[\mathsf{E}]_0$ is taken to be a parameter[5].

[5] Based on the derivation from mass-action kinetics, $K_M$ is proportional to $[\mathsf{E}]_0$.

Another example is *mass-action kinetics*, which we visit in more detail in Sections 1.3 and 2.3. It assumes that $\nu_{ij}(\boldsymbol{x}, t) = \kappa_{ij}\boldsymbol{x}^{\boldsymbol{y}_i}$ where $\kappa_{ij} > 0$ is a proportionality constant, and $\boldsymbol{x}^{\boldsymbol{y}_i}$ is the monomial whose exponents comes from the stoichiometric coefficients of the source complex. Mass-action kinetics can be derived from first principles; the monomial $\boldsymbol{x}^{\boldsymbol{y}_i}$ reflects the collision probability of the reactant species (in the correct proportion) [5]. Mass-action kinetics was derived for ideal systems, and as such is only an approximation of reality. Non-idealities can occur; for example, solvent molecules can shield a protein and effectively slow ligand binding [55]. The standard treatment from a thermodynamics point of view is to replace the concentration vector $\boldsymbol{x}$ in the monomial $\boldsymbol{x}^{\boldsymbol{y}_i}$ by the vector of *activities*[6]. Mathematically, mass-action kinetics can be replaced by *power-law kinetics*, which assumes that $\nu_{ij}(\boldsymbol{x}, t) = \kappa_{ij}\boldsymbol{x}^{\boldsymbol{z}_i}$, where $\boldsymbol{z}_i$ may be different from the stoichiometric coefficients of the reactant complex $\boldsymbol{y}_i$. We explore power-law kinetics (in the framework of *generalized mass-action systems* of [107, 108]) in Chapter 3.

Note that the rate function $\nu_{ij}(\boldsymbol{x}, t)$ often depends not only on concentration, but also on environmental conditions such as temperature, pressure, pH. If these external conditions are kept constant, then most often they are reflected in the value of the proportionality constants $\kappa_{ij}$. In short, deterministic kinetic models are at best approximations of reaction kinetics, and the factors that perhaps should be taken into consideration are plentiful.

Suppose a network has $n$ species and $R$ reactions. Equation (1.1) can be written as

$$\frac{d\boldsymbol{x}}{dt} = \boldsymbol{\Gamma}\boldsymbol{\nu}(\boldsymbol{x}, t), \tag{1.2}$$

where the columns of the ***stoichiometric matrix*** $\boldsymbol{\Gamma} \in \mathbb{R}^{n\times R}$ are the reaction vectors of the network, and $\boldsymbol{\nu} = (\nu_1, \nu_2, \ldots, \nu_R)^\top$ is the vector of rate functions. Clearly $\dot{\boldsymbol{x}}$ is confined to the linear space $S = \operatorname{ran}\boldsymbol{\Gamma}$, and any trajectory is confined to the affine space $\boldsymbol{x}(0) + S$, where

[6] Informally, the activity of a chemical species is its "effective concentration" when it comes to reactivity.

$\boldsymbol{x}(0) \in \mathbb{R}^n_{\geq}$ is the initial condition. The ***stoichiometric subspace***

$$S = \operatorname{span}\{\boldsymbol{y}_j - \boldsymbol{y}_i \,:\, \boldsymbol{y}_i \to \boldsymbol{y}_j \in E\} = \operatorname{ran} \boldsymbol{\Gamma} \tag{1.3}$$

can easily be read from the Euclidean embedded graph. For example, the stoichiometric subspace of the Lotka–Volterra model in Figure 1.4(a) is $S = \mathbb{R}^2$, while that of the SIR model in Figure 1.4(b) is the two dimensional subspace $S = \operatorname{span}\{(-1, 1, 0)^\top, (0, -1, 1)^\top\}$ with the ordering $\mathsf{X}_1 = \mathsf{S}$, $\mathsf{X}_2 = \mathsf{I}$, and $\mathsf{X}_3 = \mathsf{R}$. Sometimes $\dim S$ is referred to as the ***rank*** of the network. Notice that for the SIR model, $S^\perp = \operatorname{span}(1, 1, 1)^\top$, reflecting the fact that the total population $[\mathsf{S}] + [\mathsf{I}] + [\mathsf{R}]$ is constant; no births or deaths are included in the dynamics. We call this a ***conservation relation*** of the system[7].

### 1.3.1 Mass-action systems

Mass-action kinetics is an assumption on the reaction rate functions. We define a mass-action system as a mathematical object that has the dynamics expected from a reaction network under mass-action kinetics. To properly introduce mass-action kinetics, consider the reaction

$$\mathsf{X} + \mathsf{Y} \longrightarrow 2\mathsf{X}$$

where $\mathsf{X}$ converts a molecule of $\mathsf{Y}$ to a copy of itself. We assume this reaction proceeds at a rate proportional to the concentration of the reactant species, i.e., the rate function is $\nu(\boldsymbol{x}) = \kappa xy = \kappa x^1 y^1$, where the rate constant[8] $\kappa > 0$ is a proportionality constant. Note that the exponents in the monomial are the stoichiometric coefficients of the source complex. A proper model needs to account for the relative change of the different species' concentrations. Thus, we multiply the rate function by the reaction vector and arrive at the

[7] In the literature, *conservation relation* or *conservation law* may refer to not a vector in $S^\perp$, but rather one in $S^\perp \cap \mathbb{R}^n_>$ as a nod towards conservation of mass. We do not require this more stringent condition here.

[8] The word "constant" can be misleading, as the proportionality constant $\kappa$ depends on external conditions such as temperature, pressure, pH.

system of differential equations

$$\frac{d\boldsymbol{x}}{dt} = \kappa xy \begin{pmatrix} 1 \\ -1 \end{pmatrix}.$$

If a reaction network contains multiple reactions, we simply add together the relevant terms. For example, say the conversion reaction we considered above is actually reversible:

$$\mathsf{X} + \mathsf{Y} \rightleftharpoons 2\mathsf{X} \quad .$$

Since there are two source complexes, there are two monomials — $xy$ as well as $x^2$ — in the associated system of ODEs

$$\frac{d\boldsymbol{x}}{dt} = \kappa_+ xy \begin{pmatrix} 1 \\ -1 \end{pmatrix} + \kappa_- x^2 \begin{pmatrix} -1 \\ 1 \end{pmatrix}.$$

There are two (possibly different) rate constants, one for each reaction.

**Definition 1.3.1.** A ***mass-action system*** is a weighted directed graph $(G, \boldsymbol{\kappa})$, where $G = (V, E)$ is a reaction network, and $\boldsymbol{\kappa} \in \mathbb{R}^E_>$ is a ***vector of rate constants***. Its ***associated system of differential equations*** on $\mathbb{R}^n_\geq$ is

$$\frac{d\boldsymbol{x}}{dt} = \sum_{(i,j)\in E} \kappa_{ij} \boldsymbol{x}^{\boldsymbol{y}_i} \left(\boldsymbol{y}_j - \boldsymbol{y}_i\right), \tag{1.4}$$

where $\boldsymbol{x}^{\boldsymbol{y}} = x_1^{y_1} x_2^{y_2} \cdots x_n^{y_n}$.

To say $\boldsymbol{x}(t)$ is a solution to the mass-action system, we mean it is a solution to the associated system of ODEs (1.4) for some initial value in $\mathbb{R}^n_>$.

Under mass-action kinetics, $\mathbb{R}^n_\geq$ is forward invariant, i.e., if $\boldsymbol{x}(0) \in \mathbb{R}^n_\geq$, then the solution $\boldsymbol{x}(t) \in \mathbb{R}^n_\geq$ for all $t \geq 0$ for which the solution is defined. We often start with a *positive* initial condition $\boldsymbol{x}(0) \in \mathbb{R}^n_>$. Recall that the vector field lies in the stoichiometric subspace $S$. Thus

for any initial condition $\boldsymbol{x}(0) \in \mathbb{R}^n_>$, the solution $\boldsymbol{x}(t)$ to (1.4) is confined to the affine space $\boldsymbol{x}(0) + S$, where the addition is over the elements of $S$. The ***stoichiometric compatibility class*** of $\boldsymbol{x}(0)$ is the polytope $(\boldsymbol{x}(0) + S)_> = (\boldsymbol{x}(0) + S) \cap \mathbb{R}^n_>$. Finally, we remark that if the stoichiometric coefficients are restricted to $y_i = 0$ or $y_i = 1$ for any complex $\boldsymbol{y}$, then the right-hand side of (1.4) is Lipschitz, so uniqueness of solution is guaranteed.

**Example 1.3.2.** We write down the SIR model for infectious disease, whose reaction network appears in Figure 1.4(b). The network has two reactions with different source complexes; hence the associated system of ODEs has two monomials. Let $x = [\mathsf{S}]$ represent the fraction of the population that is susceptible to the disease, $y = [\mathsf{I}]$ the fraction that is infected and also infectious, and $z = [\mathsf{R}]$ the fraction that has recovered and immune to the disease. The associated system (with arbitrary rate constants $\kappa_i > 0$) is

$$\begin{aligned} \frac{dx}{dt} &= -\kappa_1 xy \\ \frac{dy}{dt} &= \kappa_1 xy - \kappa_2 y \\ \frac{dz}{dt} &= \kappa_2 y. \end{aligned}$$

If we think of Equation (1.4) as a "species-centric" view, then a "reaction-centric" formulation is the matrix equation

$$\frac{d\boldsymbol{x}}{dt} = \boldsymbol{\Gamma} \begin{pmatrix} \kappa_1 \boldsymbol{x}^{\boldsymbol{y}_1} \\ \kappa_2 \boldsymbol{x}^{\boldsymbol{y}_2} \\ \vdots \\ \kappa_R \boldsymbol{x}^{\boldsymbol{y}_R} \end{pmatrix}. \tag{1.5}$$

The same monomial may appear more than once in Equation (1.5) with different rate constants, if multiple reactions share the same source complex.

We introduce yet another matrix decomposition of the system (1.4) that is "complex-centric". Suppose the reaction network $G$ has $m$ vertices. Let $\kappa_{ij}$ be the rate constant of

$\boldsymbol{y}_i \to \boldsymbol{y}_j$ for $i, j = 1, 2, \ldots, m$, with the convention that $\kappa_{ij} = 0$ whenever $\boldsymbol{y}_i \to \boldsymbol{y}_j \notin E$. Define the ***complex matrix*** $\mathbf{Y} \in \mathbb{R}^{n \times m}$ to have the complexes as its columns. The ***Laplacian matrix***[9] (or the ***kinetic matrix***) of the weighted directed graph $(G, \boldsymbol{\kappa})$ is given by

$$[\mathbf{A}_{\boldsymbol{\kappa}}]_{ij} = \begin{cases} \kappa_{ji} & \text{if } i \neq j \\ -\sum_p \kappa_{jp} & \text{if } i = j \end{cases}. \tag{1.6}$$

It is normally written as $\mathbf{A}_{\boldsymbol{\kappa}} = (\mathbf{W} - \mathbf{D})^\top$, where $[\mathbf{W}]_{ij} = \kappa_{ij}$ is the matrix of weights on the edges, and $\mathbf{D} = \text{diag}(d_1, d_2, \ldots d_m)$ with $d_i = \sum_{p=1}^m [\mathbf{W}]_{ip}$ [66]. Equation (1.4) can then be written as

$$\frac{d\boldsymbol{x}}{dt} = \mathbf{Y}\mathbf{A}_{\boldsymbol{\kappa}}\boldsymbol{x}^{\mathbf{Y}}, \tag{1.7}$$

where $\boldsymbol{x}^{\mathbf{Y}} = (\boldsymbol{x}^{\boldsymbol{y}_1}, \boldsymbol{x}^{\boldsymbol{y}_2}, \ldots, \boldsymbol{x}^{\boldsymbol{y}_m})^\top$ is exponentiation with the columns of $\mathbf{Y}$. The vector $\boldsymbol{x}^{\mathbf{Y}}$ consists of the monomials defined by the complexes. We illustrate these different formulations with examples.

**Example 1.3.3.** Consider two reversible pairs of reactions

$$2\mathsf{X} \underset{\kappa_{21}}{\overset{\kappa_{12}}{\rightleftharpoons}} \mathsf{X} + \mathsf{Y} \underset{\kappa_{32}}{\overset{\kappa_{23}}{\rightleftharpoons}} 2\mathsf{Y}$$

with rate constants as labelled. Under mass-action kinetics, the variables $x$ and $y$, for the concentrations of $\mathsf{X}$ and $\mathsf{Y}$ respectively, evolve according to

$$\begin{aligned} \frac{d}{dt}\begin{pmatrix} x \\ y \end{pmatrix} &= \kappa_{12}x^2\begin{pmatrix} -1 \\ 1 \end{pmatrix} + \kappa_{21}xy\begin{pmatrix} 1 \\ -1 \end{pmatrix} + \kappa_{23}xy\begin{pmatrix} -1 \\ 1 \end{pmatrix} + \kappa_{32}y^2\begin{pmatrix} 1 \\ -1 \end{pmatrix} \\ &= \begin{pmatrix} -\kappa_{12}x^2 + \kappa_{21}xy - \kappa_{23}xy + \kappa_{32}y^2 \\ \kappa_{12}x^2 - \kappa_{21}xy + \kappa_{23}xy - \kappa_{32}y^2 \end{pmatrix}. \end{aligned}$$

[9] What is defined here is actually the negative transpose of the Laplacian matrix; however, since we refer to this matrix repeatedly, we call the matrix (1.6) the Laplacian.

Let $\boldsymbol{x} = (x, y)^\top$. Another way to rewrite the system of ODEs above is

$$\frac{d\boldsymbol{x}}{dt} = \boldsymbol{\Gamma}\boldsymbol{\nu}(\boldsymbol{x}) = \begin{pmatrix} -1 & 1 & -1 & 1 \\ 1 & -1 & 1 & -1 \end{pmatrix} \begin{pmatrix} \kappa_{12}x^2 \\ \kappa_{21}xy \\ \kappa_{23}xy \\ \kappa_{32}y^2 \end{pmatrix}.$$

Note the columns of $\boldsymbol{\Gamma}$ are the reaction vectors. For a reversible system like this, there is a certain amount of redundancy. We can combine reaction pairs and instead write

$$\frac{d\boldsymbol{x}}{dt} = \begin{pmatrix} -1 & -1 \\ 1 & 1 \end{pmatrix} \begin{pmatrix} \kappa_{12}x^2 - \kappa_{21}xy \\ \kappa_{23}xy - \kappa_{32}y^2 \end{pmatrix}.$$

While this may be useful for certain purposes, and indeed sometimes the literature takes this perspective, we avoid this, thereby restricting the vector of rate functions $\boldsymbol{\nu}(\boldsymbol{x})$ to take non-negative or positive values.

The "complex-centric" formulation captures the network structure. Numbering the complexes from left to right, the complex matrix and the Laplacian matrix are

$$\mathbf{Y} = \begin{pmatrix} 2 & 1 & 0 \\ 0 & 1 & 2 \end{pmatrix} \quad \text{and} \quad \mathbf{A}_{\boldsymbol{\kappa}} = \begin{pmatrix} -\kappa_{12} & \kappa_{21} & \\ \kappa_{12} & -\kappa_{21} - \kappa_{23} & \kappa_{32} \\ & \kappa_{23} & -\kappa_{32} \end{pmatrix}.$$

The second column of $\mathbf{A}_{\boldsymbol{\kappa}}$ reflects the fact that two reactions are leaving the second complex $\mathsf{X}+\mathsf{Y}$: one to the first complex $2\mathsf{X}$ with rate constant $\kappa_{21}$ and another to the third complex $2\mathsf{Y}$ with rate constant $\kappa_{23}$. The vector $\boldsymbol{x}^{\mathbf{Y}} = (x^2, xy, y^2)^\top$ is precisely the monomials associated to the three complexes in this order. Thus, the system of ODEs can also be written as

$$\frac{d\boldsymbol{x}}{dt} = \mathbf{Y}\mathbf{A}_{\boldsymbol{\kappa}}\boldsymbol{x}^{\mathbf{Y}} = \begin{pmatrix} 2 & 1 & 0 \\ 0 & 1 & 2 \end{pmatrix} \begin{pmatrix} -\kappa_{12} & \kappa_{21} & \\ \kappa_{12} & -\kappa_{21} - \kappa_{23} & \kappa_{32} \\ & \kappa_{23} & -\kappa_{32} \end{pmatrix} \begin{pmatrix} x^2 \\ xy \\ y^2 \end{pmatrix}.$$

By *flux* across the reaction $\boldsymbol{y}_i \to \boldsymbol{y}_j$, we refer to the value of the rate function $\kappa_{ij}\boldsymbol{x}^{\boldsymbol{y}_i}$ at a specified concentration level $\boldsymbol{x} > \mathbf{0}$. Observe that any component of

$$\mathbf{A}_{\boldsymbol{\kappa}}\boldsymbol{x}^{\mathbf{Y}} = \begin{pmatrix} \kappa_{21}xy - \kappa_{12}x^2 \\ \kappa_{12}x^2 + \kappa_{32}y^2 - (\kappa_{21}+\kappa_{23})xy \\ \kappa_{23}xy - \kappa_{32}y^2 \end{pmatrix}$$

is the net difference, at the corresponding complex, between incoming and outgoing fluxes at the current state. We study the structure of $\mathbf{A}_{\boldsymbol{\kappa}}\boldsymbol{x}^{\mathbf{Y}}$ as it relates to the class of *complex-balanced* steady states more generally in Section 1.4.1.

**Example 1.3.4.** Consider a version of Sel'kov's model of glycolysis with an ordering of the complexes in Figure 1.6(a). Let $\kappa_{ij}$ be the rate constant of the reaction $\boldsymbol{y}_i \to \boldsymbol{y}_j$. The mass-action system defined by this network is

$$\frac{d\boldsymbol{x}}{dt} = \begin{pmatrix} \kappa_{12} - \kappa_{21}x - \kappa_{23}x & + \kappa_{32}y - \kappa_{45}x^3 + \kappa_{54}x^2y \\ \kappa_{13} & + \kappa_{23}x - \kappa_{31}y - \kappa_{32}y + \kappa_{45}x^3 - \kappa_{54}x^2y \end{pmatrix},$$

or with the complex and Laplacian matrices,

$$\frac{d\boldsymbol{x}}{dt} = \begin{pmatrix} 0 & 1 & 0 & 3 & 2 \\ 0 & 0 & 1 & 0 & 1 \end{pmatrix} \begin{pmatrix} -(\kappa_{12}+\kappa_{13}) & \kappa_{21} & \kappa_{31} & & \\ \kappa_{12} & -(\kappa_{21}+\kappa_{23}) & \kappa_{32} & & \\ \kappa_{13} & \kappa_{23} & -(\kappa_{31}+\kappa_{32}) & & \\ & & & -\kappa_{45} & \kappa_{54} \\ & & & \kappa_{45} & -\kappa_{54} \end{pmatrix} \begin{pmatrix} 1 \\ x \\ y \\ x^3 \\ x^2y \end{pmatrix}.$$

The non-linearity of mass-action systems lies with the monomials. The *Newton polytope*[10], or *reactant polytope* [69], can be used to see which monomial *dominates*, i.e., is orders of magnitude stronger than, other monomials in certain region of the state space [22, 31, 45, 69].

[10] In algebra, the Newton polytope is defined for a single polynomial, while here, we use all the polynomials appearing on the right-hand side.

**Definition 1.3.5.** The ***Newton polytope*** of a reaction network $G = (V, E)$ is the convex hull of the source complexes, i.e.,

$$\text{Newt}(G) = \left\{ \sum_{\boldsymbol{y} \in V_s} \alpha_{\boldsymbol{y}} \boldsymbol{y} \ : \ \alpha_{\boldsymbol{y}} \geq 0 \text{ and } \sum_{\boldsymbol{y} \in V_s} \alpha_{\boldsymbol{y}} = 1 \right\},$$

where $V_s \subseteq V$ is the set of source complexes. The ***relative interior of the Newton polytope*** is the set

$$\text{Newt}(G)^\circ = \left\{ \sum_{\boldsymbol{y} \in V_s} \alpha_{\boldsymbol{y}} \boldsymbol{y} \ : \ \alpha_{\boldsymbol{y}} > 0 \text{ and } \sum_{\boldsymbol{y} \in V_s} \alpha_{\boldsymbol{y}} = 1 \right\}.$$

The Newton polytopes of two networks are shown in Figures 1.5(a) and 1.6(a). Figures 1.5(b) and 1.6(b) roughly splits the state space into regions where a single monomial dominates; between these regions, there is no clear winner. The precise boundary of these regions depend on the relative magnitude of rate constants. Shown in each region is the reaction vector(s) associated to the dominant monomial. For details on how these regions are determined and which monomial dominates where, see [22, 31].

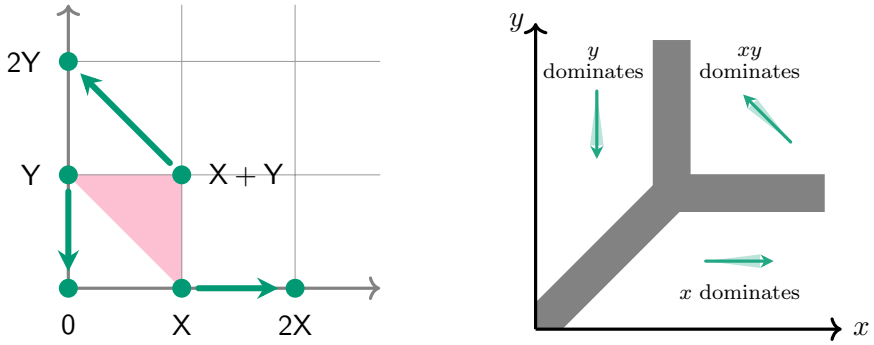


(a) (b)

Figure 1.5: (a) Highlighted is the Newton polytope of the Lotka–Volterra model. (b) The regions of state space where a monomial dominates over all others. The vector shows the corresponding dominant reaction in each region, while the cone shows the possible direction of the vector field.

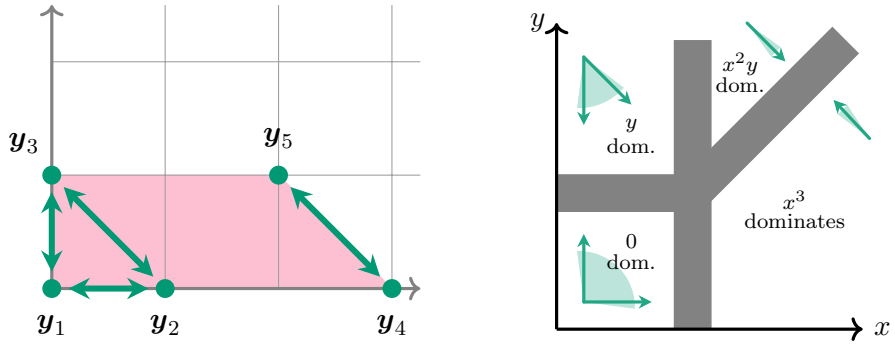


Figure 1.6: (a) Highlighted is the Newton polytope of a version of the Sel'kov model. (b) The regions of state space where a monomial dominates over all others. The vector(s) shows the corresponding dominant reaction(s) in each region, while the cone shows the possible direction of the vector field.

## 1.4 Toric systems

In this section, we introduce two classes of positive steady states for mass-action systems — *detailed-balanced* and *complex-balanced* — that enjoy remarkable stability and algebraic properties. Detailed-balancing dates back to Boltzmann [13,14,15]. Complex-balancing, which generalizes the former, was analyzed extensively in the 1970's [56, 60, 76, 78].

Boltzmann introduced detailed-balancing for the collision of ideal gas particles. He assumed *microscopic reversibility*, that is, one cannot distinguish between the process forward in time and backward in time. Later, Wegscheider and Lewis, among others, generalized it to chemical processes, where *detailed-balanced* implies that across every reversible pair of reactions, the forward reaction proceeds at the same rate as the backward reaction [93,109,133]. Detailed-balancing has thermodynamic implications. Horn and Jackson called complex-balancing a *quasi-thermodynamics* property [78]. While kinetics has deep connection to thermodynamics, we will not broach this broad subject. The reader is referred to [59, Chapter 13] for an introduction.

**Definition 1.4.1.** Let $(G, \boldsymbol{\kappa})$ be a mass-action system with associated system of ODEs $\frac{d\boldsymbol{x}}{dt} = \boldsymbol{f}(\boldsymbol{x})$.

(a) Its ***set of positive***[11] ***steady states*** is

$$E_{\boldsymbol{\kappa}} = \{\boldsymbol{x}^* > \mathbf{0} \,:\, \boldsymbol{f}(\boldsymbol{x}^*) = \mathbf{0}\}\,. \tag{1.8}$$

(b) A positive steady state $\boldsymbol{x}^*$ is ***detailed-balanced*** if for every $\boldsymbol{y}_i \to \boldsymbol{y}_j \in E$, we have

$$\kappa_{ij}(\boldsymbol{x}^*)^{\boldsymbol{y}_i} = \kappa_{ji}(\boldsymbol{x}^*)^{\boldsymbol{y}_j}. \tag{1.9}$$

Let $D_{\boldsymbol{\kappa}}$ denote the set of detailed-balanced steady states. If $D_{\boldsymbol{\kappa}} \neq \emptyset$, we say the mass-action system $(G, \boldsymbol{\kappa})$ is ***detailed-balanced***.

(c) A positive steady state $\boldsymbol{x}^*$ is ***complex-balanced*** if for every complex $\boldsymbol{y}_i \in V$, we have

$$\sum_{(i,j)\in E} \kappa_{ij}(\boldsymbol{x}^*)^{\boldsymbol{y}_i} = \sum_{(j,i)\in E} \kappa_{ji}(\boldsymbol{x}^*)^{\boldsymbol{y}_j}. \tag{1.10}$$

Let $Z_{\boldsymbol{\kappa}}$ denote the set of complex-balanced steady states. If $Z_{\boldsymbol{\kappa}} \neq \emptyset$, we say the mass-action system $(G, \boldsymbol{\kappa})$ is ***complex-balanced***.

The detailed-balancing condition (1.9) ensures that the fluxes across each reversible pair are equal. For this reason, a system that admits a detailed-balanced steady state is necessarily reversible. The complex-balancing condition (1.10) ensures that the net flux flowing across each vertex is zero. For this reason, a system that admits a complex-balanced steady state is necessarily weakly reversible [31, 136]. In the literature, detailed-balancing is also known as *edge-balancing*, while complex-balancing is also called *vertex-balancing*. In Chapter 3, we extend the notion of vertex-balancing beyond mass-action systems.

[11] The relevant steady states are non-negative. In this thesis, we are only concerned about *positive* steady states.

**Example 1.4.2.** Consider the simple reaction network

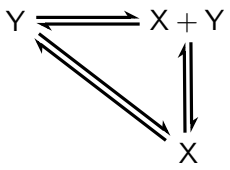


with complexes ordered clockwise, starting with Y being $\boldsymbol{y}_1$. If all rate constants are $\kappa_{ij} = 1$, then the steady state $(x, y) = (1, 1)^\top$ is detailed-balanced, hence also complex-balanced. However, if the rate constants are chosen such that the clockwise ones are $\kappa_{12} = \kappa_{23} = \kappa_{31} = 1$, while the counterclockwise ones are $\kappa_{21} = \kappa_{32} = \kappa_{13} = 2$, then $(x, y) = (1, 1)^\top$ is complex-balanced but not detailed-balanced.

If a steady state is detailed-balanced, then it is complex-balanced, i.e., $D_{\boldsymbol{\kappa}} \subseteq Z_{\boldsymbol{\kappa}}$, although the converse may not be true. More surprisingly, if a mass-action system has one complex-balanced steady state, then all its positive steady states are complex-balanced, i.e., $Z_{\boldsymbol{\kappa}} = E_{\boldsymbol{\kappa}}$ if $Z_{\boldsymbol{\kappa}} \neq \emptyset$. Similarly, if a mass-action system has one detailed-balanced steady state, then all its positive steady states are detailed balanced, i.e., $D_{\boldsymbol{\kappa}} = E_{\boldsymbol{\kappa}}$ if $D_{\boldsymbol{\kappa}} \neq \emptyset$ [78]. Therefore, it makes sense to call a mass-action system *complex-balanced* or *detailed-balanced*.

Generally, the rate constants need to satisfy some algebraic constraints for a weakly reversible system to be complex-balanced [35, 56, 76]. If in addition, the network is reversible and the rate constants satisfy additional constraints known as *formal-balancing* [49], then the system is also detailed-balanced. See [35] for a discussion on a necessary and sufficient condition on the rate constants for complex-balancing, and [59, Chapter 14.4] for detailed-balancing.

In what follows, we limit our discussion to complex-balanced systems, while keeping in mind that detailed-balanced systems share the same properties. We list the most foundational results below [76, 78, 82]. An assumption behind this list is the existence of a complex-balanced steady state. In Section 1.4.1 we look at conditions for when such a steady state exists.

**Theorem 1.4.3.** *Let $(G, \boldsymbol{\kappa})$ be a complex-balanced system, with complex-balanced steady state $\boldsymbol{x}^* \in Z_{\boldsymbol{\kappa}}$. Let $\dot{\boldsymbol{x}} = \mathbf{Y}\mathbf{A}_{\boldsymbol{\kappa}}\boldsymbol{x}^{\mathbf{Y}}$ be its associated system of ODEs, and $S$ its stoichiometric subspace.*

(a) *Then $\boldsymbol{x}^*$ is a solution to $\mathbf{A}_{\boldsymbol{\kappa}}(\boldsymbol{x}^*)^{\mathbf{Y}} = \mathbf{0}$.*

(b) *Every positive steady state is complex-balanced, i.e., $Z_{\boldsymbol{\kappa}} = E_{\boldsymbol{\kappa}}$.*

(c) *The set $Z_{\boldsymbol{\kappa}}$ can be represented as*

$$Z_{\boldsymbol{\kappa}} = \left\{\boldsymbol{x} > \mathbf{0} \ : \ \ln \boldsymbol{x} - \ln \boldsymbol{x}^* \in S^{\perp}\right\} = \boldsymbol{x}^* \circ \exp S^{\perp}, \tag{1.11}$$

*where $\ln(\cdot)$, $\circ$, and $\exp(\cdot)$ are the component-wise logarithm, multiplication and exponentiation respectively.*

(d) *There is exactly one positive steady state in every stoichiometric compatibility class.*

(e) *The function*

$$L(\boldsymbol{x}) = \sum_{i=1}^{n} x_i \left(\ln x_i - \ln x_i^* - 1\right) + x_i^* \tag{1.12}$$

*is a strictly convex Lyapunov function on $\mathbb{R}^n_>$ for the mass-action system, with global minimum at $\boldsymbol{x} = \boldsymbol{x}^*$.*

(f) *Every positive steady state is asymptotically stable within its stoichiometric compatibility class.*

(g) *Every positive steady state is linearly stable within its stoichiometric compatibility class.*

Theorem 1.4.3(a)–(d) are algebraic in nature. In Section 1.4.1, we look more closely at these algebraic properties, and explain why in a sense, the system has toricity. Theorem 1.4.3(e)–(g) focus on the dynamics of complex-balanced systems, which is the focus of Section 1.4.2.

### 1.4.1 Algebraic properties of complex-balanced systems

In this section, we focus on some algebraic properties of complex-balanced systems. Mathematically, complex-balanced and detailed-balanced systems — collectively called toric systems in this thesis, for reason to be seen in this section — enjoy a variety of algebraic properties in addition to their stable dynamics. Algebraists and algebraic geometers are bringing their tool-kits to biology and chemistry [35, 50, 62, 63, 64, 67, 68, 70, 71, 87, 88, 108]. We can only expect more algebraic structure in nature to be discovered.

Horn and Jackson called a system whose positive steady state set has the representation $\boldsymbol{x}^* \circ \exp S^\perp$ *quasi-thermostatic* [78]; elsewhere such a system is called a *toric dynamical system* [35]. At the heart of both works are complex-balanced systems. Notably, Horn and Jackson thought of the algebraic and the dynamical aspects separately, referring to Lyapunov stability (Theorem 1.4.3(e)) as *quasi-thermodynamic*. Craciun et al. were mostly focused on the algebraic aspect of complex-balanced systems[12]. In Chapter 3, we see that certain non-mass-action systems also share the same algebraic properties as complex-balancing, sometimes without the dynamical properties [107, 108].

If we accept that $Z_{\boldsymbol{\kappa}} = \boldsymbol{x}^* \circ \exp S^\perp$ [59, 73, 78], where $\boldsymbol{x}^*$ is one complex-balanced steady state of the system, it follows that $Z_{\boldsymbol{\kappa}}$ admits a monomial parametrization. For example, suppose $\{\boldsymbol{u}, \boldsymbol{v}\}$ is a basis for $S^\perp$. If $t$ is a positive scalar and $\boldsymbol{u} \in \mathbb{R}^n$ is a vector, denote by $t^{\boldsymbol{u}}$ the vector $(t^{u_1}, t^{u_2}, \ldots, t^{u_n})^\top$. Then

$$\begin{aligned} Z_{\boldsymbol{\kappa}} &= \{\boldsymbol{x}^* \circ \exp(a\boldsymbol{u} + b\boldsymbol{v}) \ : \ a, b \in \mathbb{R}\} \\ &= \left\{\boldsymbol{x}^* \circ (e^a)^{\boldsymbol{u}} \circ (e^b)^{\boldsymbol{v}} \ : \ a, b \in \mathbb{R}\right\} \\ &= \{\boldsymbol{x}^* \circ s^{\boldsymbol{u}} \circ t^{\boldsymbol{v}} \ : \ s, t > 0\}\,. \end{aligned}$$

In other words, $Z_{\boldsymbol{\kappa}}$ admits the parametrization $(x_1^* s^{u_1} t^{v_1}, x_2^* s^{u_2} t^{v_2}, \ldots, x_n^* s^{u_n} t^{v_n})^\top$ with $s$, $t > 0$. The same calculation holds even when $S^\perp$ is of higher dimensions.

[12] In the second half of [35], they studied stability and proved the Global Attractor Conjecture for detailed-balanced systems whose stoichiometric compatibility class is two-dimensional and bounded.

The existence and uniqueness of a complex-balanced steady state within every stoichiometric compatibility class can be interpreted as the intersection of two surfaces. This result, by the name of **Birch's Theorem** [11], is also related to the maximum likelihood estimate in algebraic statistics [111].

**Theorem 1.4.4.** *Let $S \subseteq \mathbb{R}^n$ be a vector subspace. Then for any $\boldsymbol{x}_0$, $\boldsymbol{x}^* \in \mathbb{R}^n_>$, the intersection $(\boldsymbol{x}_0 + S) \cap (\boldsymbol{x}^* \circ \exp S^\perp)$ has exactly one point.*

In Section 3.3, we generalize this to the existence and uniqueness of intersection points in $(\boldsymbol{x}_0 + S) \cap (\boldsymbol{x}^* \circ \exp \tilde{S}^\perp)$ for any $\boldsymbol{x}_0$, $\boldsymbol{x}^* > \mathbf{0}$, where $S$ and $\tilde{S}$ are two vector subspaces that satisfy certain geometric conditions. Although for now we leave behind Birch's Theorem, in Corollary 2.2.5, we apply this in a surprising way to show that the family of *single-target networks*, though not weakly reversible, are essentially always detailed-balanced (up to *dynamical equivalence*; see Definition 2.1.1).

That a complex-balanced steady state $\boldsymbol{x}^*$ is a solution to $\mathbf{A}_{\boldsymbol{\kappa}} \boldsymbol{x}^{\mathbf{Y}} = \mathbf{0}$ follows from our observation in Example 1.3.3 that the components $\mathbf{A}_{\boldsymbol{\kappa}} \boldsymbol{x}^{\mathbf{Y}}$ measure the net flux flowing across the vertices. We now look at the kernel of $\mathbf{A}_{\boldsymbol{\kappa}}$ in more depth. Because $\mathbf{A}_{\boldsymbol{k}}$ is column-conserving, i.e., $(1, 1, \ldots, 1)^\top \in \ker \mathbf{A}_{\boldsymbol{\kappa}}^\top$, it is not full ranked. Theorem 1.4.7 describes a basis for $\ker \mathbf{A}_{\boldsymbol{\kappa}}$.

Suppose there are $m$ complexes in the mass-action system $(G, \boldsymbol{\kappa})$, i.e., $\mathbf{A}_{\boldsymbol{\kappa}} \in \mathbb{R}^{m \times m}$. For simplicity, let $\kappa_{ij} = 0$ whenever $\boldsymbol{y}_i \to \boldsymbol{y}_j$ is not a reaction. The components of

$$\mathbf{A}_{\boldsymbol{\kappa}} \boldsymbol{x}^{\mathbf{Y}} = \begin{pmatrix} -\left(\sum_j \kappa_{1j}\right) \boldsymbol{x}^{\boldsymbol{y}_1} + \sum_j \kappa_{j1} \boldsymbol{x}^{\boldsymbol{y}_j} \\ \vdots \\ -\left(\sum_j \kappa_{mj}\right) \boldsymbol{x}^{\boldsymbol{y}_m} + \sum_j \kappa_{jm} \boldsymbol{x}^{\boldsymbol{y}_j} \end{pmatrix}$$

measure the net flux flowing across each complex. If one imagines each vertex as a bucket, and edges allow the flow of water between buckets, then $\mathbf{A}_{\boldsymbol{\kappa}} \boldsymbol{x}^{\mathbf{Y}}$ measures the net flow of water into each bucket. Complex-balancing occurs precisely when the net flow across vertices is zero.

Before continuing, we need some graph-theoretic objects and a generalization of the Matrix-Tree Theorem [35, 74, 76, 83]. A subgraph of $G$ is *connected* if in the undirected version of $G$, there exists a path between any two of its vertices. A maximally connected subgraph is a ***connected component*** or ***linkage class***, of $G$. A subgraph of $G$ is *strongly connected* if there exists a directed path between any two of its vertices. A maximally strongly connected subgraph is a ***strongly connected component*** or ***strong linkage class***. A ***terminal strongly connected component*** or ***terminal strong linkage class*** is a strongly connected component with no edge leaving it. Figure 1.7 illustrates these terms with an example.

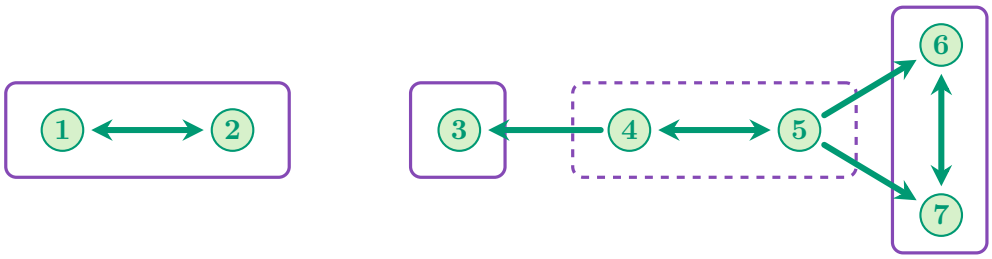


Figure 1.7: A directed graph with two connected components (linkage classes); emphasized are its four strongly connected components (strong linkage classes), of which three are terminal strongly connected (terminal strong linkage classes).

**Definition 1.4.5.** Let $\mathcal{G} = (\mathcal{V}, \mathcal{E})$ be a directed graph, with no loops and no isolated vertices. Label each edge $(i, j)$ with the variable $\kappa_{ij}$.

(a) If $\mathcal{G}$ is connected, a ***spanning tree*** $\mathcal{T}$ is a directed tree of $\mathcal{G}$ containing all of $\mathcal{V}$. Let

$$\kappa(\mathcal{T}) = \prod_{(i,j)\in\mathcal{T}} \kappa_{ij}.$$

(b) For a fixed vertex $i$, a ***spanning tree rooted at*** $i$ is a spanning tree of the connected component of $i$, such that its unique sink is $i$. Let $\mathfrak{T}_i$ be the set of all spanning trees rooted at $i$.

(c) The ***tree constant*** of the vertex $i$ is the polynomial

$$K_i = \sum_{\mathcal{T} \in \mathfrak{T}_i} \kappa(\mathcal{T}). \tag{1.13}$$

We take $\mathcal{G}$ to be a reaction network without the information about the complexes, and $\kappa_{ij}$ to be the rate constants. The formula for the tree constants is not as important as the fact that there is an explicit way to compute them, and that each $K_i$ is a polynomial in the labels $\kappa_{ij}$. Indeed, Kirchoff's Matrix Theorem states that $K_i$ is equal to the determinant of $M_i$, where $M_i$ is obtained by deleting the $i$th row and $i$th column from $\mathbf{A}_{\boldsymbol{\kappa}}$ [48].


Figure 1.8: A graph with two connected components, whose rooted spanning trees are shown in Figure 1.9. See Example 1.4.6 for detail.

**Example 1.4.6.** Consider the graph with two connected components in Figure 1.8, whose rooted spanning trees are shown in Figure 1.9. For example, there are two spanning trees rooted at the vertex 1. As the figure shows, the more edges are present, the more rooted spanning trees there are. For example, by Cayley's formula, a complete graph with $m$ nodes has $m^{m-2}$ spanning trees [25]. More generally in a directed graph, the number of spanning trees rooted at the vertex $i$ is the determinant of $M_i$, where $M_i$ is obtained by deleting the $i$th row and $i$th column from $\mathbf{A}_{\boldsymbol{\kappa}}$, with $\boldsymbol{\kappa} = (1)_{ij}$ [26].

Let $\kappa_{ij}$ be the label on the edge $(i, j)$ in the graph of Figure 1.8. The tree constants are

$$K_1 = \kappa_{21}\kappa_{31} + \kappa_{23}\kappa_{31}, \quad K_2 = \kappa_{31}\kappa_{12}, \quad K_3 = \kappa_{12}\kappa_{23},$$
$$K_4 = \kappa_{56}\kappa_{67}\kappa_{74}, \quad K_5 = \kappa_{67}\kappa_{74}\kappa_{45}, \quad K_7 = \kappa_{45}\kappa_{56}\kappa_{67} + \kappa_{46}\kappa_{56}\kappa_{67},$$
$$K_6 = \kappa_{45}\kappa_{56}\kappa_{76} + \kappa_{46}\kappa_{56}\kappa_{76} + \kappa_{74}\kappa_{46}\kappa_{56} + \kappa_{74}\kappa_{45}\kappa_{56}.$$

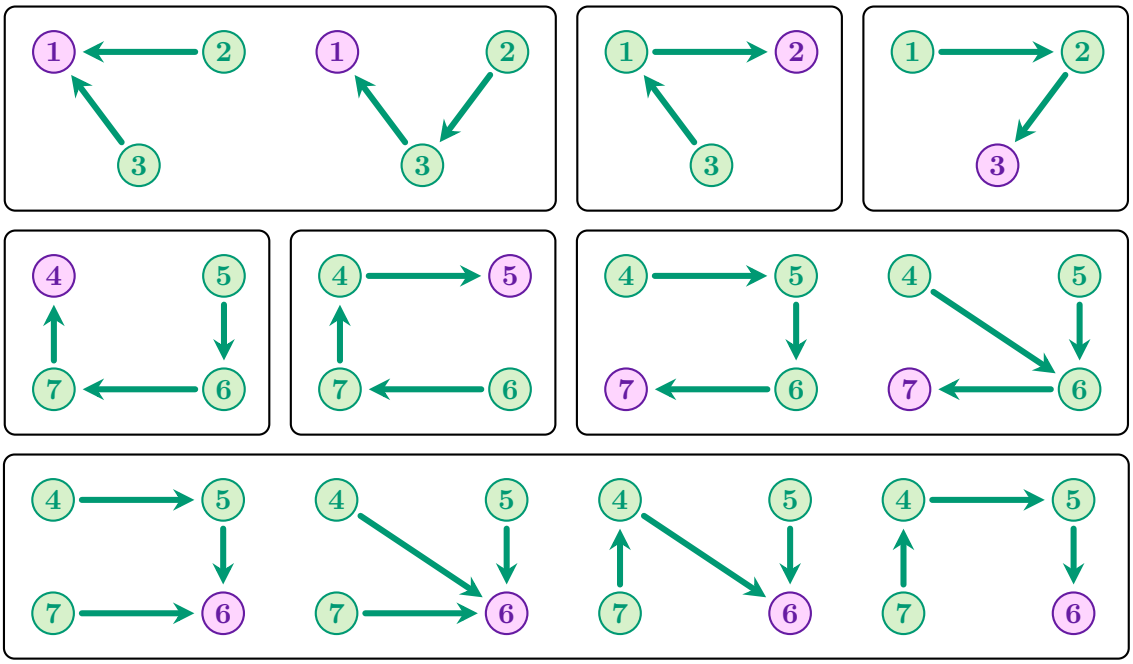


Figure 1.9: The rooted spanning trees of the graph in Figure 1.8.

The tree constants play a prominent role in the kernel of the Laplacian matrix $\mathbf{A}_{\boldsymbol{\kappa}}$, which is supported on the terminal strongly connected components of a reaction network $G$. Moreover, $\dim(\mathbf{A}_{\boldsymbol{\kappa}})$ is equal to the number of terminal strongly connected components. The following result and example are drawn from [35, 61, 73, 74, 83, 103, 108].

**Theorem 1.4.7.** *Let $(G, \boldsymbol{\kappa})$ be a mass-action system with Laplacian matrix $\mathbf{A}_{\boldsymbol{\kappa}}$. Suppose $T_1$, $T_2, \ldots, T_t$ are the terminal strongly connected components, and let $V_j \subseteq V$ be the subset of complexes in a terminal strongly connected component. For each terminal strongly connected component $T_j$, define a vector in $\mathbb{R}^m$ by*

$$\boldsymbol{\chi}_j(i) = \begin{cases} K_i & \text{if } \boldsymbol{y}_i \in V_j \\ 0 & \text{otherwise} \end{cases} \tag{1.14}$$

*where $K_i$ is the tree constant of vertex $i$ as defined in* (1.13)*. Then $\{\boldsymbol{\chi}_1, \boldsymbol{\chi}_2, \ldots, \boldsymbol{\chi}_t\}$ is a basis for* $\ker \mathbf{A}_{\boldsymbol{\kappa}}$.

If the network is weakly reversible, then every connected component is strongly connected and terminal. Hence the above, when applied to a weakly reversible mass-action system, can be used to determine when a system is complex-balancing.

**Example 1.4.8.** With respect to the network in Figure 1.8, the kernel of $\mathbf{A}_{\boldsymbol{\kappa}}$ is spanned by

$$\Big(K_1, K_2, K_3, 0, 0, 0, 0\Big)^\top \quad \text{and} \quad \Big(0, 0, 0, K_4, K_5, K_6, K_7\Big)^\top,$$

where the constants $K_i$ are given in Example 1.4.6. The vector $\boldsymbol{x}^{\mathbf{Y}}$ is in $\ker \mathbf{A}_{\boldsymbol{\kappa}}$ if and only if it is orthogonal to a basis for $(\ker \mathbf{A}_{\boldsymbol{\kappa}})^\perp$. A basis for $(\ker \mathbf{A}_{\boldsymbol{\kappa}})^\perp$ is

$$\Big(-K_2, K_1, 0, 0, 0, 0, 0\Big)^\top, \quad \Big(0, -K_3, K_2, 0, 0, 0, 0, 0\Big)^\top,$$
$$\Big(0, 0, 0, -K_5, K_4, 0, 0\Big)^\top, \quad \Big(0, 0, 0, 0, -K_6, K_5, 0\Big)^\top, \quad \Big(0, 0, 0, 0, 0, -K_7, K_6\Big)^\top.$$

So $\boldsymbol{x}^{\mathbf{Y}} \in \ker \mathbf{A}_{\boldsymbol{\kappa}}$ if and only if

$$K_1\boldsymbol{x}^{\boldsymbol{y}_2} - K_2\boldsymbol{x}^{\boldsymbol{y}_1} = 0, \quad K_2\boldsymbol{x}^{\boldsymbol{y}_3} - K_3\boldsymbol{x}^{\boldsymbol{y}_2} = 0,$$
$$K_4\boldsymbol{x}^{\boldsymbol{y}_5} - K_5\boldsymbol{x}^{\boldsymbol{y}_4} = 0, \quad K_5\boldsymbol{x}^{\boldsymbol{y}_6} - K_6\boldsymbol{x}^{\boldsymbol{y}_5} = 0, \quad K_6\boldsymbol{x}^{\boldsymbol{y}_7} - K_7\boldsymbol{x}^{\boldsymbol{y}_6} = 0.$$

This calculation generalizes to any weakly reversible mass-action system. In other words, when the network is weakly reversible, $\mathbf{A}_{\boldsymbol{\kappa}}\boldsymbol{x}^{\mathbf{Y}} = \mathbf{0}$ if and only if for every complexes $\boldsymbol{y}_i$ and $\boldsymbol{y}_j$ in the same connected component,

$$K_i\boldsymbol{x}^{\boldsymbol{y}_j} - K_j\boldsymbol{x}^{\boldsymbol{y}_i} = 0, \tag{1.15}$$

where $K_i$ is the tree constant of the vertex $i$.

Indeed, now we see why complex-balanced systems are also called *toric systems*; they are characterized by the binomials $K_i\boldsymbol{x}^{\boldsymbol{y}_j} - K_j\boldsymbol{x}^{\boldsymbol{y}_i}$. The authors of [35] used these binomials to define the *toric balancing ideal* of a reaction network. They also eliminated the state variables

$\boldsymbol{x}$ from the binomials[13], and obtain a necessary and sufficient condition on the rate constants for the system to be complex-balanced. The number of polynomial equations on the tree constants (hence the number of polynomial equations on the rate constants) is given by the network's *deficiency*. This important invariant measures how far is the set of positive steady state from being complex-balanced.

**Definition 1.4.9.** Let $G = (V, E)$ be a reaction network with $\ell$ connected components and let $S$ be its stoichiometric subspace. The ***deficiency*** of the network is

$$\delta = |V| - \ell - \dim S. \tag{1.16}$$

Equivalently, $\delta = \dim(\ker \mathbf{Y} \cap \operatorname{ran} \mathbf{I}_E)$, where $\mathbf{I}_E$ is the incidence matrix of $G$ [83].

**Example 1.4.10.** Consider the mass-action system $(G, \boldsymbol{\kappa})$ given by

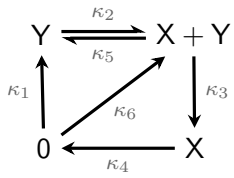


where the rate constants $k_i > 0$ are not yet specified. The network has $|V| = 4$ complexes, $\ell = 1$ connected component, and $S = \mathbb{R}^2$, so $\delta = 1$. The system is complex-balanced if and only if the rate constants satisfy some algebraic constraints, which we now derive.

A steady state $(x, y) > \mathbf{0}$ is complex-balanced if and only if

$$\kappa_1 + \kappa_6 = \kappa_4 x, \quad \kappa_2 y = \kappa_1 + \kappa_5 xy, \quad (\kappa_3 + \kappa_5)xy = \kappa_6 + \kappa_2 y, \quad \text{and} \quad \kappa_4 x = \kappa_3 xy.$$

Using the first and last equations rewrite the state variables $x$, $y$ as polynomials of the rate

[13] This is accomplished using Gröbner basis, or if the example is small, by hand.

constants, and subbing these into the second equation leads to

$$\kappa_1\kappa_3 + \kappa_1\kappa_5 + \kappa_5\kappa_6 = \kappa_2\kappa_4,$$

which is necessary and sufficient for the system to be complex-balanced. Slices of this variety are shown in Figure 1.10.

For a different approach, order the vertices as $\boldsymbol{y}_1 = 0$, $\boldsymbol{y}_2 = \mathsf{Y}$, $\boldsymbol{y}_3 = \mathsf{X}+\mathsf{Y}$, and $\boldsymbol{y}_4 = \mathsf{X}$. The characterizing binomial equations for complex-balancing are $K_1 y = K_2$, $K_2 xy = K_3 y$ and $K_3 x = K_4 xy$, from which we can easily derive $K_1 K_4 = K_2 K_3$, where $K_i$ is the tree constant of the complex $\boldsymbol{y}_i$. Given that the tree constants are polynomials in the rate constants, the resulting polynomial could be complicated, e.g.,

$$[\kappa_2\kappa_4(\kappa_1 + \kappa_6)]\kappa_2\kappa_3^2 = [\kappa_2\kappa_4(\kappa_1 + \kappa_6)]\kappa_4(\kappa_1\kappa_3 + \kappa_5(\kappa_1 + \kappa_6)).$$

After simplification, $\kappa_2\kappa_3^2 = \kappa_4(\kappa_1\kappa_3 + \kappa_5(\kappa_1 + \kappa_6))$, which still looks quite different from the condition derived directly from the complex-balancing condition (1.10), even though each of the two polynomial equations is necessary and sufficient for complex-balancing, since $\delta = 1$ [35].

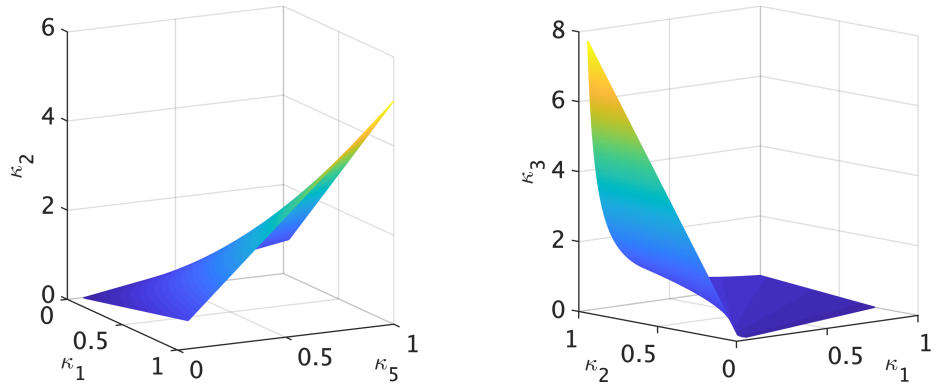


(a) (b)

Figure 1.10: Slices in parameter space for when the mass-action system in Example 1.4.10 is complex-balanced. Parameters chosen in (a) are $\kappa_3 = 0.1$, $\kappa_4 = 0.25$, $\kappa_6 = 0.15$; and in (b) $\kappa_5 = \kappa_6 = 0.1$, $\kappa_4 = 5$.

Geometrically, the deficiency $\delta$ measures the linear independence of the stoichiometric subspaces, as well as the affine independence of the complexes within each connected component [59, Chapter 6.4].

**Theorem 1.4.11.** *A reaction network has deficiency zero if and only if*

(a) *the complexes within each connected component are affinely independent, and*

(b) *the stoichiometric spaces of the connected components are linearly independent.*

*Proof.* A description of the notation is longer than the proof. Let $G_1$, $G_2, \ldots, G_\ell$ be the connected components of the reaction network, and $S_i$ the stoichiometric subspace of the $i$th connected component, i.e., it is the span of reaction vectors in the $i$th connected component. Finally let $\delta_i = |V_i| - 1 - \dim S_i$ be the deficiency of the $i$th connected component. Then

$$\begin{aligned}\delta &= |V| - \ell - \dim S \\ &= \sum_{i=1}^{\ell} (|V_i| - 1 - \dim S_i) + \sum_{i=1}^{\ell} \dim S_i - \dim S \\ &= \sum_{i=1}^{\ell} \delta_i + \sum_{i=1}^{\ell} \dim S_i - \dim S \geq \sum_{i=1}^{\ell} \delta_i,\end{aligned}$$

with equality if and only if the vector spaces $S_1$, $S_2, \ldots, S_\ell$ are linearly independent. Moreover, $\delta = 0$ if and only if $\delta_i = 0$ for all $i$, which implies that $\dim S_i = |V_i| - 1$, i.e., the complexes within any connected component are affinely independent. □

Deficiency zero networks not only have a nice geometric interpretation, but also there is no condition on the rate constants for the system to be complex-balanced. This is the well-known **Deficiency Zero Theorem** [56, 57, 60, 76, 78].

**Theorem 1.4.12.** *Let $G$ be a weakly reversible reaction network. The mass-action system $(G, \boldsymbol{\kappa})$ is complex-balancing for all choice of rate constants $\boldsymbol{\kappa} > \mathbf{0}$ if and only if the deficiency is $\delta = 0$.*

There is also the Deficiency One Theorem [57]. More recently, we relax the algebraic conditions on the rate constants while keeping the same dynamics as those of complex-balanced systems. We search for possible network structures (along with their rate constants) that would give rise to the same associated system of ODEs; these new mass-action systems are said to be *dynamically equivalent* to the original one [39, 40]. See Section 2.1 for more detail.

As a nod to the efforts characterizing rate constants needed for equilibrium, we mention the Wegscheider condition for detailed-balancing [109,133]. A more nuanced algebraic condition for detailed-balancing can be found in [58].

Let $G$ be a reversible network with $p$ reversible pairs of edges, i.e., the network has $2p$ reactions. Choose a forward direction for each reversible pair and let $\kappa_{r+}$ be its rate constant; let $\kappa_{r-}$ be the rate constant of the backward direction. Let $\mathbf{\Gamma'} \in \mathbb{R}^{n\times p}$ be the matrix whose columns are the reaction vector of the forward directions. The ratio $\kappa_{r+}/\kappa_{r-}$ is the equilibrium constant from thermodynamics, appearing, for example, in balancing Gibbs free energy[14].

**Theorem 1.4.13** (Wegscheider Condition)**.** *The reversible mass-action system* $(G, \boldsymbol{\kappa})$ *is detailed-balanced if and only if every* $\boldsymbol{\gamma} \in \ker \mathbf{\Gamma'} \subseteq \mathbb{R}^{n\times p}$ *satisfies the Wegscheider condition*

$$\prod_{r=1}^{p} (\kappa_{r+})^{\gamma_r} = \prod_{r=1}^{p} (\kappa_{r-})^{\gamma_r}.$$

*Proof.* For a fixed reversible pair $\boldsymbol{y}_r \rightleftharpoons \boldsymbol{y}'_r$, whose rate constants are $\kappa_{r+}$ and $\kappa_{r-}$ for the forward and backward reaction respectively, detailed-balancing occurs if and only if $\kappa_{r+}\boldsymbol{x}^{\boldsymbol{y}_r} = \kappa_{r-}\boldsymbol{x}^{\boldsymbol{y}'_r}$. Equivalently,

$$\ln\left(\frac{\kappa_{r+}}{\kappa_{r-}}\right) = \ln \boldsymbol{x}^{\boldsymbol{y}'_r - \boldsymbol{y}_r} = \langle \boldsymbol{y}'_r - \boldsymbol{y}_r, \ln \boldsymbol{x}\rangle,$$

[14] Gibbs free energy is used if temperature and pressure are constant. Other free energies are used for different environmental conditions.

where $\langle \cdot, \cdot \rangle$ is the standard inner product of $\mathbb{R}^n$. Collecting these terms into a vector leads to

$$\ln\left(\frac{\kappa_{r+}}{\kappa_{r-}}\right)_r = \boldsymbol{\Gamma}'^{\top} \ln \boldsymbol{x}.$$

In other words, $\ln(\kappa_{r+}/\kappa_{r-})$ lies in $\operatorname{ran}(\boldsymbol{\Gamma}'^{\top})$. Since $\operatorname{ran}(\boldsymbol{\Gamma}'^{\top}) = (\ker \boldsymbol{\Gamma}')^{\perp}$, the linear system is solvable, i.e., a solution $\ln \boldsymbol{x}$ exists, if and only if for every $\boldsymbol{\gamma} \in \ker \boldsymbol{\Gamma}'$, we have

$$0 = \left\langle \ln\left(\frac{\kappa_{r+}}{\kappa_{r-}}\right)_r, \boldsymbol{\gamma} \right\rangle = \sum_{r=1}^{p} \gamma_r \ln\left(\frac{\kappa_{r+}}{\kappa_{r-}}\right) = \prod_{r=1}^{p} \ln\left(\frac{\kappa_{r+}}{\kappa_{r-}}\right)^{\gamma_r}.$$

Rearranging this equation gives the Wegscheider condition. □

### 1.4.2 Dynamical properties of complex-balanced systems

One reason why complex-balanced (and detailed-balanced) systems are fascinating is their stability: admitting a Lyapunov function, linear stability; conjectured to be globally stable, *persistent*, and *permanent* (Definition 1.4.19). As is convention, when we speak about a steady state's stability, we refer to its stability relative to its stoichiometric compatibility class.

Most of what will be discussed in this section are well-known within the *Chemical Reaction Network Theory* community. Arguably, much of it dates back to Horn and Jackson's seminal paper [78]. As such, our aim is to review the most important results and conjectures. Proofs of these results can be found in [45, 59, 73, 78, 82, 122].

We introduced in Theorem 1.4.3 the Lyapunov function

$$L(\boldsymbol{x}) = \sum_{i=1}^{n} x_i \left(\ln x_i - \ln x_i^* - 1\right) + x_i^*, \tag{1.17}$$

which Horn and Jackson used to show asymptotic stability of a complex-balanced steady state [78]. Shown in Figure 1.11 are level sets of $L(\boldsymbol{x})$ in various dimensions. Horn and Jackson called $L(\boldsymbol{x})$ a pseudo-Helmholtz function, acknowledging that it plays a similar role as

the Helmholtz free energy[15] in thermodynamics. Horn and Jackson in [78] were interested in systems that display properties expected at thermodynamic equilibrium, regardless of whether or not the system is at equilibrium.

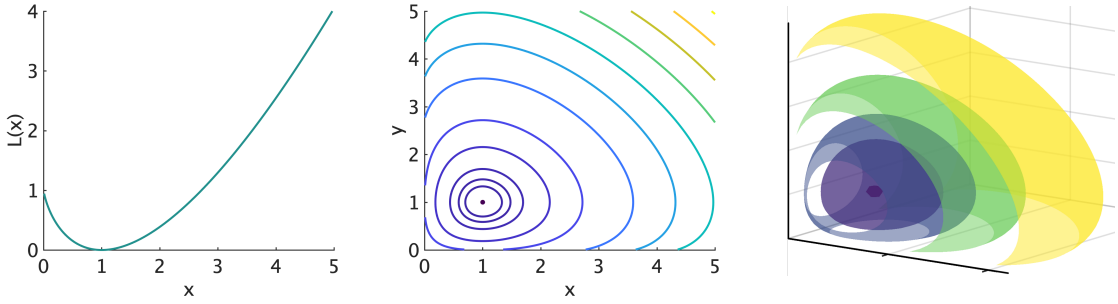


(a) (b) (c)

Figure 1.11: The Horn–Jackson Lyapunov function $L(\boldsymbol{x})$ in (1.17): (a) its graph on $\mathbb{R}_>$, (b) level sets on $\mathbb{R}^2_>$ and (c) level sets on $\mathbb{R}^3_>$. In (b) and (c), some level sets intersect the coordinate faces.

As Figures 1.11(b) and 1.11(c) illustrate, some of the level sets of $L(\boldsymbol{x})$ on $\mathbb{R}^2_>$ and $\mathbb{R}^3_>$ intersect the faces of the state space. Nonetheless, $L(\boldsymbol{x})$ is a strict Lyapunov function on $\mathbb{R}^n_>$ and also within each stoichiometric compatibility class. Horn and Jackson called a mass-action system *quasi-thermodynamic* if the system is *quasi-thermostatic* (i.e., toric, see Section 1.4.1) and the inequality (1.18) holds [78]. The inequality $A(\ln B - \ln A) \leq B - A$ is critical to the proof; for a full proof of the following theorem, see [3, 78].

**Theorem 1.4.14.** *Let $\dot{\boldsymbol{x}} = \boldsymbol{f}(\boldsymbol{x})$ be a complex-balanced system, and let $\boldsymbol{x}^*$ be a complex-balanced steady state. For any $\boldsymbol{x} \in (\boldsymbol{x}^* + S)_>$, we have*

$$\nabla L(\boldsymbol{x}) \cdot \boldsymbol{f}(\boldsymbol{x}) \leq 0, \tag{1.18}$$

*with equality if and only if $\boldsymbol{x} = \boldsymbol{x}^*$. In particular, for any trajectory $\boldsymbol{x}(t) > \boldsymbol{0}$, we have $\frac{d}{dt}L(\boldsymbol{x}(t)) \leq 0$, with equality at the complex-balanced steady state of the stoichiometric compatibility class.*

[15] The Helmholtz free energy is useful when temperature and volume are held constant. Gibbs free energy is used when temperature and pressure are constant. The form of $L(\boldsymbol{x})$ also appears as the entropy function; for example, see Boltzmann's work on the $H$-theorem [13].

Not only is a complex-balanced steady state asymptotically stable within its stoichiometric compatibility class (via the Horn–Jackson Lyapunov function), it is *linearly stable*. Indeed, a complex-balanced steady state is what is known as *D-stable* — when the Jacobian matrix is stable even after multiplying by arbitrary positive diagonal matrices [19]. We will not concern ourselves with D-stability or the slightly different notion of *diagonal stability*, but instead refer the reader to [19].

For a linear system $\dot{\boldsymbol{x}} = \mathbf{J}\boldsymbol{x}$, its *stable* (respective *unstable* and *centre*) subspace is the span of eigenspaces whose eigenvalues have negative (respectively positive and zero) real parts. Suppose $\dot{\boldsymbol{x}} = \mathbf{J}\boldsymbol{x}$ arises as the linearization of a non-linear system $\dot{\boldsymbol{x}} = \boldsymbol{f}(\boldsymbol{x})$ about a *hyperbolic* steady state $\boldsymbol{x}^*$, i.e., the centre subspace of the linearized system is trivial. The stable (respectively unstable) subspace of $\dot{\boldsymbol{x}} = \mathbf{J}\boldsymbol{x}$ is tangent to the stable (respectively unstable) manifold of $\dot{\boldsymbol{x}} = \boldsymbol{f}(\boldsymbol{x})$. Moreover, the Hartman–Grobman Theorem guarantees that $\dot{\boldsymbol{x}} = \boldsymbol{f}(\boldsymbol{x})$ and $\dot{\boldsymbol{x}} = \mathbf{J}\boldsymbol{x}$ share the same qualitative dynamics [113]. Let $S = \operatorname{span}\{\boldsymbol{f}(\boldsymbol{x}) : \boldsymbol{x} \in \mathbb{R}^n_>\}$; unsurprisingly, if $S = \operatorname{ran}\mathbf{J}$ coincides with the stable subspace, then trajectories that start near the steady state $\boldsymbol{x}^*$ exponentially converge to it.

For a complex-balanced system, the stable manifold coincides with the stoichiometric subspace $S$. For a proof of the following theorem, see [19, 122].

**Theorem 1.4.15.** *Let $\dot{\boldsymbol{x}} = \boldsymbol{f}(\boldsymbol{x})$ be a complex-balanced system, with complex-balanced steady state $\boldsymbol{x}^*$. Then the linearized system $\dot{\boldsymbol{x}} = \mathbf{J}\boldsymbol{x}$ about $\boldsymbol{x}^*$ has eigenvalues with non-positive real parts. Moreover, the stable subspace coincides with the stoichiometric subspace $S$, and the centre subspace is $\operatorname{diag}(\boldsymbol{x}^*)S^\perp$. In particular, $\boldsymbol{x}^*$ is linearly stable within its stoichiometric compatibility class.*

When discussing the stability of complex-balanced systems, one cannot avoid the *Global Attractor Conjecture* and the related *Persistence* and *Permanence Conjectures*. In 1974, Horn identified that the Horn–Jackson Lyapunov function $L(\boldsymbol{x})$ is not sufficient to prevent trajectories from converging to a face of $\mathbb{R}^n_>$; nonetheless he conjectured that indeed a complex-balanced steady state is globally attracting within its stoichiometric compatibility class [77].

The conjecture was christianed in [35].

**Conjecture 1.4.16** (**Global Attractor Conjecture** [35])**.** *For a complex-balanced system, any positive steady state is a global attractor within its stoichiometric compatibility class.*

This is one of the most important open problems in the field. Many special cases have been proved, with some of the more well-known and recent ones being:

- networks with a single connected component [2, 17];
- systems in $\mathbb{R}^3_>$ [45];
- networks whose stoichiometric subspace has $\dim S = 3$ [112];
- *strongly endotactic* networks [4, 69].

A proof for the general case has been proposed [30, 31]. Most of the results above attempt to prove the stronger *Persistence Conjectures*, which claims that trajectories do not converge to the faces of $\mathbb{R}^n_>$, highlighting the problem the Horn–Jackson Lyapunov function has near the boundary of the state space.

We formally introduce two more network structures that captures the notion of "inward pointing" [45, 69, 85]. Some examples are shown in Figure 1.12.

**Definition 1.4.17.** Let $G = (V, E)$ be a reaction network.

(a) It is said to be ***endotactic*** if, for every $\boldsymbol{w} \in \mathbb{R}^n$ and any $\boldsymbol{y}_i \to \boldsymbol{y}'_i \in E$ with $\langle \boldsymbol{w},\, \boldsymbol{y}'_i - \boldsymbol{y}_i \rangle < 0$, there exists another reaction $\boldsymbol{y}_p \to \boldsymbol{y}'_p \in E$ such that $\langle \boldsymbol{w},\, \boldsymbol{y}'_p - \boldsymbol{y}_p \rangle > 0$ and $\langle \boldsymbol{w},\, \boldsymbol{y}_p - \boldsymbol{y}_i \rangle < 0$.

(b) A reaction network is ***strongly endotactic*** if it is endotactic and the reaction $\boldsymbol{y}_p \to \boldsymbol{y}'_p$ can be chosen such that $\langle \boldsymbol{w},\, \boldsymbol{y}_p - \boldsymbol{y} \rangle \leq 0$ for every source complex $\boldsymbol{y}$.

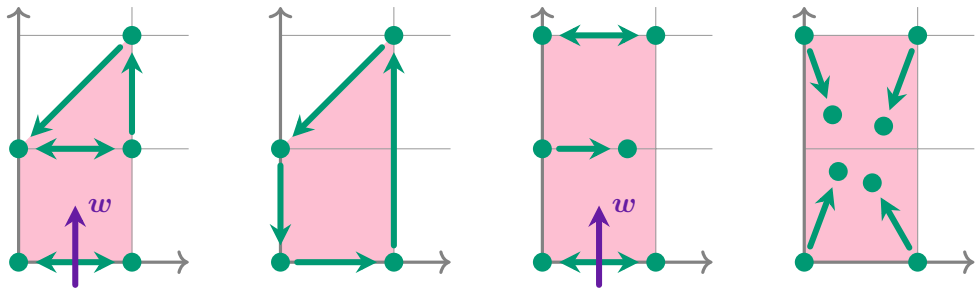


(a) (b) (c) (d)

Figure 1.12: Networks that are (a) weakly reversible and endotactic; (b) weakly reversible, endotactic and strongly endotactic; (c) endotactic; (d) endotactic and strongly endotactic. In (a) and (c), labelled is the direction $\boldsymbol{w}$ for which the network fails the strongly endotactic condition.

For technical reasons, instead of working with complex-balanced systems (with fixed rate constants), attempts at the Global Attractor and Persistence Conjectures worked with weakly reversible systems whose rate constants are allowed to vary. These are called *variable-$\boldsymbol{\kappa}$* systems [30, 31, 45], or systems with *bounded kinetics* [2, 17].

**Definition 1.4.18.** Let $G = (V, E)$ be a reaction network, and fix $0 < \varepsilon < 1$. A ***variable-$\boldsymbol{\kappa}$ mass-action system*** $(G, \boldsymbol{\kappa}(t))$ is associated to the non-autonomous system of ODEs on $\mathbb{R}^n_{\geq}$

$$\frac{d\boldsymbol{x}}{dt} = \sum_{(i,j)\in E} \kappa_{ij}(t)\boldsymbol{x}^{\boldsymbol{y}_i}\left(\boldsymbol{y}_j - \boldsymbol{y}_i\right), \tag{1.19}$$

where $\varepsilon \leq \kappa_{ij}(t) \leq 1/\varepsilon$ for all $t \geq 0$.

In a nutshell, persistence occurs when trajectories always stay away from the faces of $\mathbb{R}^n_{>}$, while permanence implies there is a globally attracting compact set within a forward invariant set.

**Definition 1.4.19.** Let $\dot{\boldsymbol{x}} = \boldsymbol{f}(\boldsymbol{x}, t)$ be a system of ODEs on $\mathbb{R}^n_{>}$.

(a) It is ***persistent*** if for any initial condition $\boldsymbol{x}(0) \in \mathbb{R}^n_{>}$, the solution $\boldsymbol{x}(t)$ satisfies $\liminf_{t\to\infty} x_i(t) > 0$ for all $i = 1,, 2, \ldots, n$.

(b) It is ***permanent on a forward invariant set*** $U \subseteq \mathbb{R}^n_>$ if there exists a compact set $K \subseteq U$ such that for any initial condition $\boldsymbol{x}(0) \in U$, the solution $\boldsymbol{x}(t)$ is eventually in $K$, i.e., there exists $t_0 \geq 0$ such that for all $t \geq t_0$ we have $\boldsymbol{x}(t) \in K$.

For a mass-action system (autonomous or variable-$\boldsymbol{\kappa}$), we say it is ***permanent*** if it is permanent on every stoichiometric compatibility class. In Section 2.3, we prove that the *Extended Permanence Conjecture* implies not only that complex-balanced systems are globally stable, but that the system is globally stable even after its rate constants have been perturbed. Since for networks with positive deficiencies, complex-balancing is sensitive to the choice of rate constants, the result in Section 2.3 proves global stability for a family of mass-action systems.

**Conjecture 1.4.20** (**Persistence Conjecture** [45, 57])**.**
*A weakly reversible mass-action system is persistent.*

**Conjecture 1.4.21** (**Permanece Conjecture** [45])**.**
*A weakly reversible mass-action system is permanent.*

**Conjecture 1.4.22** (**Persistence Conjecture for variable-$\boldsymbol{\kappa}$ systems**)**.**
*A weakly reversible variable-$\boldsymbol{\kappa}$ system is persistent.*

**Conjecture 1.4.23** (**Permanece Conjecture for variable-$\boldsymbol{\kappa}$ systems**)**.**
*A weakly reversible variable-$\boldsymbol{\kappa}$ system is permanent.*

**Conjecture 1.4.24** (**Extended Persistence Conjecture** [45])**.**
*An endotactic variable-$\boldsymbol{\kappa}$ mass-action system is persistent.*

**Conjecture 1.4.25** (**Extended Permanence Conjecture** [45])**.**
*An endotactic variable-$\boldsymbol{\kappa}$ mass-action system is permanent.*

Clearly there are more conjectures with slightly different assumptions. For example, one can study instead endotactic mass-action system with constant rate constants. Let v-$\boldsymbol{\kappa}$ be short for variable-$\boldsymbol{\kappa}$. The above conjectures are logically related in the following way.

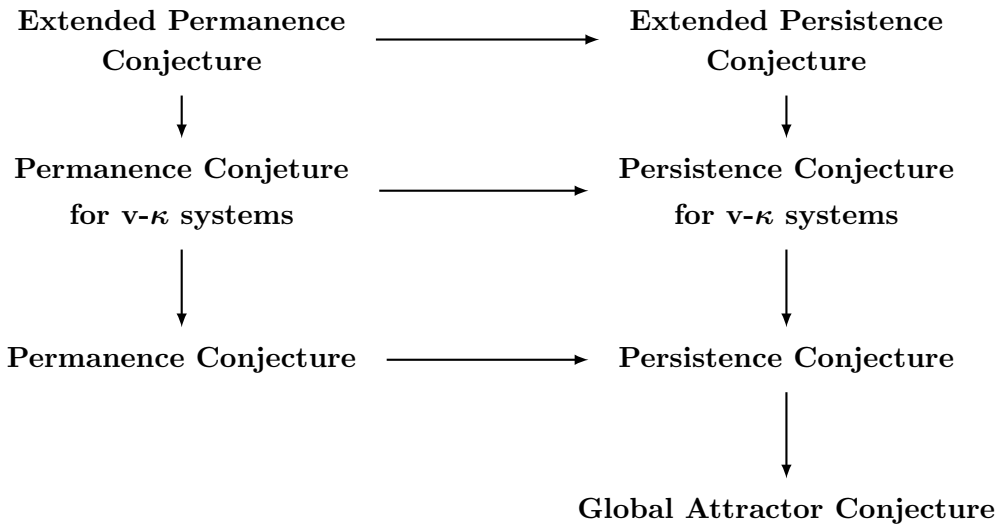

# Chapter 2

# Beyond deficiency theory

In this chapter, we extend some global stability results of mass-action systems, particularly those of detailed-balancing and complex-balancing, in two directions. First, we introduce the notion of *dynamical equivalence*, and how a system that is not weakly reversible can be dynamically equivalent to a complex-balanced or detailed-balanced one, thus enjoying all of their nice dynamical properties. In Section 2.1, we characterize all single-target networks under mass-action kinetics based on the geometry of the network. These networks — possibly with high deficiencies — either have no positive steady state for any rate constants, or are dynamically equivalent to a detailed-balanced system for any rate constant. Second, we introduce the notion of *robust permanence*, and prove in Section 2.3 that even when the rate constants of a complex-balanced system have been perturbed, the system is still globally stable as long as the complex-balanced system is robustly permanent.

## 2.1 Dynamical equivalence

The associated dynamical system (1.4) of a mass-action system $(G, \boldsymbol{\kappa})$ is uniquely defined; however, different reaction networks can give rise to the same system of ODEs under mass-action kinetics [39, 46, 127]. When studying mass-action kinetics, it is the associated system of ODEs that is of interest. *Dynamical equivalence* occurs when different mass-action systems (networks along with their rate constants) have the same differential equations. Regardless of the initial network structure, if a system is dynamically equivalent to a complex-balanced one, then it shares the same algebraic and dynamical properties expected of one [23,39,40]. In what follows, we adopt the convention that the empty sum is $\mathbf{0}$, i.e., $\sum_{(i,j)\in\emptyset} \kappa_{ij}(\boldsymbol{y}_j - \boldsymbol{y}_i) = \mathbf{0}$.

**Definition 2.1.1.** Let $G = (V, E)$ and $G' = (V', E')$ be two reaction networks. We say the mass-action systems $(G, \boldsymbol{\kappa})$ and $(G', \boldsymbol{\kappa}')$ are ***dynamically equivalent*** if their associated systems of ODEs agree on all of $\mathbb{R}^n_{\geq}$. Equivalently, for all vertices[1] $\boldsymbol{y}_i \in V \cup V'$, we have

$$\sum_{(i,j)\in E} \kappa_{ij}(\boldsymbol{y}_j - \boldsymbol{y}_i) = \sum_{(i,k)\in E'} \kappa'_{ik}(\boldsymbol{y}_k - \boldsymbol{y}_i). \tag{2.1}$$

We say that $(G', \boldsymbol{\kappa}')$ is another ***realization*** of $(G, \boldsymbol{\kappa})$, or that $(G, \boldsymbol{\kappa})$ and $(G', \boldsymbol{\kappa}')$ ***realize*** the common system of ODEs.

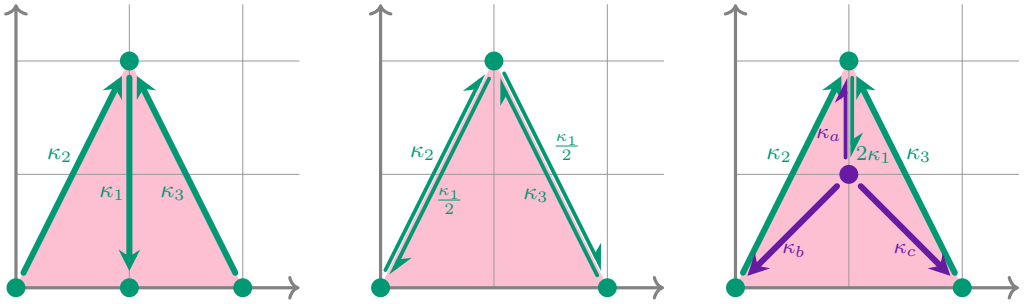


(a) (b) (c)

Figure 2.1: Three dynamically equivalent mass-action systems: (a) not weakly reversible with $\delta = 1$, (b) reversible and $\delta = 0$, (c) weakly reversible and $\delta = 1$, assuming $\kappa_b = \kappa_c$ and $\kappa_a = \kappa_b + \kappa_c$.

**Example 2.1.2.** Figure 2.1 shows three dynamically equivalent mass-action systems. In Figure 2.1(c), there is a linear relation on the rate constants $\kappa_a$, $\kappa_b$, and $\kappa_c$, namely,

$$\kappa_a \begin{pmatrix} 0 \\ 1 \end{pmatrix} + \kappa_b \begin{pmatrix} -1 \\ -1 \end{pmatrix} + \kappa_c \begin{pmatrix} 1 \\ -1 \end{pmatrix} = \begin{pmatrix} 0 \\ 0 \end{pmatrix}.$$

All three has as its associated system of ODEs

$$\frac{d\boldsymbol{x}}{dt} = \kappa_1 xy^2 \begin{pmatrix} 0 \\ -2 \end{pmatrix} + \kappa_2 \begin{pmatrix} 1 \\ 2 \end{pmatrix} + \kappa_3 x^2 \begin{pmatrix} -1 \\ 2 \end{pmatrix}.$$

[1] By which we mean either $\boldsymbol{y}_i \in V$ or $\boldsymbol{y}_i \in V'$. It suffices to check for source vertices in $V$ and $V'$.

The relation (2.1) only needs to be checked on all the *source* vertices, namely at

$$\begin{pmatrix}0\\0\end{pmatrix}, \quad \begin{pmatrix}1\\2\end{pmatrix}, \quad \begin{pmatrix}2\\0\end{pmatrix}, \quad \text{and} \quad \begin{pmatrix}1\\1\end{pmatrix}.$$

Dynamical equivalence as defined in Definition 2.1.1, which utilizes the linear independence of monomials, is truly a linear property.

**Remark 2.1.3.** The stoichiometric subspaces for dynamically equivalent systems can in principle be different. However, the two systems share the same *kinetic subspaces*, the smallest vector space containing the image of the right-hand side of the associated system of ODEs [61]. For example, in Figure 2.2 the four new reactions in Figure 2.2(b) that are not in (a) contribute the zero vector to the system of ODEs. In particular, trajectories of both systems in Figure 2.2 are confined to an affine line parallel to $(-1, 1)^\top$.

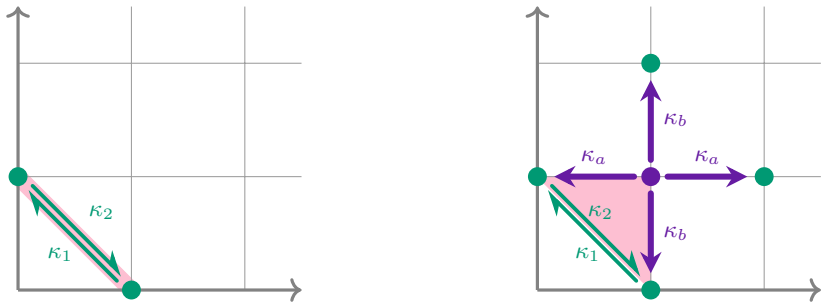


(a) (b)

Figure 2.2: Two dynamically equivalent mass-action systems with different stoichiometric subspaces and Newton polytopes.

To go from having the same associated ODEs to the linear relation (2.1), we looked at each monomial independently. For other types of kinetics, one can analogously define dynamical equivalence using Equation (2.1) if each rate function depends only on the source vertex and they are linearly independent[2]. This chapter focuses on mass-action kinetics.

[2]One can relax this further by grouping all linearly dependent rate functions to originate from one source vertex, in a sense, by replacing the Euclidean embedded graph with a directed graph, whose source vertices are labelled with (linearly independent) rate functions, and stoichiometric coefficients to define the reaction vectors.

We divorce the non-linear from the linear in the definition of dynamical equivalence. Another notion that divorces the non-linear from the linear is fluxes. The *flux* of an edge $\boldsymbol{y}_i \to \boldsymbol{y}_j$ in a mass-action system $(G, \boldsymbol{\kappa})$ is the quantity $\kappa_{ij}\boldsymbol{x}^{\boldsymbol{y}_i}$ where $\boldsymbol{x} > \mathbf{0}$ is a fixed state.

**Definition 2.1.4.** A ***flux vector*** $\boldsymbol{J} \in \mathbb{R}^E_>$ on a reaction network $G = (V, E)$ is a vector of *positive* numbers, one for each edge. We call the tuple $(G, \boldsymbol{J})$ a ***flux system***.

This idea of fluxes on a reaction network may be familiar to anyone who has worked with stoichiometric network analysis or flux balance analysis. One form of the analysis is to solve the linear equation $\boldsymbol{\Gamma J} = \mathbf{0}$, where $\boldsymbol{\Gamma}$ is the stoichiometric matrix, and the unknown vector $\boldsymbol{J}$ has nonnegative coordinates [28,110,129]. Since we are interested in relating network structure with dynamics, if $\boldsymbol{y}_i \to \boldsymbol{y}_j \in G$, we ask that $J_{ij} > 0$. Also if $\boldsymbol{y}_i \rightleftharpoons \boldsymbol{y}_j$ is a reversible reaction in $G$, then $J_{ij}$ and $J_{ji}$ are two positive components of the vector $\boldsymbol{J}$. At steady state, we do not require that detailed-balancing or $J_{ij} = J_{ji}$. A positive solution $\boldsymbol{J}$ to the equation $\boldsymbol{\Gamma J} = \mathbf{0}$ corresponds to a positive steady state $\boldsymbol{x}_0$ if $\boldsymbol{J} = \boldsymbol{\nu}(\boldsymbol{x}_0)$, where $\boldsymbol{\nu}(\boldsymbol{x}_0)$ is a vector of rate functions evaluated at $\boldsymbol{x}_0$. We define the flux analogues of positive steady state, detailed-balanced steady state, and complex-balanced steady state.

**Definition 2.1.5.** A ***steady state flux*** on a network $G = (V, E)$ is a flux vector $\boldsymbol{J} \in \mathbb{R}^E_>$ in the cone $\ker \boldsymbol{\Gamma} \cap \mathbb{R}^E_>$, i.e.,

$$\sum_{(i,j)\in E} J_{ij}(\boldsymbol{y}_j - \boldsymbol{y}_i) = \mathbf{0}. \tag{2.2}$$

A steady state flux $\boldsymbol{J} \in \mathbb{R}^E_>$ is said to be ***detailed-balanced*** if for every $\boldsymbol{y} \to \boldsymbol{y}' \in E$, we have

$$J_{ij} = J_{ji}. \tag{2.3}$$

A steady state flux $\boldsymbol{J} \in \mathbb{R}^E_>$ is said to be ***complex-balanced*** if for every $\boldsymbol{y}_i \in V$, we have

$$\sum_{(i,j)\in E} J_{ij} = \sum_{(j,i)\in E} J_{ji}. \tag{2.4}$$

As a shorthand, we refer to the flux system $(G, \boldsymbol{J})$ as detailed-balanced if $\boldsymbol{J}$ is a detailed-balanced flux on $G$. Similarly defined is a complex-balanced flux on $G$. It will be clear from context whether a complex-balanced (respectively detailed-balanced) system refers to a mass-action system or a flux system.

Indeed, the relevant concepts in a mass-action system $(G, \boldsymbol{\kappa})$ and a flux system $(G, \boldsymbol{J})$ are strongly related by taking $J_{ij} = \kappa_{ij}\boldsymbol{x}^{\boldsymbol{y}_i}$. We relate the two frameworks, with details in [39].

**Definition 2.1.6.** Two flux systems $(G, \boldsymbol{J})$ and $(G', \boldsymbol{J'})$ are ***flux equivalent*** if for every vertex $\boldsymbol{y}_i \in V \cup V'$, we have

$$\sum_{(i,j)\in E} J_{ij}(\boldsymbol{y}_j - \boldsymbol{y}_i) = \sum_{(i,k)\in E'} J'_{ik}(\boldsymbol{y}_k - \boldsymbol{y}_i). \tag{2.5}$$

We say that $(G', \boldsymbol{J'})$ is another ***realization*** of $(G, \boldsymbol{J})$.

**Proposition 2.1.7.** *Let $(G, \boldsymbol{\kappa})$ be a mass-action system, and fix a state $\boldsymbol{x} \in \mathbb{R}^n_>$. For each reaction $\boldsymbol{y}_i \to \boldsymbol{y}_j \in G$, let $J_{ij} = \kappa_{ij}\boldsymbol{x}^{\boldsymbol{y}_i}$ so $\boldsymbol{J}$ is a flux vector on $G$. For a different mass-action system $(G', \boldsymbol{\kappa}')$, define $(G', \boldsymbol{J'})$ analogously with $J'_{ij} = \kappa'_{ij}\boldsymbol{x}^{\boldsymbol{y}_i}$.*

(a) *The flux vector $\boldsymbol{J}$ is a steady state flux on $G$ if and only if $\boldsymbol{x}$ is a positive steady state of $(G, \boldsymbol{\kappa})$. Indeed, $\boldsymbol{J}$ is detailed-balanced (respectively complex-balanced) if and only if $\boldsymbol{x}$ is detailed-balanced (respectively complex-balanced) for $(G, \boldsymbol{\kappa})$.*

(b) *The mass-action systems $(G, \boldsymbol{\kappa})$, $(G', \boldsymbol{\kappa}')$ are dynamically equivalent if and only if $(G, \boldsymbol{J})$ and $(G', \boldsymbol{J'})$ are flux equivalent*[3]*.*

(c) *Suppose $(G, \boldsymbol{J})$ is flux equivalent to $(G', \boldsymbol{J'})$ where $\boldsymbol{J'}$ is detailed-balanced (respectively complex-balanced). Then $(G, \boldsymbol{\kappa})$ is dynamically equivalent to a mass-action system $(G', \boldsymbol{\kappa}')$ with detailed-balanced (respectively complex-balanced) steady state $\boldsymbol{x}$. Moreover,*

$$\kappa'_{ij} = \frac{J'_{ij}}{\boldsymbol{x}^{\boldsymbol{y}_i}} > 0.$$

[3] We only require this for $\boldsymbol{J}$ and $\boldsymbol{J'}$ defined at some state $\boldsymbol{x}$, not necessarily for all $\boldsymbol{x} \in \mathbb{R}^n_>$.

In the parallels between dynamical equivalence and flux equivalence, we see that dynamical equivalence is truly a linear property. Indeed, one might have noticed that the dynamical equivalence condition (2.1) and the flux equivalence condition (2.5) are, for all intent and purpose, the same[4]. While the non-uniqueness of reaction networks giving rise to the same dynamics pose a challenge for network identifiability, it provides a mathematical tool to analyze the dynamics of non-linear systems in general.

There are many numerical methods, mostly based on linear programming, for searching dynamically equivalent mass-action systems that have special properties [41, 86, 94, 95, 96, 116, 128], e.g., detailed-balanced, complex-balanced, reversible, weakly reversible, deficiency zero. In those works, one searches for networks after fixing a set of complexes. For every new choice of complex set, among which must be the monomials of the associated system of ODEs, there is a new linear feasibility problem. See [39] for proof of the following result, that when searching for a complex-balanced realization, it suffices to consider the set of complexes associated to the monomials appearing explicitly in system of ODEs. The theorem still holds when "complex-balanced" is replaced with "detailed-balanced", "reversible", or "weakly reversible".

**Theorem 2.1.8.** *A mass-action system $(G, \boldsymbol{\kappa})$ is dynamically equivalent to a complex-balanced system if and only if it is dynamically equivalent to a complex-balanced system $(G', \boldsymbol{\kappa}')$ that only uses the source vertices, i.e., $V' \subseteq V_s$, where $V_s \subseteq V$ is the set of source vertices of $G$.*

## 2.2 Single-target networks

We apply the notions of dynamical equivalence and fluxes to study the family of *single-target networks*. In [40], we classify all single-target networks under mass-action kinetics: those that have a globally attracting positive steady state for any choice of positive rate constants, and those that have no positive steady state for any choice of rate constants. The former occurs if and only if the target is in the relative interior of the Newton polytope.

[4] Theorem 8 of [41] used this flexibility to scale the rate constants originating from any complex of the reaction network, to prove that the sign pattern of the matrix $\mathbf{YA}_{\boldsymbol{\kappa}}$ admitting a complex-balanced realization is the same sign pattern as that admitting a weakly reversible realization.

It is not difficult to show that if every reaction vector points to the relative interior of the Newton polytope, then the mass-action system is always dynamically equivalent to a (weakly) reversible system. It follows immediately that the system has a positive steady state [16] and conjectured to be permanent [45]. In the case of a single-target network with such "inward pointing" reaction vectors, we show that under mass-action kinetics, the dynamics is essentially that of a detailed-balanced system. Single-target networks are reminiscent of *star-like networks* in [59], which are reversible networks connected at a centre vertex. These have been shown to have a unique asymptotically stable steady state within each stoichiometric compatibility class under mass-action kinetics. We show that a strongly endotactic single-target network always gives rise to a dynamically equivalent star-like system, which is detailed-balanced.

**Definition 2.2.1.** A reaction network $G = (V, E)$ is a ***single-target network*** if there exists a vertex $\boldsymbol{y}^*$ such that $V \setminus \{\boldsymbol{y}^*\}$ is the set of source vertices, and the set of edges is $E = \{\boldsymbol{y} \to \boldsymbol{y}^* : \boldsymbol{y} \neq \boldsymbol{y}^*\}$. We call $\boldsymbol{y}^*$ the ***target vertex***, while the remaining vertices are ***source vertices***.

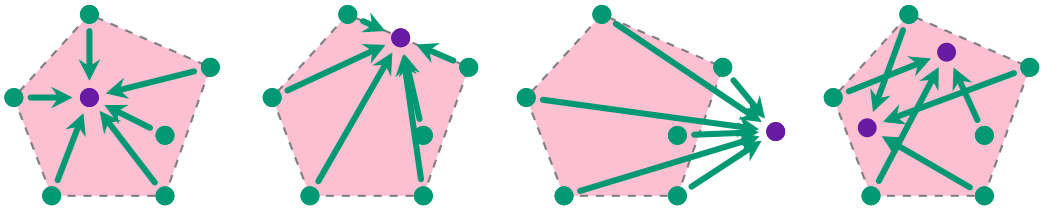


Figure 2.3: (a) A single-target network that is globally stable under mass-action kinetics. (b)–(c) Single-target networks that do not admit any positive steady state. (d) Not a single-target network.

**Example 2.2.2.** The reaction networks (a)–(c) in Figure 2.3 are single-target networks, while (d) is not a single-target network. The target vertex of (a) is in the relative interior of its Newton polytope. We show that network (a) is typical of single-target networks that gives rise to detailed-balanced dynamics, while the networks (b) and (c) have no positive steady state under any reasonable kinetics. More precisely, there can be no steady state flux on the networks (b) and (c). The deficiencies of these networks depend on the dimension $s$ of the

stoichiometric subspace. The deficiencies of the networks (a)–(c) are $\delta = 6 - s$, whille that of (d) is $\delta = 7 - s$.

The geometry of a single-target network, namely whether the target is in the relative interior of the Newton polytope, determines whether the network admits a steady state flux, a necessary condition for positive steady states under mass-action kinetics. In particular, the geometry can rule out the existence of positive steady states under any reasonable kinetics with a vector of rate functions $\boldsymbol{\nu}\colon \mathbb{R}^n_> \to \mathbb{R}^E_>$.

**Lemma 2.2.3.** *Let $G$ be a single-target network. There exists a steady state flux on $G$ if and only if the target vertex is in the relative interior of its Newton polytope.*

*Proof.* Let $\boldsymbol{y}^*$ denote the target vertex, and enumerate the source vertices $\boldsymbol{y}_1, \boldsymbol{y}_2, \ldots, \boldsymbol{y}_m$. Let $J_i$ be the flux on the edge $\boldsymbol{y}_i \to \boldsymbol{y}^*$. The flux vector $\boldsymbol{J}$ is a steady state flux if and only if

$$\sum_{i=1}^{m} J_i(\boldsymbol{y}^* - \boldsymbol{y}_i) = \boldsymbol{0}.$$

Rearranging, we see that $\boldsymbol{y}^* = \sum_i \frac{J_i}{J_T}\boldsymbol{y}_i$, where $J_T = \sum_j J_j$, and each $J_i > 0$. By definition, $\boldsymbol{y}^* \in \mathrm{Newt}(G)^\circ$. □

For a single-target network $G$ whose target vertex is outside of $\mathrm{Newt}(G)^\circ$, there can be no positive steady state under mass-action kinetics. For example, the networks in Figure 2.3(b)–(c) can have no positive steady states for any choice of rate constants under mass-action kinetics or Michaelis–Menten kinetics.

Even with the target vertex in $\mathrm{Newt}(G)^\circ$, to deduce a positive steady state from a steady state flux $\boldsymbol{J}$ involves finding a positive solution $\boldsymbol{x}$ to the nonlinear equations $J_i = k_i\boldsymbol{x}^{\boldsymbol{y}_i}$ for every $\boldsymbol{y}_i \to \boldsymbol{y}^* \in E$. Moreover, there is the entire cone of steady state flux from which to draw $\boldsymbol{J}$. We prove the existence of a steady state for such single-target mass-action systems in Corollary 2.2.5. Our proof of the existence and global stability of a positive state makes use of

Birch's Theorem [11, 78, 111] (see Theorem 1.4.4) and the Global Attractor Theorem for one connected component [2, 17] (see Conjecture 1.4.16).

As a quick reminder, Birch's Theorem states that the intersection $(\boldsymbol{x}_0+S)\cap(\boldsymbol{x}^*\circ\exp S^\perp)$ consists of exactly one point for any $\boldsymbol{x}_0$, $\boldsymbol{x}^* \in \mathbb{R}^n_>$, where $S \subseteq \mathbb{R}^n$ is any vector subspace. The Global Attractor Conjecture has been proven for when the network has one connected component; therefore any complex-balanced (or detailed-balanced) steady state $\boldsymbol{x}^* \in \mathbb{R}^n_>$ of such a system is globally stable within its stoichiometric compatibility class.

**Theorem 2.2.4.** *Let $G$ be a single-target network whose target vertex is in the relative interior of the Newton polytope. Then for any vector of rate constants $\boldsymbol{\kappa} > \mathbf{0}$, the mass-action system $(G, \boldsymbol{\kappa})$ is dynamically equivalent to a detailed-balanced system that has a single connected component.*

*Proof.* Let $\boldsymbol{y}^*$ denote the target vertex, and enumerate the source vertices $\boldsymbol{y}_1, \boldsymbol{y}_2, \ldots, \boldsymbol{y}_m$. Let $\boldsymbol{\Gamma} \in \mathbb{R}^{n\times m}$ be the stoichiometric matrix, whose $j$th column is the reaction vector $\boldsymbol{y}^* - \boldsymbol{y}_j$. Let $\kappa_j > 0$ be an arbitrary rate constant for the edge $\boldsymbol{y}_j \to \boldsymbol{y}^*$. Let $\mathrm{Newt}(G)^\circ$ be the relative interior of the Newton polytope, i.e.,

$$\mathrm{Newt}(G)^\circ = \left\{ \sum_{j=1}^m \alpha_j \boldsymbol{y}_j \ : \ \alpha_j > 0 \text{ and } \sum_{j=1}^m \alpha_j = 1 \right\}.$$

We want to prove that $(G, \boldsymbol{\kappa})$ is dynamically equivalent to a detailed-balanced system with vertex set $V_{G'} = V_G$ and edge set $E_{G'} = E_G \cup \{\boldsymbol{y}^* \to \boldsymbol{y}_j\}_{j=1}^m$. Moreover, for the original edges $\boldsymbol{y}_j \to \boldsymbol{y}^*$, we keep the same rate constants $\kappa_j$. Let $\kappa'_j$ denote the rate constant of the reversible edge $\boldsymbol{y}^* \to \boldsymbol{y}_j$, whose value is to be determined. Thus our goal is to find positive rate constants $\kappa'_j$ for each edge $\boldsymbol{y}^* \to \boldsymbol{y}_j$ and a positive state $\boldsymbol{x} \in \mathbb{R}^n_>$ satisfying two conditions:

$$\sum_{j=1}^m \kappa'_j(\boldsymbol{y}_j - \boldsymbol{y}^*) = \mathbf{0}, \tag{2.6}$$

$$\kappa_j \boldsymbol{x}^{\boldsymbol{y}_j} = \kappa'_j \boldsymbol{x}^{\boldsymbol{y}^*} \qquad \text{for all } 1 \le j \le m. \tag{2.7}$$

The first condition (2.6) ensures that the resulting system $(G', \boldsymbol{\kappa}')$ is dynamically equivalent to the original. The second ensures that $(G', \boldsymbol{\kappa}')$ is a detailed-balanced system with positive steady state $\boldsymbol{x}$. Condition (2.6) written in matrix form is $\boldsymbol{\kappa}' \in \ker \boldsymbol{\Gamma}$, where $\dim(\ker \boldsymbol{\Gamma}) = m - s$. Isolating $\kappa'_j$ in condition (2.7), we obtain

$$\kappa'_j = \kappa_j \boldsymbol{x}^{\boldsymbol{y}_j - \boldsymbol{y}^*} = \kappa_j e^{\langle \boldsymbol{y}_j - \boldsymbol{y}^*, \log \boldsymbol{x} \rangle},$$

where $\log \boldsymbol{x}$ is the component-wise logarithm. Let $\exp(\boldsymbol{z})$ denote component-wise exponentiation, and $\circ$ component-wise multiplication. Then condition (2.7) is equivalent to $\boldsymbol{\kappa}' \in \boldsymbol{\kappa} \circ \exp(\operatorname{ran} \boldsymbol{\Gamma}^\top)$. Therefore, the existence of a vector of rate constants $\boldsymbol{\kappa}' \in \mathbb{R}^m_>$ and a positive vector $\boldsymbol{x}$ for a dynamically equivalent system that is detailed-balanced is reduced to the existence of $\boldsymbol{\kappa}'$ in the intersection $\ker \boldsymbol{\Gamma} \cap (\boldsymbol{\kappa} \circ \exp(\operatorname{ran} \boldsymbol{\Gamma}^\top)) \subseteq \mathbb{R}^m_>$.

By Lemma 2.2.3, there exists a steady state flux $\boldsymbol{J}$ on $G$, i.e., $\boldsymbol{J} \in \ker \boldsymbol{\Gamma}$. Hence,

$$\ker \boldsymbol{\Gamma} \cap (\boldsymbol{\kappa} \circ \exp(\operatorname{ran} \boldsymbol{\Gamma}^\top)) = (\boldsymbol{J} + \ker \boldsymbol{\Gamma}) \cap (\boldsymbol{\kappa} \circ \exp(\ker \boldsymbol{\Gamma})^\perp),$$

which is guaranteed to be non-empty for any positive $\boldsymbol{J}$, $\boldsymbol{\kappa}$ by Birch's Theorem (Theorem 1.4.4) [11,78]. In other words, $(G, \boldsymbol{\kappa})$ is dynamically equivalent to a detailed-balanced system $(G', \boldsymbol{\kappa}')$, where $G'$ consists of the edges $\{\boldsymbol{y}_i \rightleftharpoons \boldsymbol{y}^*\}_{i=1}^m$. □

The results above classify all single-target networks under mass-action kinetics.

**Corollary 2.2.5.** *Let $G$ be a single-target network. For any vector of rate constants $\boldsymbol{\kappa} > \boldsymbol{0}$, let $(G, \boldsymbol{\kappa})$ denote the corresponding mass-action system. Then exactly one of the following holds.*

1. *For any $\boldsymbol{\kappa}$, the mass-action system $(G, \boldsymbol{\kappa})$ has no positive steady states.*

2. *For any $\boldsymbol{\kappa}$, the mass-action system $(G, \boldsymbol{\kappa})$ has exactly one positive steady state within each of its stoichiometric compatibility class. Furthermore, this steady state is globally stable within its compatibility class.*

*The latter occurs if and only if the target vertex of $G$ is in the relative interior of the Newton polytope.*

*Proof.* If $\boldsymbol{y}^* \notin \mathrm{Newt}(G)^\circ$, by Lemma 2.2.3 the network $G$ admits no positive steady state flux, i.e., $\ker \boldsymbol{\Gamma} \cap \mathbb{R}^m_> = \emptyset$; therefore, any mass-action system generated by $G$ cannot have a positive steady state. However, if $\boldsymbol{y}^* \in \mathrm{Newt}(G)^\circ$, then by Theorem 2.2.4 the mass-action system is dynamically equivalent to a detailed-balanced system with one connected component for any choice of rate constants. Since detailed-balanced systems are complex-balanced, this system, with one connected component, has within each of its stoichiometric compatibility class exactly one positive steady state, which is globally stable [2, 17]. □

## 2.3 Global stability of perturbed complex-balanced systems

In the previous section, we saw a family of networks, possibly with high deficiencies, that nonetheless enjoy all the dynamical properties of complex-balanced systems. Recall that for a reaction network with positive deficiency, the rate constants must satisfy certain polynomial constraints for the resulting mass-action system to be complex-balanced. In this section, we show under an assumption implied by the Permanence Conjecture for variable-$\boldsymbol{\kappa}$ system (Conjecture 1.4.23), the rate constants only need to approximately satisfy those algebraic equations for the system to be globally stable.

Recall from Definition 1.4.19 that a system $\dot{\boldsymbol{x}} = \boldsymbol{f}(\boldsymbol{x}, t)$ is said to be *permanent* on a forward invariant set $U \subseteq \mathbb{R}^n$ if there exists a globally attracting compact set $K \subseteq U$. In the context of mass-action system, $U$ is taken to be a certain compatibility class $U = (\boldsymbol{x}_0 + S)_>$, and the mass-action system is simply said to be permanent if it is permanent on every stoichiometric compatibility class. We define the stronger notion of ***robust permanence***, when there is a common globally attracting set for the family of systems obtained by perturbing the rate constants. Let $\|\cdot\|_\infty$ denote the maximum norm on $\mathbb{R}^n$.

**Definition 2.3.1.** Consider a system of differential equations $\dot{\boldsymbol{x}} = \boldsymbol{f}(\boldsymbol{x};\boldsymbol{\kappa})$ on $U \subseteq \mathbb{R}^n$, with unspecified parameters $\boldsymbol{\kappa} \in \mathbb{R}^R_>$. The system $\dot{\boldsymbol{x}} = \boldsymbol{f}(\boldsymbol{x};\boldsymbol{\kappa}^*)$ is ***robustly permanent*** on $U$ if there exist $\delta > 0$ and a compact set $K \subseteq U$ such that whenever $\|\boldsymbol{\kappa} - \boldsymbol{\kappa}^*\|_\infty < \delta$, the solution $\boldsymbol{x}(t)$ of $\dot{\boldsymbol{x}} = \boldsymbol{f}(\boldsymbol{x};\boldsymbol{\kappa})$ with initial condition $\boldsymbol{x}(0) \in \mathbb{R}^n_>$ is eventually in $K$, i.e., there exists some $t_0 > 0$ such that $\boldsymbol{x}(t) \in K$ for all $t \geq t_0$.

We say a mass-action system $(G, \boldsymbol{\kappa}^*)$ is ***robustly permanent*** if the associated system of ODEs $\dot{\boldsymbol{x}} = \boldsymbol{f}(\boldsymbol{x};\boldsymbol{\kappa}^*)$ is robustly permanent on every stoichiometric compatibility class. Not surprisingly, robust permanence follows from the Permanence Conjecture for variable-$\boldsymbol{\kappa}$ systems: a weakly reversible variable-$\boldsymbol{\kappa}$ mass-action system is permanent.

**Proposition 2.3.2.** *Assume the Permanence Conjecture for variable-$\boldsymbol{\kappa}$ systems. Then a complex-balanced system $(G, \boldsymbol{\kappa}^*)$ is robustly permanent.*

*Proof.* Let $(G, \boldsymbol{\kappa}^*)$ be a complex-balanced system. Choose $\varepsilon > 0$ such that $\varepsilon \leq \kappa^*_{ij} \leq 1/\varepsilon$ for every $\boldsymbol{y}_i \to \boldsymbol{y}_j \in E$. There exists $\delta > 0$ such that whenever $|\kappa_{ij} - \kappa^*_{ij}| < \delta$, we still have $\varepsilon \leq \kappa_{ij} \leq 1/\varepsilon$. Fix a stoichiometric compatibility class $(\boldsymbol{x}_0 + S)_>$. The Permanence Conjecture for variable-$\boldsymbol{\kappa}$ systems implies that there exists a compact set $K_\varepsilon \subseteq (\boldsymbol{x}_0 + S)_>$ that is globally attracting for any variable-$\boldsymbol{\kappa}$ system with parameter $\varepsilon$. Indeed, $K_\varepsilon$ is a globally attracting compact set for the mass-action system $(G, \boldsymbol{\kappa})$ for any $\|\boldsymbol{\kappa} - \boldsymbol{\kappa}^*\|_\infty < \delta$. □

**Remark 2.3.3.** Robust permanence implies permanence. If a complex-balanced system is also permanent, then each complex-balanced steady state is globally stable within its stoichiometric compatibility class. The goal is to extend this global stability to a perturbation of the system.

We now show that a robustly permanent complex-balanced system is *globally stable* even when its rate constants are perturbed. In other words, global stability for complex-balanced systems is robust. We make use of a result from [124]. Consider a system of differential equations (with parameters $\boldsymbol{\kappa}$)

$$\frac{d\boldsymbol{z}}{dt} = \boldsymbol{F}(\boldsymbol{z};\boldsymbol{\kappa}), \tag{2.8}$$

where $\boldsymbol{F} : U \times \Lambda \to \mathbb{R}^n$ with $U \subseteq \mathbb{R}^n$, $\Lambda \subseteq \mathbb{R}^R$, and the Jacobian matrix $D_{\boldsymbol{z}}\boldsymbol{F}(\boldsymbol{z};\boldsymbol{\kappa})$ is continuous on $U \times \Lambda$. Assume that solutions of the initial value problems are unique and remain in $U$ for all $t \geq 0$ and for any $\boldsymbol{\kappa} \in \Lambda$. Let $\boldsymbol{z}(t;\boldsymbol{\kappa},\boldsymbol{z}_0)$ denote the solution with initial value $\boldsymbol{z}(0) = \boldsymbol{z}_0$.

**Theorem 2.3.4** (Corollary 2.3 [124])**.** *Consider the system* (2.8)*. Assume that*

(a) $\boldsymbol{F}(\boldsymbol{z}^*;\boldsymbol{\kappa}^*) = \boldsymbol{0}$*, where* $\boldsymbol{z}^*$ *is an interior point of* $U$*;*

(b) *all eigenvalues of* $D_{\boldsymbol{z}}\boldsymbol{F}(\boldsymbol{z}^*;\boldsymbol{\kappa}^*)$ *have negative real parts; and*

(c) $\boldsymbol{z}^*$ *is globally attracting for solutions of the system* (2.8) *when* $\boldsymbol{\kappa} = \boldsymbol{\kappa}^*$

*Suppose there is a compact set* $K \subseteq U$ *such that for each* $\boldsymbol{\kappa} \in \Lambda$ *and initial condition* $\boldsymbol{z}_0 \in U$*, we have* $\boldsymbol{z}(t;\boldsymbol{\kappa},\boldsymbol{z}_0) \in K$ *for all large* $t$*. Then there exist* $\varepsilon > 0$ *and a unique point* $\hat{\boldsymbol{z}}(\boldsymbol{\kappa}) \in U$ *for all* $\|\boldsymbol{\kappa} - \boldsymbol{\kappa}^*\| < \varepsilon$ *such that* $\boldsymbol{F}(\hat{\boldsymbol{z}}(\boldsymbol{\kappa});\boldsymbol{\kappa}) = \boldsymbol{0}$ *and* $\lim_{t\to\infty} \boldsymbol{z}(t;\boldsymbol{\kappa},\boldsymbol{z}_0) = \hat{\boldsymbol{z}}(\boldsymbol{\kappa})$ *for all* $\boldsymbol{z}_0 \in U$*.*

**Remark 2.3.5.** The function $\boldsymbol{\kappa} \mapsto \hat{\boldsymbol{z}}(\boldsymbol{\kappa})$ is continuous on a neighbour of $\boldsymbol{\kappa}^*$ [124]. It follows that $\hat{\boldsymbol{z}}(\boldsymbol{\kappa})$ is an interior point of $U$.

Recall from Theorem 1.4.15 that if $\boldsymbol{x}^*$ is a complex-balanced steady state, then the stable manifold coincides with the stoichiometric compatibility class $(\boldsymbol{x}_0 + S)_>$, the unstable manifold is trivial, and the tangent space of the centre manifold is $\operatorname{diag}(\boldsymbol{x}^*)S^\perp$ [82, 122]. In other words, the dynamics along the centre manifold is stationary, and the dynamics along the stable manifold is diffeomorphic to some non-linear system

$$\frac{d\boldsymbol{Z}_s}{dt} = \tilde{\boldsymbol{F}}(\boldsymbol{Z}_s, \boldsymbol{Z}_c), \tag{2.9}$$

where $\boldsymbol{Z}_c$ the state variables of the centre manifold, determined by the initial condition (the compatibility class), stays constant for $t \geq 0$. Therefore, a change of coordinates reduces to the autonomous non-linear system (2.9) in the state variables $\boldsymbol{Z}_s$. Combining the results of [122, 124] leads to the main theorem of this section.

**Theorem 2.3.6.** *Let $(G, \boldsymbol{\kappa}^*)$ be a robustly permanent complex-balanced system. Then for every stoichiometric compatibility class, there exists $\varepsilon > 0$ such that whenever $\|\boldsymbol{\kappa} - \boldsymbol{\kappa}^*\|_\infty < \varepsilon$, the mass-action system $(G, \boldsymbol{\kappa})$ has a unique globally stable positive steady state within every stoichiometric compatibility class.*

*Proof.* For a mass-action system $(G, \boldsymbol{\kappa})$, denote its associated system by

$$\dot{\boldsymbol{x}} = \boldsymbol{f}(\boldsymbol{x}; \boldsymbol{\kappa}). \tag{2.10}$$

If $\boldsymbol{\kappa} = \boldsymbol{\kappa}^*$, the system is complex-balanced. Fix a stoichiometric compatibility compatibility class $\tilde{U} = (\boldsymbol{x}_0 + S)_>$, and let $\boldsymbol{x}^*$ be the unique linearly stable steady state in $\tilde{U}$ [78,82]. Indeed, $\boldsymbol{x}^*$ is globally stable by Remark 2.3.3. Let $\Lambda$ be the $\delta$-ball in $\mathbb{R}^R_>$ around $\boldsymbol{\kappa}^*$ that implies robust permanence, and $\tilde{K}$ be the attracting compact set in $\tilde{U}$. In other words, whenever $\|\boldsymbol{\kappa} - \boldsymbol{\kappa}^*\|_\infty < \delta$, the solution $\boldsymbol{x}(t)$ to the system (2.10) is eventually in the compact set $\tilde{K}$, for any initial condition in $\tilde{U}$.

The complex-balanced system $\dot{\boldsymbol{x}} = \boldsymbol{f}(\boldsymbol{x}; \boldsymbol{\kappa}^*)|_{\tilde{U}}$ is diffeomorphic (say via $\Phi$) to a $s$-dimensional dynamical system

$$\dot{\boldsymbol{z}} = \boldsymbol{F}(\boldsymbol{z}; \boldsymbol{\kappa}^*). \tag{2.11}$$

Let $U = \Phi(\tilde{U})$ be the domain of the system (2.11). The reduced system (2.11) has a unique steady state $\boldsymbol{z}^* = \Phi(\boldsymbol{x}^*)$ in the interior of $U$, because $\boldsymbol{x}^*$ is an interior point of its stoichiometric compatibility class. The steady state $\boldsymbol{z}^*$ inherits linear stability as well, i.e., all the eigenvalues of the Jacobian $D_{\boldsymbol{z}}\boldsymbol{F}(\boldsymbol{z}^*; \boldsymbol{\kappa}^*)$ have negative real parts. Moreover, $\boldsymbol{z}^*$ is a global attractor for the system (2.11) on $U$.

Let $K = \Phi(\tilde{K})$ be the image of the compact set under the diffeomorphism. For any $\|\boldsymbol{\kappa} - \boldsymbol{\kappa}^*\|_\infty < \delta$ and any initial condition in $U$, the solution $\boldsymbol{z}(t)$ to the system (2.11) is eventually in $K$. By Theorem 2.3.4, there exists some $\varepsilon > 0$ such that for all $\|\boldsymbol{\kappa} - \boldsymbol{\kappa}^*\|_\infty < \varepsilon$, there is a unique globally attracting steady state $\hat{\boldsymbol{z}}(\boldsymbol{\kappa}) \in U$ to the system $\dot{\boldsymbol{z}} = \boldsymbol{F}(\boldsymbol{z}; \boldsymbol{\kappa})$, where

$\hat{\boldsymbol{z}}(\boldsymbol{\kappa})$ is an interior point of $U$.

Let $\hat{\boldsymbol{x}}(\boldsymbol{\kappa})$ be the preimage of $\hat{\boldsymbol{z}}(\boldsymbol{\kappa})$ under the diffeomorphism $\Phi$. Then in the stoichiometric compatibility class $\tilde{U} = (\boldsymbol{x}_0 + S)_>$, the point $\hat{\boldsymbol{x}}(\boldsymbol{\kappa})$ is the unique positive steady state of the system $\dot{\boldsymbol{x}} = \boldsymbol{f}(\boldsymbol{x}; \boldsymbol{\kappa})$, and $\hat{\boldsymbol{x}}(\boldsymbol{\kappa})$ is globally stable. □

**Remark 2.3.7.** The bound $\varepsilon$ depends on $\boldsymbol{\kappa}^*$ and the stoichiometric compatibility class.

**Corollary 2.3.8.** *Assume the Permanence Conjecture for variable-$\boldsymbol{\kappa}$ systems. Let $(G, \boldsymbol{\kappa}^*)$ be a complex-balanced system. Then there exists $\varepsilon > 0$ such that whenever $\|\boldsymbol{\kappa} - \boldsymbol{\kappa}^*\|_\infty < \varepsilon$, the mass-action system $(G, \boldsymbol{\kappa})$ is globally stable.*

We conclude this chapter with a conjecture. In Chapter 3 we introduce *generalized mass-action systems*; these can arise in several manners, one of which is by perturbing the reaction vectors in a mass-action system [106][5]. The dynamics of interest is given by

$$\frac{d\boldsymbol{x}}{dt} = \sum_{(i,j)\in E} \kappa_{ij} \boldsymbol{x}^{\boldsymbol{y}_i} \boldsymbol{w}_{ij}^{\varepsilon}, \tag{2.12}$$

where $\boldsymbol{w}_{ij}^{\varepsilon} \approx \boldsymbol{y}_j - \boldsymbol{y}_i$. Viewing the reaction vectors $\{\boldsymbol{w}_{ij}^{\varepsilon} : (i,j) \in G\}$ as parameters instead of the rate constants, one can try to apply Theorem 2.3.4 by Smith and Waltman. Clearly, linear stability is inherited for small perturbations. Less obvious is an analog of the Permanence Conjecture, a sufficient condition for robust permanence. We conjecture that under mild assumptions, system (2.12) is globally stable if the unperturbed version is complex-balanced.

**Conjecture 2.3.9.** *Let $(G, \boldsymbol{\kappa}^*)$ be a complex-balanced system. There exist $\delta > 0$ and $\varepsilon > 0$ such that the perturbed mass-action system*

$$\frac{d\boldsymbol{x}}{dt} = \sum_{(i,j)\in E} \kappa_{ij}^{\delta} \boldsymbol{x}^{\boldsymbol{y}_i} \boldsymbol{w}_{ij}^{\varepsilon} \tag{2.13}$$

[5] One can instead perturb the exponents in the monomials instead. There is a certain amount of symmetry between the two views.

*is globally stable for all* $\|\boldsymbol{\kappa} - \boldsymbol{\kappa}^*\|_\infty < \delta$, *and* $\left\|\boldsymbol{w}_{ij}^{\varepsilon} - (\boldsymbol{y}_j - \boldsymbol{y}_i)\right\|_2 < \varepsilon$ *such that the perturbed network is endotactic.*

One possible approach uses toric differential inclusions [30, 31, 45, 112]. Consider the weakly reversible network $G$ in Figure 2.4(a), which is complex-balanced for some choice of rate constants $\boldsymbol{\kappa}^*$ under mass-action kinetics. Figure 2.4(b) illustrates some permitted perturbations on reaction vectors. The key condition is no reactions may point outside the Newton polytope Newt($G$), so the network is endotactic (Definition 1.4.17). Indeed, for any such permitted perturbations, the system can be realized by the network in Figure 2.4(b).

Put another way, any variable-$\boldsymbol{\kappa}$ system on the network in (b) is dynamically equivalent to some variable-$\boldsymbol{\kappa}$ system on the reversible network $G'$ in (c). Moreover, the networks in Figures 2.4(b) and 2.4(c) are endotactic, so any variable-$\boldsymbol{\kappa}$ system on $G'$ can be embedded into a *toric differential inclusion* [34], shown in Figure 2.4(d). For systems in $\mathbb{R}^2$ like this, one can construct a polygonal forward-invariant region [45], the boundary of which is outlined in purple in Figure 2.4(d). Therefore, the system $(G', \boldsymbol{\kappa}'(t))$ is persistent. It remains to show that this region is globally attracting (Conjecture 1.4.25). For this particular example, $(G', \boldsymbol{\kappa}'(t))$ is permanent by two separate results: by [45, Theorem 6.4], any variable-$\boldsymbol{\kappa}$ endotactic system with two species is permanent; and by [17, Theorem 4.2], any weakly reversible variable-$\boldsymbol{\kappa}$ system with one connected component is permanent.

More generally, suppose the assumptions in Conjecture 2.3.9. Analogous to the network in Figure 2.4(c), consider an endotactic network $G'$ that can incorporate the perturbed system (2.13); notably there should be reaction vectors along every edge on the boundary of the Newton polytope. Next, embed $G'$ into a toric differential inclusion [34]. Either by explicit construction or by Conjecture 1.4.25, any variable-$\boldsymbol{\kappa}$ system on $G'$ is permanent. Because any of our perturbed system can be realized using the variable-$\boldsymbol{\kappa}$ system, there is a compact set in $\mathbb{R}^n_>$ that is globally attracting for any $\boldsymbol{\kappa} \approx \boldsymbol{\kappa}^*$ and $\boldsymbol{w}_{ij}^{\varepsilon} \approx \boldsymbol{y}_j - \boldsymbol{y}_i$ such that the resulting network can in realized using $G'$. By Theorem 2.3.4, the perturbed system is globally stable.

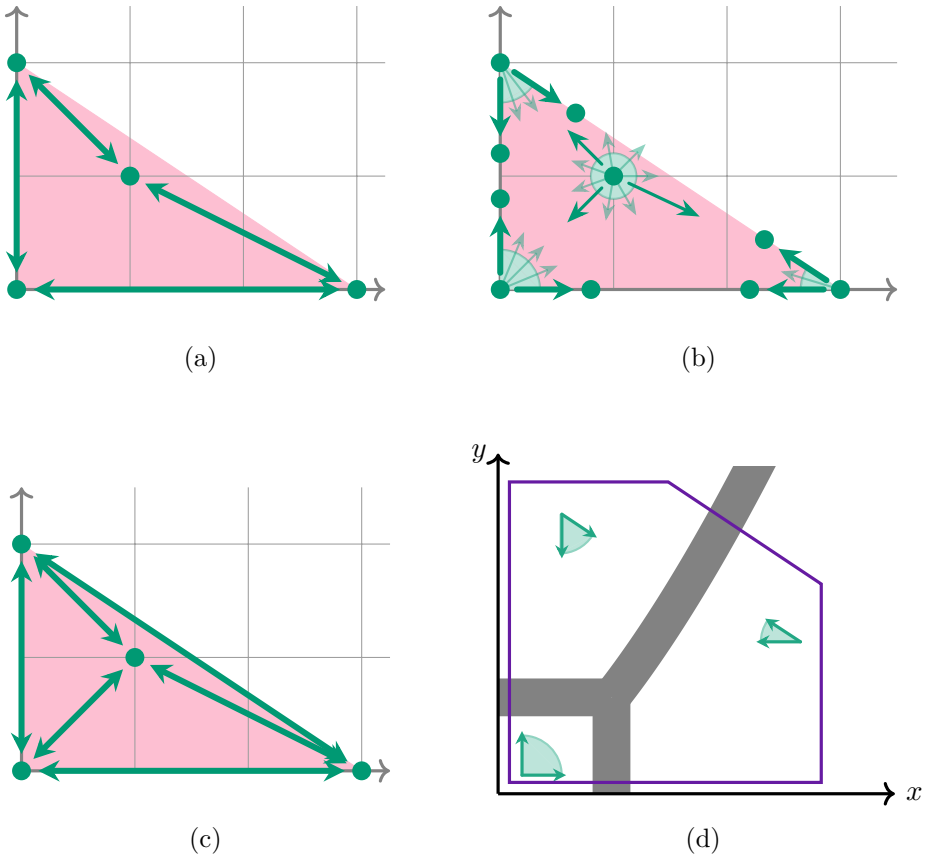


Figure 2.4: Example illustrating the idea of Conjecture 2.3.9: global stability is inherited after perturbing the reaction vectors of (a) a complex-balanced system such that (b) the resulting network is endotactic. Any variable-$\boldsymbol{\kappa}$ system (b) is always dynamically equivalent to one on (c), which can be embedded into a *toric differential inclusion*, with a forward invariant region (purple).

# Chapter 3

# Power-Law Kinetics

It was mentioned in the introductory chapter that mass-action kinetics was derived for ideal reaction systems. When those assumptions do not hold, the dynamics is expected to deviate from that modelled by a mass-action system. While other mathematical tools exist, ranging from stochastic processes to delay differential equations — the latter being the topic of the next chapter — these methods are generally more difficult to analyze. However, one can absorb the non-idealities of the system by changing the exponents in mass-action kinetics, analogous to replacing concentrations with activities in thermodynamics of reactions. This change in the reaction orders broadly fall under the name *power-law kinetics* [117, 131]. There are other methods of arriving at a power-law system, e.g., such as restricting reactants to a lower dimensional surface [91, 92].

Power-law systems are (often autonomous) systems of ordinary differential equations. What differentiates power-law kinetics from mass-action kinetics is that the exponents in the monomials may not correspond to the stoichiometric coefficient of the reactants. In the traditional view that stoichiometric coefficients are non-negative integers, mass-action systems use polynomials as the right-hand side of the ODEs[1]. In power-law kinetics, polynomials are replaced with generalized polynomials, whose exponents are real numbers. More importantly, the reaction rate function may depend on concentrations of species that are *not* reactants, a scenario that could arise when simplifying reaction mechanism diagrams and lumping several reactions together.

[1] Emphatically *not* the view we take in this thesis, and not the typical view in works that follow from those of Horn, Jackson, and Feinberg. The exponents in the non-linear rate functions are typically taken to be non-negative real numbers. In this thesis, the main difference between mass-action kinetics and power-law kinetics is whether the exponents in the rate functions correspond to the stoichiometric coefficients of the reactant complex.

In this chapter, we retain the focus on reaction networks, and decouple the stoichiometric coefficients from the rate functions. Section 3.1 reviews the framework of *generalized mass-action systems*, and the notion of complex-balancing is extended to that of *vertex-balancing* in Section 3.2. We give a condition on vector spaces in Section 3.3 for the existence and uniqueness of vertex-balanced steady states within each stoichiometric compatibility class. This generalizes Birch's Theorem (Theorem 1.4.4) for classical mass-action systems.

## 3.1 Generalized mass-action systems

In this section, we introduce yet another representation of kinetics model: that of *generalized mass-action systems*[2] as introduced by Stefan Müller and Georg Regensburger in [107, 108].

Recall from Chapter 1 that a reaction network consists of a directed graph $G = (V, E)$ whose vertices are assigned vectors in $\mathbb{R}^n_{\geq}$. A mass-action system $(G, \boldsymbol{\kappa})$ is defined when the edges of the graph are given positive weights called rate constants. The associated system of ODEs on $\mathbb{R}^n_{\geq}$ can be written as

$$\frac{d\boldsymbol{x}}{dt} = \mathbf{Y}\mathbf{A}_{\boldsymbol{\kappa}}\boldsymbol{x}^{\mathbf{Y}}. \tag{3.1}$$

The complex matrix $\mathbf{Y}$ appears once as related to the reaction vectors and once more in the monomials in $\boldsymbol{x}^{\mathbf{Y}}$. What if we are interested in decoupling these two aspects of the differential equations: the linear stoichiometric coefficients and the non-linear rate functions? In other words, what if Equation (3.1) looks like $\dot{\boldsymbol{x}} = \mathbf{Y}\mathbf{A}_{\boldsymbol{\kappa}}\boldsymbol{x}^{\tilde{\mathbf{Y}}}$ instead?

We illustrate the idea of *generalized reaction network* using two examples before the formal definition. We also illustrates what their representations as classical reaction networks would look like, if the same dynamics were generated by a classical mass-action system. The first example echoes how perhaps one might run into a generalized network in the wild, but the second example, which starts out more abstractly, better resembles the definition.

[2] In their seminal paper [78], Horn and Jackson also referred to *generalized* mass-action kinetics, whereby they meant to allow non-integer stoichiometric coefficients. Here, we refer to the Horn–Jackson framework as *classical* mass-action kinetics.

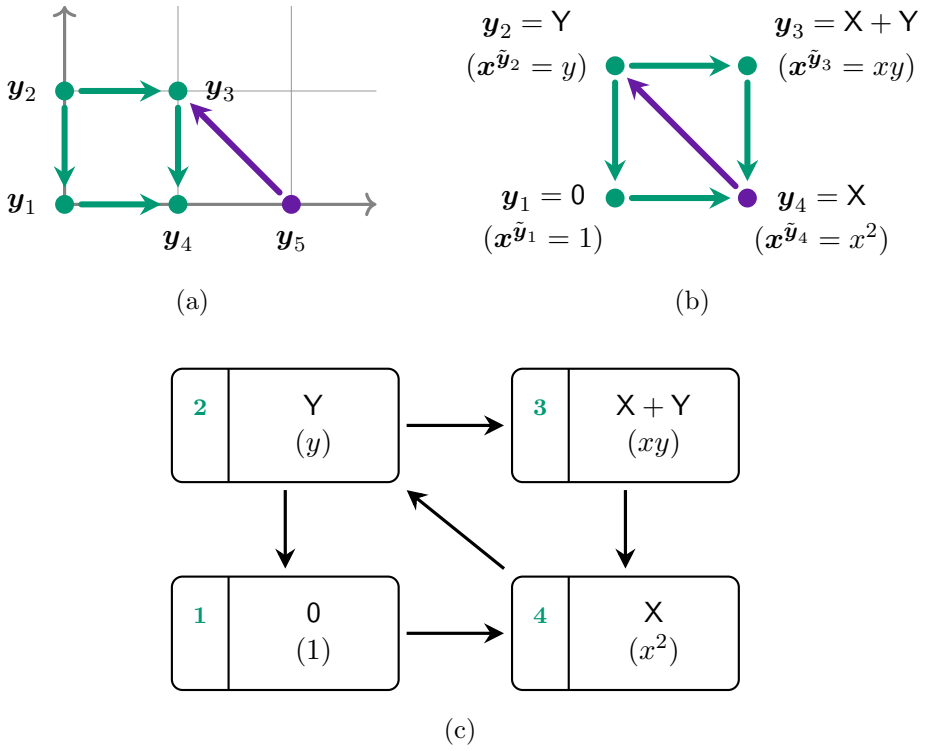


Figure 3.1: (a) A *classical* reaction network in Example 3.1.1 that is not weakly reversible. However, by "*translating*" the reaction $\boldsymbol{y}_5 \to \boldsymbol{y}_3$ left, (b) the resulting graph appears weakly reversible. To avoid changing the dynamics, one needs to keep track of the corresponding rate functions in addition to the stoichiometric coefficients. (c) How a *generalized reaction network* is usually depicted in this chapter, with the stoichiometric coefficients above the rate functions in each vertex.

**Example 3.1.1.** Consider the *classical*[3] reaction network with the complexes labelled as in Figure 3.1(a). Noting that $\boldsymbol{y}_3 - \boldsymbol{y}_5 = \boldsymbol{y}_2 - \boldsymbol{y}_4 = (-1, 1)^\top$, we can write the associated system of ODEs under mass-action kinetics as

$$\begin{aligned} \tfrac{d\boldsymbol{x}}{dt} = {} & \kappa_{14}\boldsymbol{x}^{\boldsymbol{y}_1}(\boldsymbol{y}_4 - \boldsymbol{y}_1) + \kappa_{21}\boldsymbol{x}^{\boldsymbol{y}_2}(\boldsymbol{y}_1 - \boldsymbol{y}_2) + \kappa_{23}\boldsymbol{x}^{\boldsymbol{y}_2}(\boldsymbol{y}_3 - \boldsymbol{y}_2) \\ & + \kappa_{34}\boldsymbol{x}^{\boldsymbol{y}_3}(\boldsymbol{y}_4 - \boldsymbol{y}_3) + \kappa_{53}\boldsymbol{x}^{\boldsymbol{y}_5}(\boldsymbol{y}_2 - \boldsymbol{y}_4)\,. \end{aligned} \tag{3.2}$$

At the same time, we notice that the monomial $\boldsymbol{x}^{\boldsymbol{y}_4}$ does not appear, since $\boldsymbol{y}_4$ is not a source complex in the reaction network.

[3]Emphasis added to contrast the main object of this chapter with those of previous chapters.

What if we start with the weakly reversible graph $\mathcal{G} = (\mathcal{V}, \mathcal{E})$ in Figure 3.1(b) and assign two labels to each vertex: one corresponding to the monomials, and another corresponding to stoichiometric coefficients that give the correct reaction vector? This leads to a *generalized reaction network* (Definition 3.1.3). For three of the vertices, let

$$\boldsymbol{y}_1 = \tilde{\boldsymbol{y}}_1 = (0,0)^\top, \quad \boldsymbol{y}_2 = \tilde{\boldsymbol{y}}_2 = (0,1)^\top, \quad \text{and} \quad \boldsymbol{y}_3 = \tilde{\boldsymbol{y}}_3 = (1,1)^\top.$$

For the final vertex, let

$$\boldsymbol{y}_4 = (1,0)^\top, \quad \text{while} \quad \tilde{\boldsymbol{y}}_4 = (2,0)^\top.$$

Now the system of ODEs

$$\frac{d\boldsymbol{x}}{dt} = \sum_{(i,j)\in\mathcal{E}} \kappa_{ij} \boldsymbol{x}^{\tilde{\boldsymbol{y}}_i} \left(\boldsymbol{y}_j - \boldsymbol{y}_i\right),$$

with appropriately chosen rate constants $\kappa_{ij}$ from (3.2) above.

Figure 3.1(b) contains all the information needed to define a generalized reaction network. A more standard representation of one is shown in Figure 3.1(c). Each vertex of the graph $\mathcal{G}$ is labelled with a *stoichiometric complex* on top, and a monomial corresponding to the *kinetic-order complex* below. The stoichiometric complexes $\boldsymbol{y}_i$ give rise to the relevant reaction vectors, while the kinetic-order complexes $\tilde{\boldsymbol{y}}_i$ define the respective rate functions. The motivating procedure of this example is known as *network translation* [83]. This is a common way to generate a generalized mass-action system, and has biological applications [84].

**Example 3.1.2.** Consider the abstract graph $\mathcal{G}$ in Figure 3.2(a) with two connected components. Assign two sets of vectors to the vertices, the first set as shown in Figure 3.2(b):

$$\mathbf{Y}(v_1) = \boldsymbol{y}_1 = (0,0)^\top, \quad \mathbf{Y}(v_2) = \boldsymbol{y}_2 = (1,1)^\top,$$
$$\mathbf{Y}(v_3) = \boldsymbol{y}_3 = \mathbf{Y}(v_4) = \boldsymbol{y}_4 = (2,1)^\top \quad \text{and} \quad \mathbf{Y}(v_5) = \boldsymbol{y}_5 = (1,0)^\top,$$

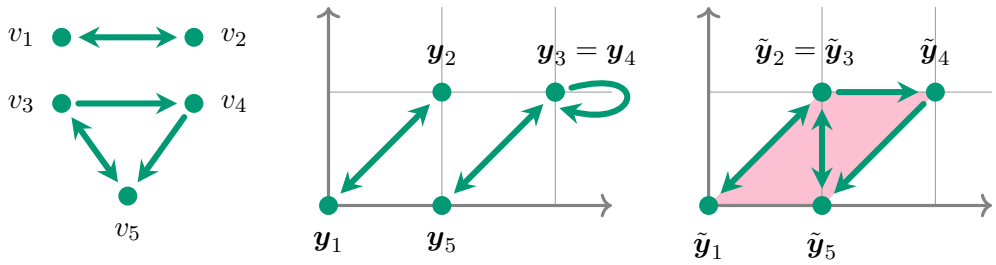


(a) $\mathcal{G}$ (b) $\mathbf{Y}(\mathcal{G})$ (c) $\tilde{\mathbf{Y}}(\mathcal{G})$

Figure 3.2: (a) An abstract graph $\mathcal{G}$, and its images under the maps (b) $\mathbf{Y}$ and (c) $\tilde{\mathbf{Y}}$ from Example 3.1.2. The Newton polytope of the associated system is shown in (c). Together, $(\mathcal{G}, \mathbf{Y}, \tilde{\mathbf{Y}})$ defines a generalized reaction network.

and the second set as seen in Figure 3.2(c):

$$\tilde{\mathbf{Y}}(v_1) = \tilde{\boldsymbol{y}}_1 = (0,0)^\top, \quad \tilde{\mathbf{Y}}(v_2) = \tilde{\boldsymbol{y}}_2 = \tilde{\mathbf{Y}}(v_3) = \tilde{\boldsymbol{y}}_3 = (1,1)^\top,$$
$$\tilde{\mathbf{Y}}(v_4) = \tilde{\boldsymbol{y}}_4 = (2,1)^\top \quad \text{and} \quad \tilde{\mathbf{Y}}(v_5) = \tilde{\boldsymbol{y}}_5 = (1,0)^\top.$$

Letting $\kappa_{ij}$ be the rate constants of the edge $(i,j)$, define the system of ODEs

$$\begin{aligned}\frac{d\boldsymbol{x}}{dt} &= \sum_{(i,j)\in\mathcal{E}} \kappa_{ij}\boldsymbol{x}^{\tilde{\boldsymbol{y}}_i}\left(\boldsymbol{y}_j - \boldsymbol{y}_i\right) \\ &= \kappa_{12}\begin{pmatrix}1\\1\end{pmatrix} + \kappa_{21}xy\begin{pmatrix}-1\\-1\end{pmatrix} + \kappa_{45}x^2y\begin{pmatrix}-1\\-1\end{pmatrix} + \kappa_{53}x\begin{pmatrix}1\\1\end{pmatrix} + \kappa_{35}xy\begin{pmatrix}-1\\-1\end{pmatrix}.\end{aligned}$$

Observe that the term corresponding to $v_3 \to v_4$ does not appear, since a self-loop in the graph $\mathbf{Y}(\mathcal{G})$ results in the zero reaction vector. Second, because $\tilde{\mathbf{Y}}$ maps both $v_2$ and $v_3$ to $(1,1)^\top$, the monomial $xy$ is associated to edges leaving those two vertices. The Newton polytope of the system is given by $\tilde{\mathbf{Y}}(\mathcal{G})$, as shown in Figure 3.2(c). As this example illustrates, the dynamics of a generalized mass-action system is determined by $(\mathcal{G}, \mathbf{Y}, \tilde{\mathbf{Y}})$ with positive rate constants assigned to each edge.

**Definition 3.1.3.** A ***generalized reaction network*** is given by $(\mathcal{G}, \mathbf{Y}, \tilde{\mathbf{Y}})$, where $\mathcal{G} = (\mathcal{V}, \mathcal{E})$ is a finite directed graph with no self-loops and no isolated vertices, and $\mathbf{Y} : \mathcal{V} \to \mathbb{R}^n$ maps

each vertex $v_j$ to a ***stoichiometric complex*** $\boldsymbol{y}_j$, while $\tilde{\mathbf{Y}}\colon \mathcal{V}_s \to \mathbb{R}^n$ maps each source vertex $v_j$ to a ***kinetic-order complex*** $\tilde{\boldsymbol{y}}_j$.

**Remark 3.1.4.** We do not assume that the maps $\mathbf{Y}$ and $\tilde{\mathbf{Y}}$ are injective (the definition initially given by Müller and Regensburger in [107]). Injectivity was dropped from the definition in [108]. Also, as in classical mass-action systems, the assumptions of no self-loops and no isolated vertices do not affect the dynamics. Instead, they pose minor inconveniences when defining the Laplacian matrix. As demonstrated in Figure 3.2, the graphs $\mathcal{G}$, $\mathbf{Y}(\mathcal{G})$, and $\tilde{\mathbf{Y}}(\mathcal{G})$ may have different topologies.

We adopt the terms ***reversible*** and ***weakly reversible*** but now referring to the abstract graph $\mathcal{G}$. While it may appear that we are stating the obvious, soon we need to distinguish between the abstract graph $\mathcal{G}$ and the images $\mathbf{Y}(\mathcal{G})$ and $\tilde{\mathbf{Y}}(\mathcal{G})$, which can be regarded as separate directed graphs themselves.

**Definition 3.1.5.** A ***generalized mass-action system*** is the quadruple $(\mathcal{G}, \mathbf{Y}, \tilde{\mathbf{Y}}, \boldsymbol{\kappa})$, where $(\mathcal{G}, \mathbf{Y}, \tilde{\mathbf{Y}})$ is a generalized reaction network, and $\boldsymbol{\kappa} \in \mathbb{R}^{\mathcal{E}}_{>}$ is a vector of rate constants. Its associated system of differential equations on $\mathbb{R}^n_{>}$ is

$$\frac{d\boldsymbol{x}}{dt} = \sum_{(i,j)\in\mathcal{E}} \kappa_{ij} \boldsymbol{x}^{\tilde{\boldsymbol{y}}_i} \left(\boldsymbol{y}_j - \boldsymbol{y}_i\right). \tag{3.3}$$

The system (3.3) can be written in matrix form. Let $m$ be the number of vertices in $\mathcal{G} = (\mathcal{V}, \mathcal{E})$. By an abuse of notation, let $\mathbf{Y}$ and $\tilde{\mathbf{Y}} \in \mathbb{R}^{n\times m}$ be matrices with columns filled by stoichiometric and kinetic-order complexes respectively; if $v_j$ is *not* a source vertex, then set the $j$th column of $\tilde{\mathbf{Y}}$ to be the zero vector $\mathbf{0}$[4]. Then the system (3.3) can be written as

$$\frac{d\boldsymbol{x}}{dt} = \mathbf{Y}\mathbf{A}_{\boldsymbol{\kappa}} \boldsymbol{x}^{\tilde{\mathbf{Y}}}, \tag{3.4}$$

[4]This choice is arbitrary since the corresponding monomial in $\boldsymbol{x}^{\tilde{\mathbf{Y}}}$ does not appear in the associated system system of ODEs or in $\mathbf{A}_{\boldsymbol{\kappa}}\boldsymbol{x}^{\tilde{\mathbf{Y}}}$.

where $\mathbf{A}_{\boldsymbol{\kappa}}$ is the Laplacian matrix or kinetic matrix[5] of the *abstract graph* $\mathcal{G}$, i.e.,

$$[\mathbf{A}_{\boldsymbol{\kappa}}]_{ij} = \begin{cases} \kappa_{ji} & \text{if } i \neq j \text{ and } (i,j) \in \mathcal{E} \\ -\sum_p \kappa_{jp} & \text{if } i = j \\ 0 & \text{otherwise} \end{cases} .$$

Let $\mathbf{I}_{\mathcal{G}} \in \mathbb{R}^{\mathcal{V}\times\mathcal{E}}$ be the incidence matrix of the graph $\mathcal{G}$. Let $S = \operatorname{span}\{\boldsymbol{y}_j - \boldsymbol{y}_i \,:\, (i,j) \in \mathcal{E}\} = \operatorname{ran} \mathbf{Y}\mathbf{I}_{\mathcal{G}}$ be the ***stoichiometric subspace***. Again $\dot{\boldsymbol{x}} \in S$, so for any positive initial condition $\boldsymbol{x}(0) > \mathbf{0}$, the solution $\boldsymbol{x}(t)$ of system (3.3) or (3.4) is confined to the invariant affine subspace $\boldsymbol{x}(0) + S$. The ***stoichiometric compatibility class*** of $\boldsymbol{x}_0 \in \mathbb{R}^n_>$ is $(\boldsymbol{x}_0 + S)_> = (\boldsymbol{x}_0 + S) \cap \mathbb{R}^n_>$. Here, we make no claim on whether $\mathbb{R}^n_>$ is forward invariant.

As observed in Example 3.1.2, the Newton polytope is given by the kinetic-order complexes. If every vertex is a source, we define ***kinetic-order subspace*** to be

$$\tilde{S} = \operatorname{span}\{\tilde{\boldsymbol{y}}_j - \tilde{\boldsymbol{y}}_i \,:\, (i,j) \in \mathcal{E}\} = \operatorname{ran} \tilde{\mathbf{Y}}\mathbf{I}_{\mathcal{G}}. \tag{3.5}$$

From here on unless otherwise stated, we assume that every vertex of $\mathcal{G}$ is a source vertex, so that the kinetic-order subspace $\tilde{S}$ is well-defined. Generally speaking, we assume that $\mathcal{G}$ is weakly reversible, unless otherwise stated (as in Remark 3.2.2 when trying to distinguish between vertex-balancing for generalized mass-action systems and complex-balancing for classical mass-action systems).

## 3.2 Vertex-balanced steady states

Given the matrix equation (3.4), it is natural to extend the notion of complex-balancing to generalized mass-action system. We shall see that these steady states enjoy some, but not all, of the algebraic properties of complex-balanced steady states of classical mass-action systems.

[5] As is the case with classical mass-action systems, strictly speaking $\mathbf{A}_{\boldsymbol{\kappa}}$ is the negative transpose of the Laplacian matrix.

**Definition 3.2.1.** Let $(\mathcal{G}, \mathbf{Y}, \tilde{\mathbf{Y}}, \boldsymbol{\kappa})$ be a generalized mass-action system with associated system $\dot{\boldsymbol{x}} = \mathbf{Y}\mathbf{A}_{\boldsymbol{\kappa}}\boldsymbol{x}^{\tilde{\mathbf{Y}}}$. A positive steady state $\boldsymbol{x}^*$ is ***vertex-balanced***[6] if for every $v_i \in \mathcal{V}$, we have

$$\sum_{(i,j)\in\mathcal{E}} \kappa_{ij}(\boldsymbol{x}^*)^{\tilde{\boldsymbol{y}}_i} = \sum_{(j,i)\in\mathcal{E}} \kappa_{ji}(\boldsymbol{x}^*)^{\tilde{\boldsymbol{y}}_j}. \tag{3.6}$$

Equivalently $\mathbf{A}_{\boldsymbol{\kappa}}(\boldsymbol{x}^*)^{\tilde{\mathbf{Y}}} = \mathbf{0}$. Let $Z_{\boldsymbol{\kappa}}$ denote the set of vertex-balanced steady states.

**Remark 3.2.2.** It is worth emphasizing that the graph on which vertex-balancing is obtained is the *abstract* graph $\mathcal{G}$, not $\mathbf{Y}(\mathcal{G})$, as this simple example $(\mathcal{G}, \mathbf{Y}, \tilde{\mathbf{Y}}, \boldsymbol{\kappa})$

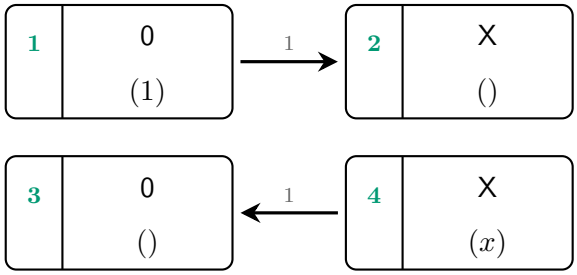


illustrates. The associated system, also generated by the classical mass-action system $(G, \boldsymbol{\kappa})$

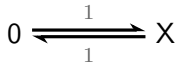


is $\dot{x} = 1 - x$. The positive steady state $x^* = 1$ is *not* vertex-balanced on $\mathcal{G}$, yet it is complex-balanced for $(G, \boldsymbol{\kappa})$. There are non-trivial biological examples of this phenomenon [84].

Despite the difference between vertex-balanced steady states (for generalized mass-action systems) and complex-balanced steady states (for classical mass-action systems), they share some algebraic properties. A generalized mass-action system $(\mathcal{G}, \tilde{\mathbf{Y}}, \tilde{\mathbf{Y}}, \boldsymbol{\kappa})$ is associated to the system of ODEs $\dot{\boldsymbol{x}} = \tilde{\mathbf{Y}}\mathbf{A}_{\boldsymbol{\kappa}}\boldsymbol{x}^{\tilde{\mathbf{Y}}}$. So a positive solution to $\mathbf{A}_{\boldsymbol{\kappa}}\boldsymbol{x}^{\tilde{\mathbf{Y}}}$ is vertex-balanced for $(\mathcal{G}, \tilde{\mathbf{Y}}, \tilde{\mathbf{Y}}, \boldsymbol{\kappa})$; it is also complex-balanced for the classical mass-action system $(\tilde{\mathbf{Y}}(\mathcal{G}), \boldsymbol{\kappa})$. As

[6] Others have also called it a *complex balancing equilibrium* [107, 108] or *generalized complex-balanced steady state* [83]. As the examples in Remark 3.2.2 and [84] illustrate, there are cases where a generalized mass-action system might have a steady state that is *complex-balanced* in a sense but certainly *not vertex-balanced*.

such, the set of vertex-balanced steady states $Z_{\boldsymbol{\kappa}}$ admits the representation

$$Z_{\boldsymbol{\kappa}} = \{\boldsymbol{x} > \mathbf{0} : \ \ln \boldsymbol{x} - \ln \boldsymbol{x}^* \in \tilde{S}^{\perp}\} = \boldsymbol{x}^* \circ \exp \tilde{S}^{\perp},$$

where $\boldsymbol{x}^*$ is a vertex-balanced steady state (if one exists). Unlike complex-balancing, without additional assumptions we cannot conclude that every positive steady state is vertex-balanced.

When thinking about complex-balancing, one cannot avoid a discussion on deficiency; similarly for vertex-balancing. Recall from Definition 1.4.9 that the deficiency of a reaction network $G$ (in the context of classical mass-action kinetics) is $\delta_G = m - \ell - \dim S$, where $m$ is the number of complexes, i.e., vertices, in the graph $G$, which has $\ell$ connected components, and $S$ is the stoichiometric subspace. In the context of generalized reaction network, there are three graphs — $\mathcal{G}$, $\mathbf{Y}(\mathcal{G})$ and $\tilde{\mathbf{Y}}(\mathcal{G})$ — and two linear subspaces — $S$ and $\tilde{S}$; there are three deficiencies for a generalized reaction network.

**Definition 3.2.3.** Let $(\mathcal{G}, \mathbf{Y}, \tilde{\mathbf{Y}})$ be a generalized reaction network, where $\mathcal{G} = (\mathcal{V}, \mathcal{E})$ has $\ell$ connected components. Let $\mathbf{I}_{\mathcal{G}}$ be the incidence matrix of $\mathcal{G}$. Assume that every vertex is a source. Let $S$ and $\tilde{S}$ be the stoichiometric and kinetic-order subspaces respectively.

(a) The ***stoichiometric deficiency*** is the non-negative integer $\delta = |\mathcal{V}| - \ell - \dim S$. Equivalently, $\delta = \dim(\ker \mathbf{Y} \cap \operatorname{ran} \mathbf{I}_{\mathcal{G}})$.

(b) The ***kinetic deficiency***[7] is the non-negative integer $\tilde{\delta} = |\mathcal{V}| - \ell - \dim \tilde{S}$. Equivalently, $\tilde{\delta} = \dim(\ker \tilde{\mathbf{Y}} \cap \operatorname{ran} \mathbf{I}_{\mathcal{G}})$.

(c) The ***effective deficiency*** is the non-negative integer $\delta' = m' - \ell' - \dim S$, where $m'$ and $\ell'$ are the number of vertices and connected components respectively in $\mathbf{Y}(\mathcal{G})$. Equivalently, $\delta' = \dim(\ker \mathbf{Y}' \cap \operatorname{ran} \mathbf{I}_{\mathbf{Y}(\mathcal{G})})$, where $\mathbf{Y}' \in \mathbb{R}^{n \times m'}$ is the truncated complex matrix[8] and $\mathbf{I}_{\mathbf{Y}(\mathcal{G})}$ is the incidence matrix of the graph $\mathbf{Y}(\mathcal{G})$ [84].

[7] Also called *kinetic-order deficiency* in [44].

[8] By truncating from $\mathbf{Y}$ the repeated columns that come from different vertices being mapped to the same stoichiometric complex.

The stoichiometric deficiency $\delta$ and kinetic deficiency $\tilde{\delta}$ were introduced in [107], while the effective deficiency $\delta'$ was introduced in [84]. Note that $\delta$ and $\tilde{\delta}$ depend on the *abstract* graph $\mathcal{G}$ and on $\mathbf{Y}$ and $\tilde{\mathbf{Y}}$ respectively, while $\delta'$, which is less than or equal to $\delta$, depends only on the graph $\mathbf{Y}(\mathcal{G})$. Finally, when $\mathcal{G}$ is weakly reversible, we can replace $\operatorname{ran}\mathbf{I}_{\mathcal{G}}$ with $\operatorname{ran}\mathbf{A}_{\boldsymbol{\kappa}}$ in the formulae for $\delta$ and $\tilde{\delta}$ above [73]. Similarly, if $\mathbf{Y}(\mathcal{G})$ is weakly reversible, then $\operatorname{ran}\mathbf{I}_{\mathbf{Y}(\mathcal{G})}$ can be replaced by the range of the Laplacian matrix of $\mathbf{Y}(\mathcal{G})$. For example, the generalized network in Figure 3.2 has

$$\delta = 5 - 2 - 1 = 2, \quad \tilde{\delta} = 5 - 2 - 2 = 1, \quad \text{and} \quad \delta' = 4 - 2 - 1 = 1.$$

As another example, the generalized network in Remark 3.2.2 has

$$\delta = 4 - 2 - 1 = 1 \quad \text{but} \quad \delta' = 2 - 1 - 1 = 0.$$

When first seeing this latter example, no doubt the reader was extremely tempted to say this example is effectively complex-balanced and fails to be vertex-balanced for technical reasons. Indeed, the network's effective deficiency hints at as much. If $\delta' = 0$, then every positive steady state of a generalized mass-action system is complex-balanced on $\mathbf{Y}(\mathcal{G})$ [84].

**Example 3.2.4.** To illustrate this, consider this example involving histidine kinase from [84]. In this network, a histidine kinase $\mathsf{X}$ phosphorylates itself, before it transfer the phosphate group to a response regulator $\mathsf{Y}$, which then dephosphorylates [29]. The two-component system is responsible for signal-tranduction in bacteria [126]. The mass-action system

$$\begin{aligned} \mathsf{X} &\xrightarrow{\kappa_1} \mathsf{X}_p \\ \mathsf{X}_p + \mathsf{Y} &\underset{\kappa_3}{\overset{\kappa_2}{\rightleftharpoons}} \mathsf{X} + \mathsf{Y}_p \\ \mathsf{Y}_p &\xrightarrow{\kappa_4} \mathsf{Y} \end{aligned}$$

can be translated [83] by adding $\mathsf{Y}$ to the first reaction, and $\mathsf{X}$ to the last reaction. The resulting generalized mass-action system is shown in Figure 3.3. The reader may notice that

there is an additional edge in the generalized network from the third vertex to the fourth. This edge contributes nothing to the dynamics since the stoichiometric complexes are both $\mathsf{X}+\mathsf{Y}_p$.

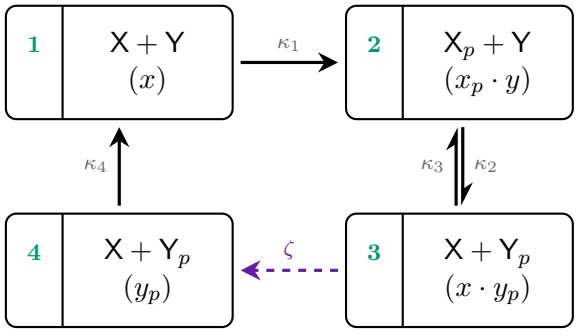


Figure 3.3: A generalized mass-action system that generates the same dynamics as the histidine kinase two-component system in Example 3.2.4.

The network in Figure 3.3, with or without the "ghost" edge with rate constant $\zeta$, has stoichiometric deficiency $\delta = 1$ but effective deficiency $\delta' = 0$. In particular, while $\dim(\mathbf{Y} \cap \operatorname{ran} \mathbf{A}_{\boldsymbol{\kappa}}(\mathcal{G})) = 1$ but $\dim(\mathbf{Y} \cap \operatorname{ran} \mathbf{A}_{\boldsymbol{\kappa}}(\mathbf{Y})) = 0$, where

$$\mathbf{A}_{\boldsymbol{\kappa}}(\mathcal{G}) = \begin{pmatrix} -\kappa_1 & & & \kappa_4 \\ \kappa_1 & -\kappa_2 & \kappa_3 & \\ & \kappa_2 & -\kappa_3 - \zeta & \\ & & \zeta & -\kappa_4 \end{pmatrix} \quad \text{and} \quad \mathbf{A}_{\boldsymbol{\kappa}}(\mathbf{Y}) = \begin{pmatrix} -\kappa_1 & & \kappa_4 \\ \kappa_1 & -\kappa_2 & \kappa_3 \\ & \kappa_2 & -\kappa_3 - \kappa_4 \end{pmatrix}$$

are the Laplacian matrices of the abstract graph $\mathcal{G}$ and the stoichiometric graph $\mathbf{Y}(\mathcal{G})$ respectively. While for any choice of rate constants, we may expect balancing across the vertices of $\mathbf{Y}(\mathcal{G})$, a scenario that is worthy of being called "*complex-balancing*", we do not expect in general balancing across vertices of $\mathcal{G}$, especially if the ghost edge is not present and the graph is not weakly reversible. We now look at this problem from two perspectives: algebraically first, then graph-theoretically for an intuitive idea.

With the ordering of species $\mathsf{X}$, $\mathsf{Y}$, $\mathsf{X}_p$, then $\mathsf{Y}_p$, the complex matrix and truncated

complex matrix are

$$\mathbf{Y} = \begin{pmatrix} 1 & 0 & 1 & 1 \\ 1 & 1 & 0 & 0 \\ 0 & 1 & 0 & 0 \\ 0 & 0 & 1 & 1 \end{pmatrix} \quad \text{and} \quad \mathbf{Y}' = \begin{pmatrix} 1 & 0 & 1 \\ 1 & 1 & 0 \\ 0 & 1 & 0 \\ 0 & 0 & 1 \end{pmatrix}.$$

Note that $(0, 0, 1, -1)^\top \in \ker \mathbf{Y}$, so $(0, 0, \zeta, -\zeta)^\top \in \ker \mathbf{Y}$. At this point, it is not difficult to show that

$$\begin{aligned} \mathbf{Y}\mathbf{A}_{\boldsymbol{\kappa}}(\mathcal{G}) &= \begin{pmatrix} 1 & 0 & 1 & 1 \\ 1 & 1 & 0 & 0 \\ 0 & 1 & 0 & 0 \\ 0 & 0 & 1 & 1 \end{pmatrix} \begin{pmatrix} -\kappa_1 & & & \kappa_4 \\ \kappa_1 & -\kappa_2 & \kappa_3 & \\ & \kappa_2 & -\kappa_3 - \zeta & \\ & & \zeta & -\kappa_4 \end{pmatrix} \\ &= \begin{pmatrix} 1 & 0 & 1 \\ 1 & 1 & 0 \\ 0 & 1 & 0 \\ 0 & 0 & 1 \end{pmatrix} \begin{pmatrix} -\kappa_1 & & \kappa_4 \\ \kappa_1 & -\kappa_2 & \kappa_3 \\ & \kappa_2 & -\kappa_3 - \kappa_4 \end{pmatrix} = \mathbf{Y}'\mathbf{A}_{\boldsymbol{\kappa}}(\mathbf{Y}). \end{aligned}$$

Next, we want to have a more intuitive and graph-theoretical understanding of why "complex-balancing", in the context of generalized mass-action systems, must imply the existence of a generalized system with the same dynamics but is also vertex-balancing. First recognize that that "complex-balancing" means balancing the flux across the nodes of $\mathbf{Y}(\mathcal{G})$. So the graph $\mathbf{Y}(\mathcal{G})$ is necessarily weakly reversible, and there is a complex-balancing flux on $\mathbf{Y}(\mathcal{G})$. Each vertex in $\mathbf{Y}(\mathcal{G})$ can be understood as a conglomerate of vertices in $\mathcal{G}$; indeed, each vertex holds the preimage $\mathbf{Y}^{-1}(\boldsymbol{y})$ of a stoichiometric complex $\boldsymbol{y}$. Zero in on the subgraph of $\mathcal{G}$ that contains $\mathbf{Y}^{-1}(\boldsymbol{y})$ with half-edges that leave/come from all other vertices; connect these half-edges to a new vertex $v^*$ (far far away). In the case of the histidine kinase system, we would focus on vertices **3** and **4**. We already know the fluxes across the half-edges balance, so it remains to craft a new generalized subnetwork that would be vertex-balancing. Because

the vertices in this subgraph share the same stoichiometric complex, adding an edge between the vertices *do not* change the associated system of ODEs. Analogous to introducing a canal between buckets with different water level, one can add edges from vertex $v_i$ with a net in-flux $J$ to a vertex $v_j$ with net out-flux. The rate constant of this edge is $\kappa_{ij} = J/\boldsymbol{x}^{\tilde{\boldsymbol{y}}_i}$, where $\tilde{\boldsymbol{y}}_i$ is the kinetic-order complex assigned to $v_i$, and $\boldsymbol{x}$ is the "complex-balanced" steady state. This procedure can then be repeated. Moreover, it must terminate at some point; otherwise there would be a vertex with non-zero net flux, which implies that the fluxes across $v^*$ are not balanced. This procedure of diverting fluxes does not in general uniquely determine the edges needed in the abstract graph $\mathcal{G}$.

Of course, if $\delta' = \dim(\ker \mathbf{Y}' \cap \operatorname{ran} \mathbf{A}_{\boldsymbol{\kappa}}(\mathbf{Y})) = 0$, then any steady state to a generalized mass-action system $(\mathcal{G}, \mathbf{Y}, \tilde{\mathbf{Y}})$ must be "complex-balancing", regardless of the choice of rate constants $\boldsymbol{\kappa}$. Therefore, there exists a generalized mass-action system (with the construction described above) that shares the same associated system of ODEs, and the set of positive steady state of $(\mathcal{G}, \mathbf{Y}, \tilde{\mathbf{Y}}, \boldsymbol{\kappa})$ is now vertex-balanced [84].

We summarize some known algebraic properties of vertex-balanced steady states.

**Theorem 3.2.5** ([84,107,108])**.** *Let $(\mathcal{G}, \mathbf{Y}, \tilde{\mathbf{Y}}, \boldsymbol{\kappa})$ be a generalized mass-action system.*

(a) *If $Z_{\boldsymbol{\kappa}} \neq \emptyset$ for some $\boldsymbol{\kappa} > \mathbf{0}$, then the graph $\mathcal{G}$ is weakly reversible.*

(b) *If $\boldsymbol{x}^* \in Z_{\boldsymbol{\kappa}}$, then $Z_{\boldsymbol{\kappa}} = \{\boldsymbol{x} \in \mathbb{R}^n_> : \ln \boldsymbol{x} - \ln \boldsymbol{x}^* \in \tilde{S}^\perp\} = \boldsymbol{x}^* \circ \exp \tilde{S}^\perp$.*

(c) *For a weakly reversible generalized reaction network, $\tilde{\delta} = 0$ if and only if $Z_{\boldsymbol{\kappa}} \neq \emptyset$ for any choices of rate constants $\boldsymbol{\kappa} > \mathbf{0}$.*

(d) *For a weakly reversible generalized reaction network, if $\delta = 0$, then for any choice of rate constants $\boldsymbol{\kappa} > \mathbf{0}$, any positive steady state is a vertex-balanced steady state, i.e., $E_{\boldsymbol{\kappa}} = Z_{\boldsymbol{\kappa}}$.*

(e) *If $\delta' = 0$, then there exists a generalized mass-action system $(\mathcal{G}', \mathbf{Y}', \tilde{\mathbf{Y}}', \boldsymbol{\kappa}')$ with the same*

*associated systems of ODEs such that its set of vertex-balanced steady states $Z'_{\boldsymbol{\kappa}'}$ is the set of positive steady states of $(\mathcal{G}, \mathbf{Y}, \tilde{\mathbf{Y}}, \boldsymbol{\kappa})$.*

Even if $Z_{\boldsymbol{\kappa}} \neq \emptyset$, it does not follow that every stoichiometric compatibility class has a vertex-balanced steady state. This leads to the question: can we conclude the existence and uniqueness of a vertex-balanced steady state in *every* stoichiometric compatibility class under some appropriate conditions? Towards this end, there are three essentially equivalent problems: (i) about vertex-balanced steady states for generalized mass-action systems, (ii) about the intersection of an affine space with a manifold, similar in spirit to Birch's Theorem (Theorem 1.4.4), and (iii) about the bijectivity of a generalized polynomial map onto a polyhedral cone. Below, we summarize these three questions. This thesis is only concerned about the first two problems.

The first of the three is phrased in the context of generalized mass-action systems. Suppose that there is a vertex-balanced steady state $\boldsymbol{x}^* \in Z_{\boldsymbol{\kappa}}$. What is a condition (E) on the network $(\mathcal{G}, \mathbf{Y}, \tilde{\mathbf{Y}})$ for the *existence* of a vertex-balanced steady state within *every* stoichiometric compatibility class? Similarly, what condition (U) on $(\mathcal{G}, \mathbf{Y}, \tilde{\mathbf{Y}})$ characterizes *uniqueness* of a vertex-balanced steady state within its stoichiometric compatibility class? We would like these conditions to be independent of the rate constants $\boldsymbol{\kappa}$.

**Problem (1).** *Let $(\mathcal{G}, \mathbf{Y}, \tilde{\mathbf{Y}}, \boldsymbol{\kappa})$ be a generalized mass-action system. Suppose that $Z_{\boldsymbol{\kappa}} \neq \emptyset$. What are conditions (E) and (U) on $(\mathcal{G}, \mathbf{Y}, \tilde{\mathbf{Y}})$, so that the following statements are true?*

1. *If $(\mathcal{G}, \mathbf{Y}, \tilde{\mathbf{Y}})$ satisfies condition (E), then there is* **at least one** *vertex-balanced steady state in every stoichiometric compatibility class, i.e., $(\boldsymbol{x}_0 + S) \cap Z_{\boldsymbol{\kappa}}$ contains at least one point for any $\boldsymbol{x}_0 \in \mathbb{R}^n_>$.*

2. *If $(\mathcal{G}, \mathbf{Y}, \tilde{\mathbf{Y}})$ satisfies condition (U), then there is* **at most one** *vertex-balanced steady state in every stoichiometric compatibility class, i.e., $(\boldsymbol{x}_0 + S) \cap Z_{\boldsymbol{\kappa}}$ contains at most one point for any $\boldsymbol{x}_0 \in \mathbb{R}^n_>$.*

Recall that $Z_{\boldsymbol{\kappa}} = \boldsymbol{x}^* \circ \exp \tilde{S}^\perp \subseteq \mathbb{R}^n_>$ for any $\boldsymbol{x}^* \in Z_{\boldsymbol{\kappa}}$. Thus, the vertex-balanced steady

states within any stoichiometric compatibility class belong to the intersection $(\boldsymbol{x}_0 + S) \cap (\boldsymbol{x}^* \circ \exp \tilde{S}^\perp)$ for some $\boldsymbol{x}_0 > \mathbf{0}$. This leads us to the another reformulation of the problem:

**Problem (2).** *Let $S$ and $\tilde{S} \subseteq \mathbb{R}^n$ be vector subspaces. What are conditions (E) and (U) on $S$ and $\tilde{S}$, so that the following statements are true?*

1. *If $S$ and $\tilde{S}$ satisfy condition (E), then $(\boldsymbol{x}_0 + S) \cap (\boldsymbol{x}^* \circ \exp \tilde{S}^\perp)$ contains* **at least one** *point, for any $\boldsymbol{x}_0$, $\boldsymbol{x}^* \in \mathbb{R}^n_>$.*

2. *If $S$ and $\tilde{S}$ satisfy condition (U), then $(\boldsymbol{x}_0 + S) \cap (\boldsymbol{x}^* \circ \exp \tilde{S}^\perp)$ contains* **at most one** *point, for any $\boldsymbol{x}_0$, $\boldsymbol{x}^* \in \mathbb{R}^n_>$.*

If a generalized mass-action system happens to be a classical mass-action system, then its stoichiometric subspace $S$ is also the kinetic-order subspace $\tilde{S}$. The existence and uniqueness of a point in the intersection $(\boldsymbol{x}_0 + S) \cap (\boldsymbol{x}^* \circ \exp S^\perp)$ for any $\boldsymbol{x}_0$, $\boldsymbol{x}^* \in \mathbb{R}^n_>$ is the content of Birch's Theorem (Theorem 1.4.4).

Another reformulation of the above problems was introduced by Müller and Regensburger [107], in terms of injectivity/surjectivity of an exponential map or a generalized polynomial map onto a polyhedral cone. Such polynomial maps appear in other applications; for example, a renormalized version appears in computer graphics and geometric modelling, where the map being injective implies that the curve or surface does not self-intersect [38].

We need to define these maps; for details of the following, see [106,107,108]. Let $\boldsymbol{x}^* \in \mathbb{R}^n_>$ be an arbitrary vector, and $S$, $\tilde{S} \subseteq \mathbb{R}^n$ two vector subspaces, with $d = \operatorname{codim} S$, $\tilde{d} = \operatorname{codim} \tilde{S}$. Choose a basis for $S^\perp$ and let the basis vectors be the rows of the matrix $\mathbf{W} \in \mathbb{R}^{d \times n}$. Similarly, choose a basis for $\tilde{S}^\perp$ and let the basis vectors be the rows of $\tilde{\mathbf{W}} \in \mathbb{R}^{\tilde{d} \times n}$. Write the two matrices in terms of their columns: $\mathbf{W} = (\boldsymbol{w}^1, \boldsymbol{w}^2, \ldots, \boldsymbol{w}^n)$ and $\tilde{\mathbf{W}} = (\tilde{\boldsymbol{w}}^1, \tilde{\boldsymbol{w}}^2, \ldots, \tilde{\boldsymbol{w}}^n)$. In this manner, $S^\perp = \operatorname{ran} \mathbf{W}^\top$, $S = \ker \mathbf{W}$, and $\tilde{S}^\perp = \operatorname{ran} \tilde{\mathbf{W}}^\top$, $\tilde{S} = \ker \tilde{\mathbf{W}}$. Finally, let $C^\circ(\mathbf{W})$ be the set of

all positive combinations of $\{\boldsymbol{w}^i\}_{i=1}^n$. For any $\boldsymbol{x}^* \in \mathbb{R}^n_>$, define the maps

$$\begin{array}{rccccc} f_{\boldsymbol{x}^*}: & \mathbb{R}^{\tilde{d}}_> & \to & C^\circ(\mathbf{W}) \subseteq \mathbb{R}^d, & & \\ & \boldsymbol{\xi} & \mapsto & \mathbf{W}(\boldsymbol{x}^* \circ \boldsymbol{\xi}^{\tilde{\mathbf{W}}}) & = & \displaystyle\sum_{i=1}^n x_i^* \boldsymbol{\xi}^{\tilde{\boldsymbol{w}}^i} \boldsymbol{w}^i \end{array}$$

and

$$\begin{array}{rccccc} F_{\boldsymbol{x}^*}: & \mathbb{R}^{\tilde{d}} & \to & C^\circ(\mathbf{W}) \subseteq \mathbb{R}^d, & & \\ & \boldsymbol{\lambda} & \mapsto & W(\boldsymbol{x}^* \circ \exp(\tilde{\mathbf{W}}^\top \boldsymbol{\lambda})) & = & \displaystyle\sum_{i=1}^n x_i^* e^{\langle \tilde{\boldsymbol{w}}^i, \boldsymbol{\lambda} \rangle} \boldsymbol{w}^i \end{array} .$$

Then the problem about intersection is equivalent to the following.

**Problem** (3)**.** *Let $S$ and $\tilde{S} \subseteq \mathbb{R}^n$ be vector subspaces. What are conditions (E) and (U) on $S$ and $\tilde{S}$, so that the following statements are true?*

1. *If $S$ and $\tilde{S}$ satisfy condition (E), then the map $f_{\boldsymbol{x}^*}$ (respectively $F_{\boldsymbol{x}^*}$) is* **surjective** *onto $C^\circ(\mathbf{W})$, for any $\boldsymbol{x}^* \in \mathbb{R}^n_>$.*

2. *If $S$ and $\tilde{S}$ satisfy condition (U), then the map $f_{\boldsymbol{x}^*}$ (respectively $F_{\boldsymbol{x}^*}$) is* **injective***, for any $\boldsymbol{x}^* \in \mathbb{R}^n_>$.*

Müller and Regensburger characterized when the maps $f_{\boldsymbol{x}^*}$ and $F_{\boldsymbol{x}^*}$ are injective and indeed when they are in a sense robustly bijective as explained in Theorem 3.2.6 below. Their characterization — as well as ours in the following section — are in terms of the *sign vectors* of the stoichiometric subspace $S$ and the kinetic-order subspace $\tilde{S}$. Briefly, the set of sign vectors $\sigma(S)$ is the image of $S$ under the coordinate-wise sign function (Definition 3.3.1). They proved that the maps $f_{\boldsymbol{x}^*}$ and $F_{\boldsymbol{x}^*}$ are injective if and only if $\sigma(S) \cap \sigma(\tilde{S}^\perp) = \{\mathbf{0}\}$ [107, Theorem 3.6]. The authors also provided a sufficient condition for bijectivity: if $\sigma(S) = \sigma(\tilde{S})$ and $(+, \cdots, +)^\top \in \sigma(S^\perp)$, then $f_{\boldsymbol{x}^*}$ and $F_{\boldsymbol{x}^*}$ are bijective, indeed, real analytic isomorphisms) [107, Proposition 3.9].

In Theorem 3.3.10 we somewhat generalized this result; more precisely, we prove that if $\sigma(S) \subseteq \overline{\sigma(\tilde{S}^{\perp})}$, with the *closure* operation defined in Definition 3.3.1, then there always exists exactly one intersection point in $(\boldsymbol{x}_0 + S) \cap (\boldsymbol{x}^* \circ \exp \tilde{S}^{\perp})$ for all $\boldsymbol{x}_0$, $\boldsymbol{x}^* > \mathbf{0}$. In other words, the maps $f_{\boldsymbol{x}^*}$ and $F_{\boldsymbol{x}^*}$ are bijective. Müller, Hofbauer, and Regensburger characterized when $f_{\boldsymbol{x}^*}$ and $F_{\boldsymbol{x}^*}$ are bijective for arbitrary $\boldsymbol{x}^* \in \mathbb{R}^n_>$ [106]. They also proved that the sign condition $\sigma(S) \subseteq \overline{\sigma(\tilde{S}^{\perp}_{\varepsilon})}$ is necessary and sufficient for $F_{\boldsymbol{x}^*}$ to be bijective for all $\boldsymbol{x}^* > \mathbf{0}$ and all small perturbations $\tilde{S}_{\varepsilon}$ of the subspace $S$.

**Theorem 3.2.6** (**Robust Deficiency Zero Theorem** [106, Theorem 46])**.** *Let* $(\mathcal{G}, \mathbf{Y}, \tilde{\mathbf{Y}})$ *be a weakly reversible generalized reaction network. There exists a unique vertex-balanced steady state in every stoichiometric compatibility class for any choice of rate constants and for all small perturbations of kinetic-order complexes* $\tilde{\mathbf{Y}}$ *if and only if* $\delta = \tilde{\delta} = 0$ *and* $\sigma(S) \subseteq \overline{\sigma(\tilde{S}^{\perp})}$.

We were careful in not claiming that the three problems are equivalent. Problems (2) and (3) are equivalent. However, Problem (1) is weaker; it assumes the existence of a particular vertex-balanced steady state $\boldsymbol{x}^*$ to obtain a representation of $Z_{\boldsymbol{\kappa}}$. So strictly speaking, the three problems are equivalent only when the kinetic deficiency is $\tilde{\delta} = 0$, and the rate constants $\boldsymbol{\kappa}$ is chosen so that $\boldsymbol{x}^*$ has the designated values.

## 3.3 Sign condition for vertex-balancing

In this section, we give a sufficient condition for the existence and uniqueness of a vertex-balanced steady state within any stoichiometric compatibility class in a generalized mass-action system. The results here appeared in [44]. The condition is in terms of the relative *sign vectors* of the stoichiometric subspace $S$ and the kinetic-order subspace $\tilde{S}$ (Definition 3.3.1). Informally speaking, we show that if $S$ and $\tilde{S}$ point in the same orthant[9] of $\mathbb{R}^n$, then for any $\boldsymbol{x}_0$, $\boldsymbol{x}^* \in \mathbb{R}^n_>$, the intersection $(\boldsymbol{x}_0 + S) \cap (\boldsymbol{x}^* \circ \exp \tilde{S}^{\perp})$ has exactly one point. In particular, if a generalized mass-action system has a vertex-balanced steady state $\boldsymbol{x}^*$, then every stoichiometric compatibility class has exactly one vertex-balanced steady state.

[9] Along with a boundary case involving coordinate faces of neighbouring orthants.

Existence of such an intersection point make up the main difficulty. Our result relies on transversality and intersection theory. We first introduce the relevant concepts of sign vectors and transversality.

**Definition 3.3.1.** Given a vector $\boldsymbol{x} \in \mathbb{R}^n$, its ***sign vector*** is

$$\sigma(\boldsymbol{x}) = (\operatorname{sgn}(x_1), \operatorname{sgn}(x_2), \ldots, \operatorname{sgn}(x_n))^\top \in \{0, +, -\}^n. \tag{3.7}$$

The set of sign vectors for a subset $S \subseteq \mathbb{R}^n$ is the collection $\sigma(S) = \{\sigma(\boldsymbol{x}) : \boldsymbol{x} \in S\}$. Consider the partial order on $\{0, +, -\}$ where $+ > 0$ and $- > 0$; the set $\{0, +, -\}^n$ inherits this partial order, i.e., we say $\boldsymbol{\tau} \geq \boldsymbol{\tau}'$ if and only if $\tau_j \geq \tau'_j$ for all $1 \leq j \leq n$. The ***closure*** of a set $\Lambda$ of sign vectors is the set

$$\overline{\Lambda} = \{\boldsymbol{\tau} \in \{0, +, -\}^n : \text{ there exists } \boldsymbol{\tau}' \in \Lambda \text{ such that } \boldsymbol{\tau} \leq \boldsymbol{\tau}'\}. \tag{3.8}$$

Geometrically, the sign vector tells approximately which direction a vector is pointing. Define an ***orthant***[10] of $\mathbb{R}^n$ to be the preimage of any sign patterns, i.e., an orthant is a maximal subset of $\mathbb{R}^n$ on which $\sigma$ is constant. For example, in $\mathbb{R}^2$ beside the four typical quadrants, there are also the positive and negative coordinate axes and the origin. In other words, $\mathbb{R}^2$ has nine orthants in total, whose sign vectors are

$$\begin{pmatrix} + \\ + \end{pmatrix}, \begin{pmatrix} - \\ + \end{pmatrix}, \begin{pmatrix} - \\ - \end{pmatrix}, \begin{pmatrix} + \\ - \end{pmatrix}, \begin{pmatrix} + \\ 0 \end{pmatrix}, \begin{pmatrix} - \\ 0 \end{pmatrix}, \begin{pmatrix} 0 \\ + \end{pmatrix}, \begin{pmatrix} 0 \\ - \end{pmatrix}, \begin{pmatrix} 0 \\ 0 \end{pmatrix}.$$

In $\mathbb{R}^3$, there are the eight 3-dimensional orthants (whose sign vectors have only non-zero components), twelve 2-dimensional orthants (whose sign vectors have exactly one 0), six 1-dimensional orthants (the coordinate axes, and whose sign vector has exactly two 0), and finally the origin. Therefore, $\mathbb{R}^3$ has twenty-seven orthants.

[10] This differs from the typical definition of an orthant, which is full dimensional. We call lower dimensional faces orthants as well.

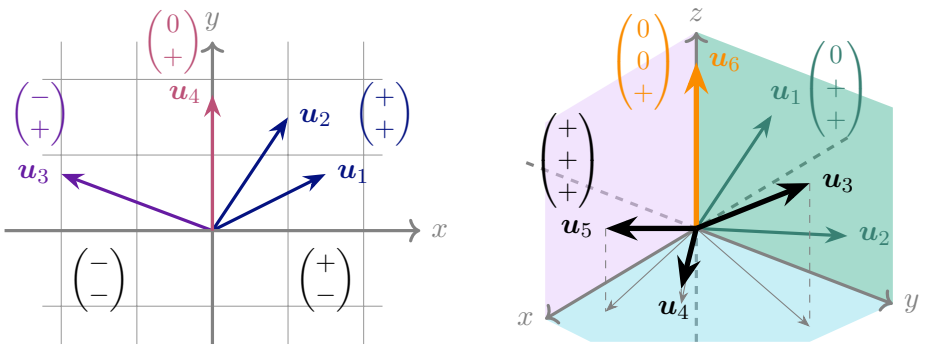


(a) (b)

Figure 3.4: Example sign vectors (colour-coded) in (a) $\mathbb{R}^2$ and (b) $\mathbb{R}^3$.

In Figure 3.4(a) are some examples in $\mathbb{R}^2$ with their sign vectors. The vectors $\boldsymbol{u}_1$, $\boldsymbol{u}_2$ share the same sign $(+,+)^\top$. The sign vector of $\boldsymbol{u}_3$ is $(-,+)^\top$. The sign vector $(0,+)^\top$ of $\boldsymbol{u}_4$ is in the closures $\overline{\sigma(\{\boldsymbol{u}_1,\boldsymbol{u}_2\})}$ and $\overline{\sigma(\boldsymbol{u}_3)}$. This reflects the fact that this coordinate face, the positive $y$-axis, borders those two orthants.

In Figure 3.4(b) are some examples in $\mathbb{R}^3$ with their sign vectors. Vectors that share the same sign are colour-coded together. The signs of $\boldsymbol{u}_1$ and $\boldsymbol{u}_2$, which lie above the positive $y$-axis, are $(0,+,+)^\top$. The vectors $\boldsymbol{u}_3$, $\boldsymbol{u}_4$, and $\boldsymbol{u}_5$ pointing out of the page towards the viewer have the sign $(+,+,+)^\top$. The closure of $(+,+,+)^\top$ includes the three coordinate faces with non-negative coordinates (shaded faces) as well as the positive $x$-, $y$- and $z$-axes and the origin. The closure of $(0,+,+)^\top$ (green shaded face) includes the positive $y$- and $z$-axes and the origin.

The closure of a set of sign vectors $\Lambda$ includes all of $\Lambda$ and any sign vector of $\Lambda$ with one or more of its components replaced by zeroes. A $+$ or a $-$ that has been replaced by 0 can be understood geometrically as sweeping a vector until it hits one of the adjacent coordinate faces that is one dimension lower.

There is also an orthogonality relation defined on $\{0,+,-\}^n$. We say two sign vectors $\boldsymbol{\tau}$ and $\boldsymbol{\tau}'$ are ***orthogonal***, denoted $\boldsymbol{\tau} \perp \boldsymbol{\tau}'$, if

i) either $\tau_j \cdot \tau'_j = 0$ for all $1 \leq j \leq n$, or

ii) there exist indices $i$, $j$ such that $\tau_i \cdot \tau'_i = +$ and $\tau_j \cdot \tau'_j = -$,

where the operation on signs is as one would expect from multiplication:

$$+ \cdot + = - \cdot - = +, \quad + \cdot - = -, \quad \text{and} \quad + \cdot 0 = - \cdot 0 = 0 \cdot 0 = 0.$$

The sign vectors $\boldsymbol{\tau}$ and $\boldsymbol{\tau}'$ are orthogonal if and only if there exist orthogonal vectors $\boldsymbol{x}$ and $\boldsymbol{y}$ such that $\sigma(\boldsymbol{x}) = \boldsymbol{\tau}$ and $\sigma(\boldsymbol{y}) = \boldsymbol{\tau}'$.

Much more could be said about the structure of sign vectors, especially in the context of oriented matroids. For a brief introduction to sign vectors of linear subspaces, we refer the reader to the appendix in [107].

The notion of *transversality* encapsulates the idea of generic intersection, that an intersection does not disappear when the surfaces are perturbed. Informally, transversal intersections is the opposite of being tangent. We do not use the full power of the theory of transversality; for a comprehensive treatment of differential topology, see [72, 121].


Figure 3.5: (a)–(b) Examples in $\mathbb{R}^3$ of transversal intersections, and (c)–(d) those in $\mathbb{R}^3$ that do not intersecting transversally.

**Definition 3.3.2.** Two manifolds $X$ and $Y$ of $\mathbb{R}^n$ ***intersect transversally*** if at each intersection point $\boldsymbol{p} \in X \cap Y$, their tangent spaces span the entire Euclidean space, i.e., $T_{\boldsymbol{p}}(X) + T_{\boldsymbol{p}}(Y) = \mathbb{R}^n$.

Transversality is quickly generalized to that between a map and a manifold, as seen in the following differential topology result.

**Theorem 3.3.3** ([121, Theorem 3.5.1]). *Let $X$ and $Y$ be manifolds and $Z \subseteq Y$ a submanifold, where $Z$ and $Y$ are boundaryless. Let $f : X \to Y$ be a smooth map. Suppose $f$ intersects $Z$ transversally and $f|_{\partial X}$ also intersects $Z$ transversally. Then $f^{-1}(Z)$ is a submanifold of $X$ with boundary $\partial(f^{-1}(Z)) = \partial X \cap f^{-1}(Z)$, and* $\operatorname{codim}_X(f^{-1}(Z)) = \operatorname{codim}_Y(Z)$.

When the ambient manifold is $Y = \mathbb{R}^n_{>0}$, and $f$ is the inclusion map of a submanifold $X$ into $\mathbb{R}^n_{>0}$, to say that the maps $f$ and $f|_{\partial X}$ intersect the manifold $Z$ transversally is equivalent to the manifolds $X$ and $\partial X$ intersect $Z$ transversally. The preimage $f^{-1}(Z)$ is the submanifold $X \cap Z$. Moreover, the dimension of the intersection $X \cap Z$ is given by the equation

$$\dim X - \dim(X \cap Z) = \operatorname{codim}_X(X \cap Z) = \operatorname{codim}_{\mathbb{R}^n_{>0}}(Z) = n - \dim Z.$$

In other words, $\dim(X \cap Z) = \dim X + \dim Z - n$. Therefore, for our purpose, we restate Theorem 3.3.3 as follows.

**Corollary 3.3.4.** *Let $X$ and $Z \subseteq \mathbb{R}^n_{>0}$ be submanifolds, where $Z$ is boundaryless. Suppose $X$ intersects $Z$ transversally and $\partial X$ also intersects $Z$ transversally. Then $X \cap Z$ is a manifold with boundary $\partial(X \cap Z) = \partial X \cap Z$ and has dimension* $\dim(X \cap Z) = \dim X + \dim Z - n$.

We first show in Lemma 3.3.6 that the sign condition $\sigma(S) \subseteq \overline{\sigma(\tilde{S})}$ implies the uniqueness condition in [107]. In Lemma 3.3.8, we establish the transversality of the manifolds $\boldsymbol{x} + S$ and $\boldsymbol{x}^* \circ \exp \tilde{S}^\perp$. Lemma 3.3.7 prevents our desired intersection point from escaping to the boundary of $\mathbb{R}^n_>$ or to infinity. Finally, these results lead to Theorem 3.3.9, concluding the existence and uniqueness of a point in the intersection $(\boldsymbol{x}_0 + S) \cap (\boldsymbol{x}^* \circ \exp \tilde{S}^\perp)$ for any $\boldsymbol{x}_0$, $\boldsymbol{x}^* \in \mathbb{R}^n_>$.

**Proposition 3.3.5** ([107, Proposition 3.1]). *Let $S$ and $\tilde{S} \subseteq \mathbb{R}^n$ be vector subspaces. The following are equivalent:*

(a) $\sigma(S) \cap \sigma(\tilde{S}^\perp) = \{\mathbf{0}\}$;

(b) *for any $\boldsymbol{x}_0$, $\boldsymbol{x}^* \in \mathbb{R}^n_>$, the intersection $(\boldsymbol{x}_0 + S) \cap (\boldsymbol{x}^* \circ \exp \tilde{S}^\perp)$ contains at most one point.*

**Lemma 3.3.6.** *Let $S$ and $\tilde{S} \subseteq \mathbb{R}^n$ be vector subspaces. If $\sigma(S) \subseteq \overline{\sigma(\tilde{S})}$, then $\sigma(S) \cap \sigma(\tilde{S}^\perp) = \{\mathbf{0}\}$. In particular, for any $\boldsymbol{x}_0$, $\boldsymbol{x}^* \in \mathbb{R}^n_>$, the intersection $(\boldsymbol{x}_0 + S) \cap (\boldsymbol{x}^* \circ \exp \tilde{S}^\perp)$ contains at most one point.*

*Proof.* By assumption, $\sigma(S) \cap \sigma(\tilde{S}^\perp) \subseteq \overline{\sigma(\tilde{S})} \cap \sigma(\tilde{S}^\perp)$. Let $\boldsymbol{\tau} \in \overline{\sigma(\tilde{S})} \cap \sigma(\tilde{S}^\perp)$ be a sign vector, so there exist vectors $\boldsymbol{u} \in \tilde{S}$ and $\boldsymbol{v} \in \tilde{S}^\perp$ such that $\boldsymbol{\tau} \leq \sigma(\boldsymbol{u})$ and $\boldsymbol{\tau} = \sigma(\boldsymbol{v})$. If $\boldsymbol{\tau} \leq \sigma(\boldsymbol{u})$ but $\boldsymbol{\tau} \perp \sigma(\boldsymbol{u})$, then $\boldsymbol{\tau} = \mathbf{0}$. Therefore, $\sigma(S) \cap \sigma(\tilde{S}^\perp) = \overline{\sigma(\tilde{S})} \cap \sigma(\tilde{S}^\perp) = \{\mathbf{0}\}$. By [107], $\sigma(S) \cap \sigma(\tilde{S}^\perp) = \{\mathbf{0}\}$ is necessary and sufficient for the intersection $(\boldsymbol{x}_0 + S) \cap (\boldsymbol{x}^* \circ \exp \tilde{S}^\perp)$ to contain at most one point for any $\boldsymbol{x}_0$, $\boldsymbol{x}^* \in \mathbb{R}^n_>$. □

**Lemma 3.3.7.** *Let $S$ and $\tilde{S} \subseteq \mathbb{R}^n$ be vector subspaces, $K \subseteq \mathbb{R}^n_>$ a compact subset, and $\boldsymbol{x}^* \in \mathbb{R}^n_>$. Suppose $\sigma(S) \subseteq \overline{\sigma(\tilde{S})}$. Then $(K + S) \cap (\boldsymbol{x}^* \circ \exp \tilde{S}^\perp)$ is a compact subset of $\mathbb{R}^n_>$.*

*Proof.* Let $\Gamma = (K + S) \cap (\boldsymbol{x}^* \circ \exp \tilde{S}^\perp)$. Since $\boldsymbol{x}^* \circ \exp \tilde{S}^\perp \subseteq \mathbb{R}^n_>$, the intersection $\Gamma$ also lies in $\mathbb{R}^n_>$. We first claim that $\Gamma$ is bounded away from infinity and from the boundary of $\mathbb{R}^n_>$. Suppose for a contradiction that this is not the case. Let $(\boldsymbol{x}^p)_p$ be a sequence in $\Gamma$ such that either $\limsup_{p\to\infty} x_i^p = \infty$ or $\liminf_{p\to\infty} x_i^p = 0$ for some $1 \leq i \leq n$. Passing to a subsequence, we may assume that

$$\begin{aligned} \lim_{p\to\infty} x_i^p &= \infty && \text{for } i \in I_1, \\ \lim_{p\to\infty} x_i^p &= 0 && \text{for } i \in I_2, \\ \lim_{p\to\infty} x_i^p &\in (0, \infty) && \text{for } i \in I_3, \end{aligned}$$

where $I_1$, $I_2$, $I_3$ partition the index set $\{1, 2, \ldots, n\}$, and $I_1 \cup I_2 \neq \emptyset$.

On one hand, $\boldsymbol{x}^p \in K + S$, with decomposition $\boldsymbol{x}^p = \boldsymbol{v}^p + \boldsymbol{s}^p$, where $\boldsymbol{v}^p \in K$ and $\boldsymbol{s}^p \in S$. Since $K \subseteq \mathbb{R}^n_>$ is compact, each component of $\boldsymbol{v}^p$ is uniformly bounded from above and below from zero. Thus for $i \in I_1$ where $x_i^p \to \infty$, we have $s_i^p \to \infty$; in particular, $s_i^p > 0$ for sufficiently large $p$. Similarly, if $i \in I_2$, then $s_i^p < 0$ for sufficiently large $p$, because $x_i^p \to 0$ and $\liminf_p v_i^p > 0$. Therefore, the sign of $s_i^p$ does not change for any $i \in I_1 \cup I_2$ and $p$ sufficiently

large. Because $\sigma(\boldsymbol{s}^p) \in \sigma(S) \subseteq \overline{\sigma(\tilde{S})}$ for sufficiently large $p$, there is a vector $\boldsymbol{u} \in \tilde{S}$ such that $u_i > 0$ if $i \in I_1$ and $u_i < 0$ if $i \in I_2$.

On the other hand, $\boldsymbol{x}^p \in \boldsymbol{x}^* \circ \exp \tilde{S}^\perp$, that is $\ln\left(\frac{\boldsymbol{x}^p}{\boldsymbol{x}^*}\right) \in \tilde{S}^\perp$, where the division is understood to be component-wise. For all $p$, we have $\boldsymbol{u} \perp \ln\left(\frac{\boldsymbol{x}^p}{\boldsymbol{x}^*}\right)$ and

$$0 = \left\langle \boldsymbol{u}\,,\, \ln\left(\frac{\boldsymbol{x}^p}{\boldsymbol{x}^*}\right)\right\rangle = \sum_{i\in I_1} u_i \ln\left(\frac{x_i^p}{x_i^*}\right) + \sum_{i\in I_2} u_i \ln\left(\frac{x_i^p}{x_i^*}\right) + \sum_{i\in I_3} u_i \ln\left(\frac{x_i^p}{x_i^*}\right).$$

The sum over $I_3$ is uniformly bounded for all $p$. Now let $p \to \infty$. For $i \in I_1$, we know $u_i > 0$ and $x_i^p \to \infty$, so the sum over $I_1$ is positive and unbounded. For $i \in I_2$, we know $u_i < 0$ and $x_i^p \to 0$, so $\ln\left(\frac{x_i^p}{x_i^*}\right) \to -\infty$, so the sum over $I_2$ is also positive and unbounded. Consequently, $0 = \lim_{p\to\infty}\langle \boldsymbol{u}, \ln\left(\frac{\boldsymbol{x}^p}{\boldsymbol{x}^*}\right)\rangle = \infty$, a contradiction. Therefore, $\Gamma \subseteq \mathbb{R}^n_>$ is bounded away from infinity and away from the boundary of $\mathbb{R}^n_>$.

Finally, we show that $\Gamma \subseteq \mathbb{R}^n_>$ is closed in the topology of $\mathbb{R}^n$. Fix $\varepsilon > 0$ such that $\Gamma$ lies inside the hypercube $Q = [\varepsilon, 1/\varepsilon]^n \subseteq \mathbb{R}^n_>$. Being the intersection of two closed sets, $Q \cap (K+S)$ is closed. The set $Q \cap (\boldsymbol{x}^* \circ \exp \tilde{S}^\perp)$ is diffeomorphic to $[\ln\varepsilon, \ln(1/\varepsilon)]^n \cap (\ln \boldsymbol{x}^* + \tilde{S}^\perp)$, which is again closed. Therefore, the set $(K+S) \cap (\boldsymbol{x}^* \circ \exp \tilde{S}^\perp) = [Q \cap (K+S)] \cap [Q \cap (\boldsymbol{x}^* \circ \exp \tilde{S}^\perp)]$ is the intersection of closed sets, thus itself closed in $\mathbb{R}^n_>$. □

In Lemma 3.3.6, we showed that the sign condition $\sigma(S) \subseteq \overline{\sigma(\tilde{S})}$ implies that the intersection $(\boldsymbol{x}_0 + S) \cap (\boldsymbol{x}^* \circ \exp \tilde{S}^\perp)$ contains at most one point. The lemma below claims that the weaker sign condition together with $\dim S = \dim \tilde{S}$ implies that the manifolds $\boldsymbol{x}_0 + S$ and $\boldsymbol{x}^* \circ \exp \tilde{S}^\perp$ intersect transversally. Figure 3.6 demonstrates how existence of an intersection point *fails* when the sign condition $\sigma(S) \subseteq \overline{\sigma(\tilde{S})}$ is not satisfied. Shown are curves $\boldsymbol{x}^* \circ \exp \tilde{S}^\perp$ (in various shades of orange) for several $\tilde{S}$; off to the right are the corresponding $\tilde{S}$, each with $\sigma(\tilde{S}) = \{\mathbf{0}, (\pm, \pm)^\top\}$. Note that $\boldsymbol{x}^* \circ \exp \tilde{S}^\perp$ and $\tilde{S}^\perp$ share the same sign vectors. Figure 3.6 also shows a compatibility class $(\boldsymbol{x}_0 + S)_>$ (blue) that does *not* intersect $\boldsymbol{x}^* \circ \exp \tilde{S}^\perp$. Note here that $\sigma(S) = \{\mathbf{0}, (\pm, \mp)^\top\}$.

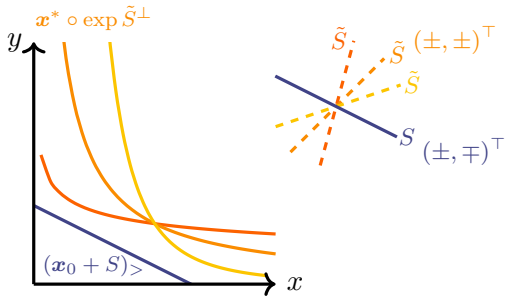


Figure 3.6: How existence of intersection point can fail when the sign condition $\sigma(S) \subseteq \overline{\sigma(\tilde{S})}$ is not satisfied. For some $\boldsymbol{x}_0 > \mathbf{0}$, the line segment $(\boldsymbol{x}_0 + S)_>$ (blue) fails to intersect with any of the curves $\boldsymbol{x}^* \circ \exp \tilde{S}^\perp$ (shades of orange) when $\sigma(S) \not\subseteq \overline{\sigma(\tilde{S}^\perp)}$.

**Lemma 3.3.8.** *Let $S$ and $\tilde{S} \subseteq \mathbb{R}^n$ be vector subspaces such that $\sigma(S) \cap \sigma(\tilde{S}^\perp) = \{\mathbf{0}\}$. Let $\boldsymbol{x}_0$, $\boldsymbol{x}^* \in \mathbb{R}^n_>$ be any positive vectors. The tangent spaces of $\boldsymbol{x}_0 + S$ and $\boldsymbol{x}^* \circ \exp \tilde{S}^\perp$ satisfy*

$$T_{\boldsymbol{p}}(\boldsymbol{x}_0 + S) \cap T_{\boldsymbol{p}}(\boldsymbol{x}^* \circ \exp \tilde{S}^\perp) = \{\mathbf{0}\}$$

*at any point $\boldsymbol{p} \in (\boldsymbol{x}_0 + S) \cap (\boldsymbol{x}^* \circ \exp \tilde{S}^\perp)$. If in addition $\dim S = \dim \tilde{S}$, then $\boldsymbol{x}_0 + S$ and $\boldsymbol{x}^* \circ \exp \tilde{S}^\perp$ intersect transversally at any intersection point $\boldsymbol{p}$.*

*Proof.* For any intersection point $\boldsymbol{p} \in (\boldsymbol{x}_0 + S) \cap (\boldsymbol{x}^* \circ \exp \tilde{S}^\perp)$, note that $T_{\boldsymbol{p}}(\boldsymbol{x}_0 + S) = S$ and $T_{\boldsymbol{p}}(\boldsymbol{x}^* \circ \exp \tilde{S}^\perp) = \boldsymbol{p} \circ \tilde{S}^\perp$ and hence $\sigma(T_{\boldsymbol{p}}(\boldsymbol{x}^* \circ \exp \tilde{S}^\perp)) = \sigma(\tilde{S}^\perp)$, because $\boldsymbol{p} > \mathbf{0}$. For any $\boldsymbol{v} \in T_{\boldsymbol{p}}(\boldsymbol{x}_0 + S) \cap T_{\boldsymbol{p}}(\boldsymbol{x}^* \circ \exp \tilde{S}^\perp)$, its sign vector is $\sigma(\boldsymbol{v}) \in \sigma(S) \cap \sigma(\tilde{S}^\perp) = \{\mathbf{0}\}$, i.e., $\boldsymbol{v} = \mathbf{0}$. Consequently, $T_{\boldsymbol{p}}(\boldsymbol{x}_0 + S) \cap T_{\boldsymbol{p}}(\boldsymbol{x}^* \circ \exp \tilde{S}^\perp) = \{\mathbf{0}\}$.

If we further assume that $\dim S = \dim \tilde{S}$, the linear space $T_{\boldsymbol{p}}(\boldsymbol{x}_0 + S) + T_{\boldsymbol{p}}(\boldsymbol{x}^* \circ \exp \tilde{S}^\perp)$ is of dimension $n$. In other words, the manifolds $\boldsymbol{x}_0 + S$ and $\boldsymbol{x}^* \circ \exp \tilde{S}^\perp$ intersect transversally. □

Now we are ready to state and prove the main result of this chapter: that the sign condition $\sigma(S) \subseteq \overline{\sigma(\tilde{S}^\perp)}$ essentially implies the existence of an intersection point in $(\boldsymbol{x}_0 + S) \cap (\boldsymbol{x}^* \circ \exp \tilde{S}^\perp)$ for any $\boldsymbol{x}_0, \boldsymbol{x}^* > \mathbf{0}$. There need not be an intersection point when the

sign condition fails; for example, see Figure 3.6. The proof starts with a known intersection point, $\boldsymbol{x}^* \in (\boldsymbol{x}^* + S) \cap (\boldsymbol{x}^* \circ \exp \tilde{S}^\perp)$. Next, we translate the affine space $(\boldsymbol{x}^* + S)$ to $(\boldsymbol{x}_0 + S)$, creating a $(d+1)$-dimensional strip of the form $K+S$, where $d = \dim S$ and $K$ is a line segment in $\mathbb{R}^n_>$. This strip intersects $\boldsymbol{x}^* \circ \exp \tilde{S}^\perp$ transversally, and we use Corollary 3.3.4 to conclude that the intersection $(K + S) \cap (\boldsymbol{x}^* \circ \exp \tilde{S}^\perp)$ is a one-dimensional manifold, whose boundary lies on the boundary of the affine strip $K + S$. Finally, the existence of a boundary point on $\boldsymbol{x}_0 + S$ follows from Lemma 3.3.6. For a visual sketch of the proof, see Figure 3.7.

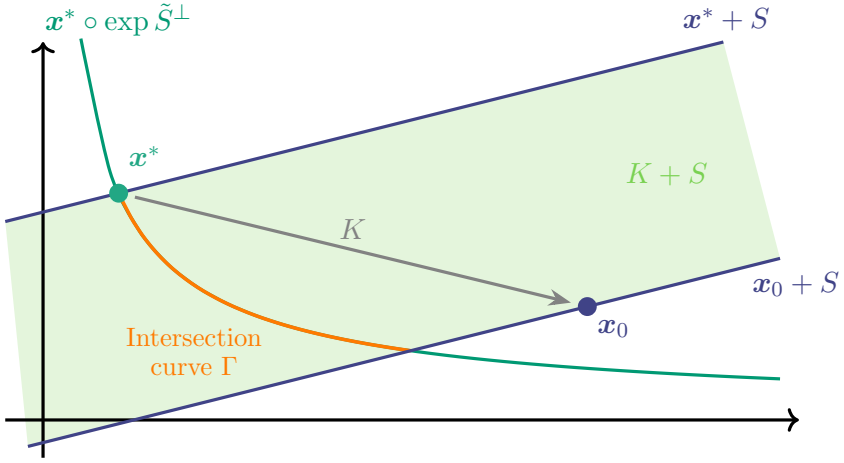


Figure 3.7: A sketch of the proof of Theorem 3.3.9. Let $K$ be the line segment between $\boldsymbol{x}^*$ and $\boldsymbol{x}_0$; then $K + S$ (shaded green) is an affine strip. It intersects the manifold $\boldsymbol{x}^* \circ \exp \tilde{S}^\perp$ along a curve $\Gamma$ (orange). If a boundary point of $\Gamma$ lies on $\boldsymbol{x}_0 + S$, then there exists a point in the intersection $(\boldsymbol{x}_0 + S) \cap (\boldsymbol{x}^* \circ \exp \tilde{S}^\perp)$.

**Theorem 3.3.9.** *Let $S$ and $\tilde{S} \subseteq \mathbb{R}^n$ be vector subspaces of equal dimension such that $\sigma(S) \subseteq \overline{\sigma(\tilde{S})}$. Then for any positive vectors $\boldsymbol{x}_0$, $\boldsymbol{x}^* \in \mathbb{R}^n_>$, the intersection $(\boldsymbol{x}_0 + S) \cap (\boldsymbol{x}^* \circ \exp \tilde{S}^\perp)$ consists of exactly one point.*

*Proof.* Let $\boldsymbol{x}_0, \boldsymbol{x}^* \in \mathbb{R}^n_>$ be arbitrary positive vectors. Lemma 3.3.6 implies that the intersection $(\boldsymbol{x}_0 + S) \cap (\boldsymbol{x}^* \circ \exp \tilde{S}^\perp)$ contains at most one point; hence it remains to show the existence of such a point. Clearly if $\boldsymbol{x}^* \in \boldsymbol{x}_0 + S$, then $(\boldsymbol{x}_0 + S) \cap (\boldsymbol{x}^* \circ \exp \tilde{S}^\perp) = \{\boldsymbol{x}^*\}$.

Suppose $\boldsymbol{x}^* \notin \boldsymbol{x}_0 + S$, and let $d = \dim S$. We define a $(d + 1)$-dimensional affine strip, which we intersect with $\boldsymbol{x}^* \circ \exp \tilde{S}^\perp$. To define this affine strip, consider the interpolation

function

$$\begin{aligned} K\colon \quad [0,1] &\to \mathbb{R}^n_>, \\ \delta &\mapsto \delta \boldsymbol{x}_0 + (1-\delta)\boldsymbol{x}^*. \end{aligned}$$

Since the line segment $K([0,1]) \subseteq \mathbb{R}^n_>$ is compact, the intersection $(K([0,1]) + S) \cap (\boldsymbol{x}^* \circ \exp \tilde{S}^\perp) \subseteq \mathbb{R}^n_>$ is compact by Lemma 3.3.7. Moreover, the manifolds $K([0,1]) + S$ and $\boldsymbol{x}^* \circ \exp \tilde{S}^\perp$ intersect transversally by Lemma 3.3.8, because

$$T_{\boldsymbol{p}}(K([0,1]) + S) + T_{\boldsymbol{p}}(\boldsymbol{x}^* \circ \exp \tilde{S}^\perp) \supseteq T_{\boldsymbol{p}}(\boldsymbol{x}^* + S) + T_{\boldsymbol{p}}(\boldsymbol{x}^* \circ \exp \tilde{S}^\perp) = \mathbb{R}^n.$$

By Corollary 3.3.4, the intersection $\Gamma = (K([0,1]) + S) \cap (\boldsymbol{x}^* \circ \exp \tilde{S}^\perp)$ is a manifold with boundary where $\partial\Gamma \subseteq \partial(K([0,1]) + S) = (\boldsymbol{x}^* + S) \cup (\boldsymbol{x}_0 + S)$. In addition, $\Gamma$ is 1-dimensional because

$$\dim(\Gamma) = \dim(K([0,1]) + S) + \dim(\boldsymbol{x}^* \circ \exp \tilde{S}^\perp) - n = 1 + \dim S + \dim \tilde{S}^\perp - n = 1.$$

Consider the connected component $\Gamma^* \subseteq \Gamma$ containing the point $\boldsymbol{x}^*$. The point $\boldsymbol{x}^*$ must be an endpoint of $\Gamma^*$; otherwise uniqueness fails at $K(\delta_0) + S$ for some small $\delta_0 > 0$. Since $\Gamma^*$ is compact, it is a curve with two endpoints. As $\partial\Gamma^* \subseteq \partial\Gamma = (\boldsymbol{x}^* + S) \cup (\boldsymbol{x}_0 + S)$, by uniqueness the other endpoint of $\Gamma^*$ must be in $\boldsymbol{x}_0 + S$. Thus, a point exists in $(\boldsymbol{x}_0 + S) \cap (\boldsymbol{x}^* \circ \exp \tilde{S}^\perp)$. □

We now apply Theorem 3.3.9 to generalized mass-action systems by combining with previously known results, especially those of [107, 108].

**Theorem 3.3.10.** *Let $(\mathcal{G}, \mathbf{Y}, \tilde{\mathbf{Y}})$ be a weakly reversible generalized reaction network, with stoichiometric subspace $S$, and kinetic-order subspace $\tilde{S}$. Assume that $\sigma(S) \subseteq \overline{\sigma(\tilde{S})}$ and $\dim S = \dim \tilde{S}$. Then the following hold.*

(a) *Suppose for some vector of rate constants $\boldsymbol{\kappa} > \mathbf{0}$, the generalized mass-action system $(\mathcal{G}, \mathbf{Y}, \tilde{\mathbf{Y}}, \boldsymbol{\kappa})$ admits a vertex-balanced steady state. Then every stoichiometric*

*compatibility class contains exactly one vertex-balanced steady state.*

(b) *If the kinetic deficiency is* $\tilde{\delta} = 0$*, then*[11] *for all choices of rate constants* $\boldsymbol{\kappa}$*, the generalized mass-action system* $(\mathcal{G}, \mathbf{Y}, \tilde{\mathbf{Y}}, \boldsymbol{\kappa})$ *admits a vertex-balanced steady state, and every stoichiometric compatibility class contains exactly one vertex-balanced steady state.*

(c) *Suppose* $(\mathcal{G}, \mathbf{Y}, \tilde{\mathbf{Y}}, \boldsymbol{\kappa})$ *admits a vertex-balanced steady state for some choice of rate constants* $\boldsymbol{\kappa}$*, and the stoichiometric deficiency is* $\delta = 0$*. Then every stoichiometric compatibility class contains exactly one positive steady state, which is vertex-balanced.*

*Proof.* As $\boldsymbol{x}^*$ is a vertex-balanced steady state for $(\mathcal{G}, \mathbf{Y}, \tilde{\mathbf{Y}}, \boldsymbol{\kappa})$, the set of vertex-balanced steady states is $Z_{\boldsymbol{\kappa}} = \boldsymbol{x}^* \circ \exp \tilde{S}^{\perp}$. By Theorem 3.3.9 $Z_{\boldsymbol{\kappa}}$ intersects the stoichiometric compatibility class $\boldsymbol{x}_0 + S$ exactly once for any $\boldsymbol{x}_0 \in \mathbb{R}^n_{>}$. This proves (a).

The first implication of (b) was proved in [108, Theorem 1(a)]. By (a), we conclude that every stoichiometric compatibility class contains exactly one vertex-balanced steady state.

If in addition we have $\delta = 0$, then $E_{\boldsymbol{\kappa}} = Z_{\boldsymbol{\kappa}}$, i.e., there is no positive steady state that is not vertex-balanced [107]. Consequently, there exists a unique steady state within each stoichiometric compatibility class, which is vertex-balanced. □

**Corollary 3.3.11.** *Let* $(\mathcal{G}, \mathbf{Y}, \tilde{\mathbf{Y}})$ *be a weakly reversible generalized reaction network, with stoichiometric subspace* $S$ *and kinetic-order subspace* $\tilde{S}$*. Suppose that* $\dim S = \dim \tilde{S}$ *and* $\sigma(S) \subseteq \overline{\sigma(\tilde{S})}$*. Further suppose that the stoichiometric deficiency and kinetic deficiency are* $\delta = \tilde{\delta} = 0$*. Then for any choice of rate constants, every stoichiometric compatibility class contains exactly one positive steady state, which is vertex-balanced.*

We conclude this chapter with several examples. The first demonstrates the necessity of the sign condition $\sigma(S) \subseteq \overline{\sigma(\tilde{S})}$. The remaining illustrate some subtleties with vertex-balancing in contrast with what is expected from complex-balancing of classical mass-action systems.

[11] By [108, Theorem 1(a)], this implication can be replaced by "if and only if".

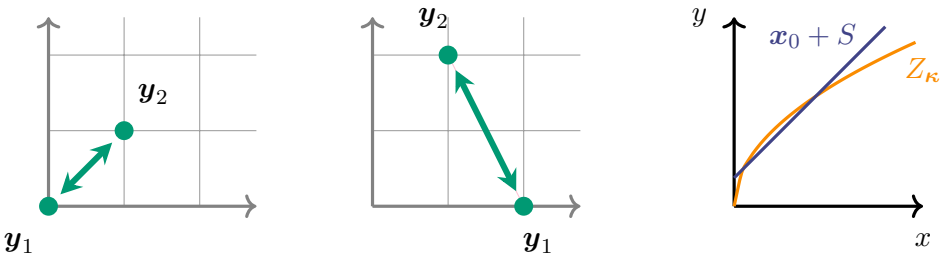


(a) $\mathbf{Y}(\mathcal{G})$ (b) $\tilde{\mathbf{Y}}(\mathcal{G})$ (c)

Figure 3.8: (a)–(b) A generalized mass-action system with two vertex-balanced steady states within the same stoichiometric compatibility class. See Example 3.3.12. (c) A stoichiometric compatibility class and the set $Z_{\boldsymbol{\kappa}=\mathbf{1}}$.

**Example 3.3.12.** Figure 3.8(a)–(b) define the generalized mass-action system $(\mathcal{G}, \mathbf{Y}, \tilde{\mathbf{Y}}, \boldsymbol{\kappa})$

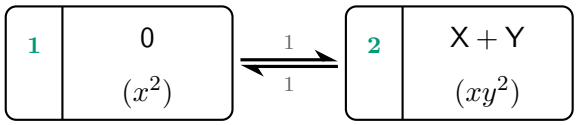


with rate constants $\boldsymbol{\kappa} = \mathbf{1}$. The stoichiometric and kinetic deficiencies are $\delta = \tilde{\delta} = 0$. By [107, 108], we conclude that there is a vertex-balanced steady state independent of choice of rate constants, and every positive steady state is vertex-balanced, i.e., $\emptyset \neq Z_{\boldsymbol{\kappa}} = E_{\boldsymbol{\kappa}}$. How the set of steady states intersects stoichiometric compatibility classes is a separate question. As seen in Figure 3.8(a)–(b), the sign condition of Corollary 3.3.11 is not satisfied, because

$$\sigma(\tilde{S}) = \left\{ \begin{pmatrix} + \\ - \end{pmatrix}, \begin{pmatrix} - \\ + \end{pmatrix} \right\} \quad \text{and} \quad \overline{\sigma(\tilde{S})} = \left\{ \begin{pmatrix} + \\ - \end{pmatrix}, \begin{pmatrix} - \\ + \end{pmatrix}, \begin{pmatrix} 0 \\ \pm \end{pmatrix}, \begin{pmatrix} \pm \\ 0 \end{pmatrix}, \begin{pmatrix} 0 \\ 0 \end{pmatrix} \right\},$$

but $(+,+)^\top$, which is in $\sigma(S)$, is not in $\overline{\sigma(\tilde{S})}$. In Figure 3.8(c) is a plot of $Z_{\boldsymbol{\kappa}} = \{(t^2, t)^\top : t > 0\}$ and a stoichiometric compatibility class that intersects $Z_{\boldsymbol{\kappa}}$ twice. Indeed, any compatibility class $\boldsymbol{x}_0 + S = \{(r, \varepsilon + r) : r \in \mathbb{R}\}$ with $0 < \varepsilon < 1/4$ would intersect $Z_{\boldsymbol{\kappa}}$ twice.

As mentioned in this chapter's introduction, beside network translation [83], generalized mass-action systems naturally arise from using power-law kinetics as an approximation of classical mass-action kinetics. For a complex-balanced mass-action system, if such

perturbations do not violate the sign condition $\sigma(S) \subseteq \overline{\sigma(\tilde{S})}$, the complex-balanced steady states naturally become vertex-balanced steady states, and inherit their predecessors' asymptotic stability.

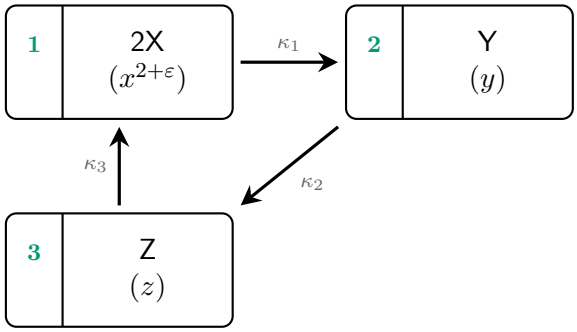


Figure 3.9: A generalized mass-action system modelling the perturbed dynamics in Example 3.3.13, where $\varepsilon > 0$. Dynamics (with $\varepsilon = 0$ and $\varepsilon > 0$) shown in Figure 3.10.

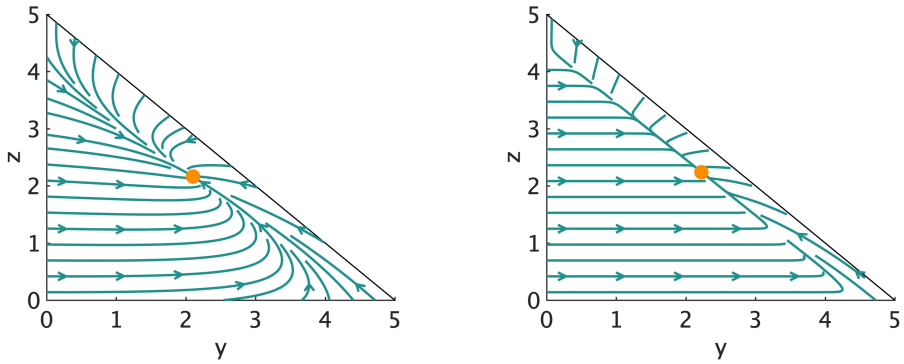


(a) (b)

Figure 3.10: Projection of phase portraits of system (3.9), and (3.10) with $\varepsilon = 10$, from Example 3.3.13, where $\kappa_i = 1$ and $x + 2y + 2z = 10$. The steady states are (a) complex-balanced and (b) vertex-balanced respectively.

**Example 3.3.13.** The mass-action system $(G, \boldsymbol{\kappa})$

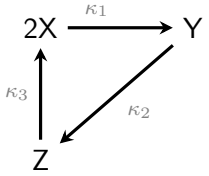

is associated to the system of ODEs

$$\begin{aligned}\frac{dx}{dt} &= -2\kappa_1 x^2 + 2\kappa_3 z\\ \frac{dy}{dt} &= \kappa_1 x^2 - \kappa_2 y\\ \frac{dz}{dt} &= \kappa_2 y - \kappa_3 z.\end{aligned} \tag{3.9}$$

Suppose the reagent $\mathsf{X}$ is confined to a fractal-like surface. Simulations and experiments show that the rate function with reactant complex $\mathsf{X}+\mathsf{X}$ is proportional to $[\mathsf{X}]^{2+\varepsilon}$, where $d_s = 2(1+\varepsilon)^{-1}$ is the spectral dimension [91, 92]. The resulting dynamics, modelled by the generalized mass-action system in Figure 3.9 with $\varepsilon > 0$, is associated to the system of ODEs

$$\begin{aligned}\frac{dx}{dt} &= -2\kappa_1 x^{2+\varepsilon} + 2\kappa_3 z\\ \frac{dy}{dt} &= \kappa_1 x^{2+\varepsilon} - \kappa_2 y\\ \frac{dz}{dt} &= \kappa_2 y - \kappa_3 z.\end{aligned} \tag{3.10}$$

Figure 3.10 shows the projected (onto the $yz$-plane) phase portraits of systems (3.9) and (3.10).

For any $\varepsilon > 0$, the stoichiometric and kinetic deficiencies are $\delta = \tilde{\delta} = 0$. Moreover, the two-dimensional subspaces $S$ and $\tilde{S}$ share the same set of sign vectors; these include the zero vector, and

$$\begin{pmatrix}+\\-\\0\end{pmatrix}, \begin{pmatrix}+\\-\\-\end{pmatrix}, \begin{pmatrix}+\\0\\-\end{pmatrix}, \begin{pmatrix}+\\+\\-\end{pmatrix}, \begin{pmatrix}0\\+\\-\end{pmatrix}, \begin{pmatrix}-\\+\\-\end{pmatrix},$$

and their negatives. Therefore the sign condition $\sigma(S) \subseteq \overline{\sigma(\tilde{S})}$ is satisfied. By Corollary 3.3.11, every stoichiometric compatibility class has exactly one positive steady state, which is vertex-balanced.

It is worth emphasizing that for a generalized mass-action system, even when every stoichiometric compatibility class has exactly one positive (vertex-balanced) steady state, one cannot expect everything from classical complex-balancing. First, we show an example with a unique vertex-balanced steady state, although there are other positive steady states of the system that are not complex-balanced.

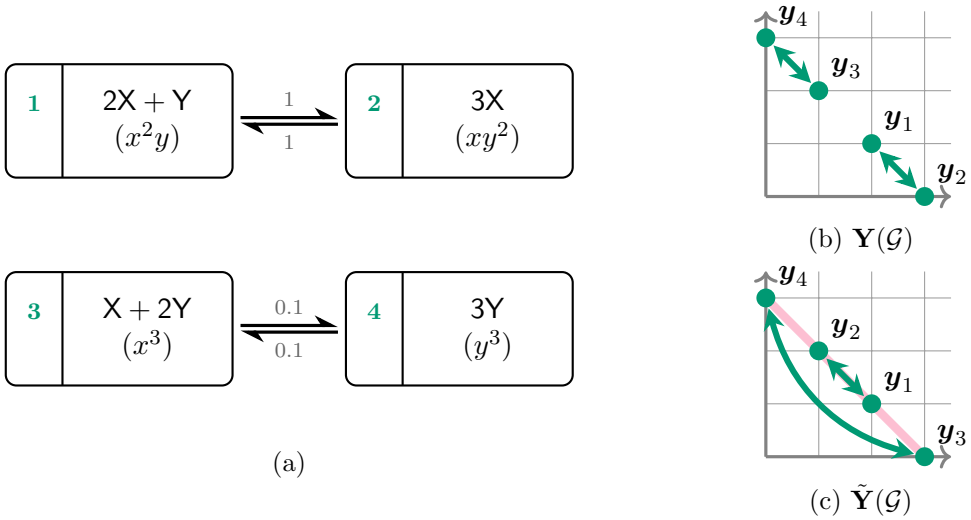


Figure 3.11: A generalized mass-action system modelling with a unique vertex-balanced steady state in addition to two non-vertex-balancing steady states in each stoichiometric compatibility class. See Example 3.3.14.

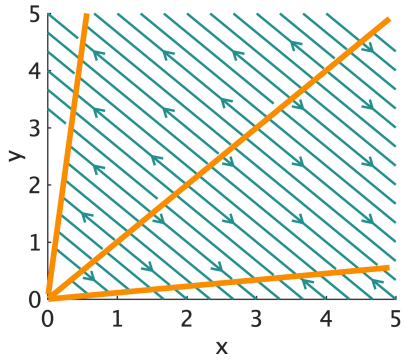


Figure 3.12: Phase portrait of the system in Example 3.3.14 and Figure 3.11(a). Each stoichiometric compatibility class has exactly one vertex-balanced steady state at $(x, x)^\top$, and two non-vertex-balancing steady states.

**Example 3.3.14.** Consider the generalized mass-action system in Figure 3.11(a). For convenience, its images under the stoichiometric and kinetic-order maps are shown in (b) and

(c) respectively. Note that $S = \tilde{S} = \text{span}(-1, 1)^\top$, so clearly the sign condition $\sigma(S) \subseteq \overline{\sigma(\tilde{S})}$ is satisfied. It follows from Theorem 3.3.9 that every stoichiometric compatibility class has exactly one vertex-balanced steady state. Note however, that the deficiencies are $\delta = \tilde{\delta} = 1$.

The associated system of ODEs

$$\begin{aligned}\frac{dx}{dt} &= \quad x^2y - xy^2 - 0.1x^3 + 0.1y^3\\ \frac{dy}{dt} &= -x^2y + xy^2 + 0.1x^3 - 0.1y^3\end{aligned}$$

has as its steady state set three lines, shown in Figure 3.12, one of which is the set of vertex-balanced steady state. Indeed, note that the vertex-balanced conditions are

$$xy^2 = xy^2 \quad \text{and} \quad x^3y^3,$$

or $x = y$. Thus, the middle line in Figure 3.12 is the set of vertex-balanced steady state. It is certainly true that each stoichiometric compatibility class has only one vertex-balanced steady state, but it is not only steady state.

One cannot expect similar dynamical behaviour as classical complex-balanced mass-action systems. We illustrate this with the Lotka–Volterra predator-prey model. Generalizations of Lotka–Volterra-type models were studied in the framework of generalized mass-action system in [18]; the authors characterized which $\tilde{\mathbf{Y}}$ would give rise to a center, like the phase portrait shown in Figure 3.13(b).

**Example 3.3.15.** Consider the generalized mass-action system in Figure 3.13(a). The associated system of the generalized mass-action system $(\mathcal{G}, \mathbf{Y}, \tilde{\mathbf{Y}}, \boldsymbol{\kappa})$

$$\begin{aligned}\frac{dx}{dt} &= \kappa_{12}x - \kappa_{23}xy\\ \frac{dy}{dt} &= \kappa_{23}xy - \kappa_{31}y\end{aligned}$$

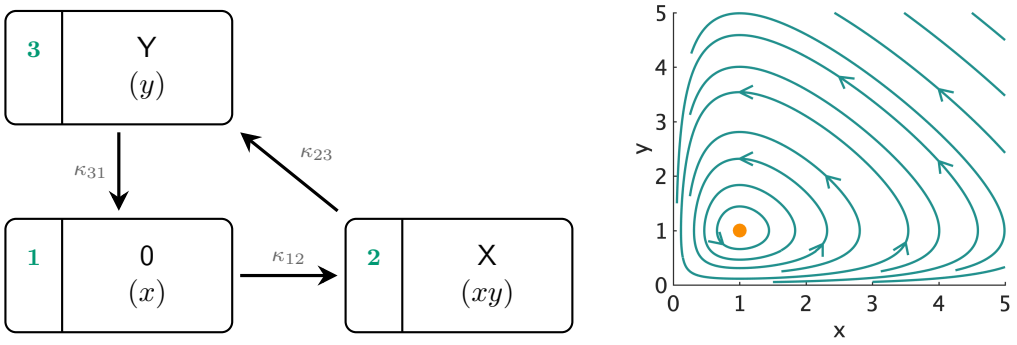


Figure 3.13: (a) A generalized mass-action system that gives rise to dynamics as that of Lotka–Volterra under mass-action kinetics. See Example 3.3.15. (b) A phase portrait, where the unique positive steady state (orange) is a center.

is the same as that generated by the network in Figure 1.4(a) under mass-action kinetics. It is known that for any choice of rate constants $\kappa_{ij} > 0$, the system has one positive steady state, surrounded by periodic solutions as seen in Figure 3.13(b). Therefore, the same dynamical behaviour is exhibited by $(\mathcal{G}, \mathbf{Y}, \tilde{\mathbf{Y}}, \boldsymbol{\kappa})$.

As for the generalized mass-action system, the stoichiometric and kinetic deficiencies are $\delta = \tilde{\delta} = 0$. Moreover, the stoichiometric and kinetic-order subspaces are both $S = \tilde{S} = \mathbb{R}^2$, so they trivially satisfy the sign condition $\sigma(S) \subseteq \overline{\sigma(\tilde{S})}$. By Corollary 3.3.11, the unique positive steady state (shown in Figure 3.13(b) surrounded by periodic orbit) is vertex-balanced.

The next example demonstrates that even having a unique positive steady states that is vertex-balanced is no guarantee that it is stable. The dynamical behaviour of generalized mass-action systems is complicated.

**Example 3.3.16.** Consider the generalized mass-action system $(\mathcal{G}, \mathbf{Y}, \tilde{\mathbf{Y}}, \boldsymbol{\kappa})$ in Figure 3.14. Its associated system of ODEs

$$\frac{dx}{dt} = -x^2 + 2y - 4x + 2y^2$$

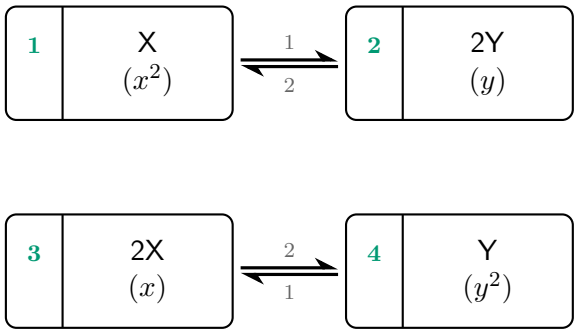


Figure 3.14: A generalized mass-action system with a unique positive steady state, which is vertex-balanced but unstable. The dynamics is shown in Figure 3.15.

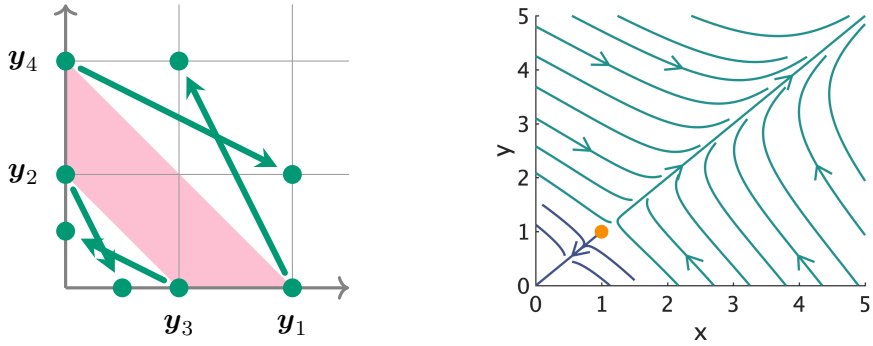


(a) (b)

Figure 3.15: (a) A classical mass-action system (with all rate constants $\kappa_{ij} = 1$) that shares the same dynamics as the generalized mass-action system of Example 3.3.16. (b) Its phase portrait showing that the only positive steady state $(1,1)^\top$ is unstable and most trajectories either converge to the origin or become unbounded.

$$\frac{dy}{dt} = 2x^2 - 4y + 2x - y^2$$

has exactly one positive steady state at $(1,1)^\top$. The same system of ODEs is generated by the classical mass-action system in Figure 3.15(a). It is not difficult to check that $\delta = \tilde{\delta} = 0$, so the steady state is vertex-balanced. However, it is unstable as the phase portrait Figure 3.15(b) shows . Indeed, the Euclidean embedded graph hints that the system is unstable, where for *any* choice of rate constants, trajectories outside of the one dimensional stable manifold either converge to the boundary or towards infinity.

We conclude this chapter with a brief remark on stability of vertex-balanced steady states. As Examples 3.3.15 and 3.3.16 illustrate, vertex-balancing enjoy many of the algebraic properties of complex-balancing; however, dynamics is a different story altogether. One cannot hope, without additional information, for even asymptotic stability. However, if similar to Example 3.3.13, a generalized mass-action system arises as a perturbation of a classical complex-balanced system, by continuity one can conclude the system is asymptotically stable, indeed linearly stable.

More precisely, let $(G, \boldsymbol{\kappa})$ be a complex-balanced system. View the network $G$ as an abstract graph $\mathcal{G}$, and let $\mathbf{Y}$ collect the complex information from $G$. Suppose $\tilde{\mathbf{Y}} \approx \mathbf{Y}$, in the $\ell^2$-norm, and $\sigma(S) \subseteq \overline{\sigma(\tilde{S})}$ where $S$ and $\tilde{S}$ are the stoichiometric and kinetic-order subspaces. Then the generalized mass-action system $(\mathcal{G}, \mathbf{Y}, \tilde{\mathbf{Y}}, \boldsymbol{\kappa})$ has a unique vertex-balanced steady state in its stoichiometric compatibility class that is asymptotically stable within its stoichiometric compatibility class. At the end of Chapter 2, we speculated on when such a generalized mass-action system is actually globally stable. For another work on the stability of vertex-balanced steady states, see [19].

# Chapter 4

# Delay Reaction Kinetics

In this chapter we investigate the stability of mass-action systems with delay. We work with a system of delay differential equations, which is appropriate when the dynamics depends not only on the current state but also at earlier times. In population dynamics and epidemiology, there may be a significant time delay between the initiation of an interaction to the observed effect [21]. In chemistry and biochemistry, time delay can be used to account for protein conformational change, or arises from clumping several reactions into one, simplifying mechanisms [52, 54, 115]. Delay models have also been used for a possible mathematical explanation of chemical oscillators [53].

There are two main types of delays. A system with *discrete delays* involves only the current state and past states at discrete times. For example, consider the SIR model with fixed period temporary immunity [21, 123]. The delay system

$$\begin{aligned}\dot{S}(t) &= -\beta I(t)S(t) + \gamma I(t-\tau)\\ \dot{I}(t) &= \beta I(t)S(t) - \gamma I(t)\\ \dot{R}(t) &= \gamma I(t) - \gamma I(t-\tau)\end{aligned}$$

depends on the current state at time $t$ as well as at a previous time at $t-\tau$ for some $\tau \geq 0$. The corresponding network (with delayed interaction labelled)

$$\mathsf{I} + \mathsf{S} \longrightarrow 2\mathsf{I}$$

$$\mathsf{I} \longrightarrow \mathsf{R} \xrightarrow{\tau} \mathsf{S}$$

illustrates how the delay system is built on top of the standard SIR model; the recovered R once again become suspectible S after a time lag.

A system with *distributed delays* involves the state variable over a continuous time interval, possibly unbounded. Volterra studied a delay predatory-prey model [119, 123]

$$\begin{aligned}\dot{x}(t) &= \kappa_1 x(t) - \kappa_2 x(t) y(t)\\ \dot{y}(t) &= -\kappa_3 y(t) + \kappa_4 \int_{-\infty}^{t} x(\tau) k(t-\tau)\, d\tau\end{aligned}$$

where $k(t-\tau)$ accounts for the time needed between feeding on prey and reproducing offsprings.

Other variations include delays that depend on the current state, on control parameters or functions of time. Similar to the case of ODEs, there are autonomous and non-autonomous delay equations. This chapter deals exclusively with autonomous systems with discrete delays.

Much could still be said about delay systems. For example, their state space, instead of being $\mathbb{R}^n_{\geq}$, is usually the Banach space of continuous (or differentiable) functions on the interval $[-\overline{\tau}, 0]$ where $\overline{\tau}$ is the maximal delay parameter. Initial conditions are also functions over the time interval. We refer the reader to textbooks on the theory of existence of solutions [9, 123]. We now deviate from the approach of previous chapters. While there has been progress extending results about complex-balanced systems [94], we do not impose such stringent condition on our reaction systems. Instead, we study delay reaction systems via linearization.

In this chapter, we focus on mass-action kinetics with delay. In Section 4.1, we linearize a delay mass-action system and discuss the various types of stability. In Section 4.2, we provide an algebraic condition for *absolute stability* — asymptotic stability independent of delay parameters. The conditions are given by principal minors of the *modified Jacobian matrix* (Equation (4.6)), aptly named because it is both a modified version of the Jacobian matrix of the system of ODEs, and the Jacobian matrix of a slightly different reaction network under mass-action kinetics. In Section 4.3, we construct this modified network. The remainder of the chapter aims to give a graph-theoretic condition for *delay stability* — asymptotic stability

independent of delay parameters and rate constants. Section 4.4 introduces the *directed species-reaction graph* while Section 4.5 proves the main result.

## 4.1 Delay mass-action systems

Delay mass-action systems are mass-action systems equipped with delay parameters. For the model to be chemically consistent, we assume that at the moment a reaction occurs, the reactant species are no longer available for other reactions, while product species only become available after a fixed time lag. Moreover, we assume that *inflow* reactions, reactions of the form $0 \to \mathsf{X}$, and *outflow* reactions, those of the form $\mathsf{X} \to 0$, do not admit delays [115]. In fact, *generalized inflow* and *outflow* reactions, those of the form $\alpha\mathsf{X} \to 0$ and $0 \to \alpha\mathsf{X}$ for some $\alpha > 0$, also occur without delays.

As a quick note about notation, in this chapter we take a reaction-centred view. Let $E = \{\boldsymbol{y}_r \to \boldsymbol{y}'_r \,:\, 1 \leq r \leq R\}$ be the set of reactions. When indexing over the set of reactions, as in $r \in E$, we really mean the reaction $\boldsymbol{y}_r \to \boldsymbol{y}'_r$. This choice is to avoid excess subscripts. The rate constant of this reaction is $\kappa_r$ and its delay parameter $\tau_r$.

**Definition 4.1.1.** A ***delay mass-action system*** $(G, \boldsymbol{\kappa}, \boldsymbol{\tau})$ is a mass-action system $(G, \boldsymbol{\kappa})$ with a vector of delays $\boldsymbol{\tau} \in \mathbb{R}^E_{\geq}$. Its associated system of delay differential equations on $\mathbb{R}^n_{\geq}$ is

$$\frac{d\boldsymbol{x}(t)}{dt} = \sum_{r \in E} \kappa_r \left( [\boldsymbol{x}(t - \tau_r)]^{\boldsymbol{y}_r} \boldsymbol{y}'_r - [\boldsymbol{x}(t)]^{\boldsymbol{y}_r} \boldsymbol{y}_r \right). \tag{4.1}$$

**Remark 4.1.2.** In principle, we allow different delay parameters for different product species of the same reaction. For example, in the following modified enzymatic reaction

$$\mathsf{E} + \mathsf{S} \rightleftharpoons \mathsf{SE} \xrightarrow{\tau_{\mathsf{P}},\ \tau_{\mathsf{E}}} \mathsf{E} + \mathsf{P}$$

the product species $\mathsf{P}$ may become available for other reactions after a delay time $\tau_{\mathsf{P}}$, while the enzyme $\mathsf{E}$ might take $\tau_{\mathsf{E}}$ for it to return to its initial conformation. The associated delay

system for this reaction scheme is

$$\begin{aligned}
\frac{d[\mathsf{E}]}{dt} &= -\kappa_1[\mathsf{S}][\mathsf{E}] + \kappa_2[\mathsf{SE}] + \kappa_3[\mathsf{SE}](t-\tau_{\mathsf{E}}) \\
\frac{d[\mathsf{S}]}{dt} &= -\kappa_1[\mathsf{S}][\mathsf{E}] + \kappa_2[\mathsf{SE}] \\
\frac{d[\mathsf{ES}]}{dt} &= \quad \kappa_1[\mathsf{S}][\mathsf{E}] - \kappa_2[\mathsf{SE}] - \kappa_3[\mathsf{SE}] \\
\frac{d[\mathsf{P}]}{dt} &= \qquad\qquad\qquad + \kappa_3[\mathsf{SE}](t-\tau_{\mathsf{P}})
\end{aligned}$$

where dependence on the current time $t$ has been suppressed for simplicity. To avoid unnecessary notation, we assume that $\boldsymbol{\tau} \in \mathbb{R}^E_{\geq}$; however, the reader should keep in mind that different delay parameters for different products is an option.

If there is no delay, i.e., $\boldsymbol{\tau} \equiv \mathbf{0}$, then the delay system reduces to the ODE model (1.4) of a mass-action system [8]. Similar to the ODE model, (4.1) has non-negative solution for initial conditions in $\mathbb{R}^n_{\geq}$ [12, 94]. Moreover, the delay and ODE models share the same *set* of positive steady states [94].

Recall that for a mass-action system (ODE model) with positive initial data $\boldsymbol{\theta} \in \mathbb{R}^n_{>}$, the solution satisfies

$$\boldsymbol{x}(t) - \boldsymbol{\theta} \in S,$$

where $S = \operatorname{span}\{\boldsymbol{y}' - \boldsymbol{y} \,:\, \boldsymbol{y} \to \boldsymbol{y}' \in E\}$ is the *stoichiometric subspace*. Similarly, the delay system (4.1), with continuous and positive initial data $\boldsymbol{\theta}$ defined on the interval $[-\overline{\tau}, 0]$ where $\overline{\tau} = \max\{\tau_r \,:\, r \in E\}$, may admit a conservation relation [94]

$$\boldsymbol{x}(t) - \boldsymbol{\theta}(0) + \sum_{r \in E} \kappa_r \left( \int_{t-\tau_r}^{t} [\boldsymbol{x}(u)]^{\boldsymbol{y}_r}\, du - \int_{-\tau_r}^{0} [\boldsymbol{\theta}(u)]^{\boldsymbol{y}_r}\, du \right) \boldsymbol{y}_r \in S.$$

While the ODE and delay models share the same set of positive equilibria, when $S \subsetneq \mathbb{R}^n$ solving for the delay model's steady states that respect the conservation relation can be difficult. This chapter is only about systems whose stoichiometric subspace $S$ is the whole $\mathbb{R}^n$.

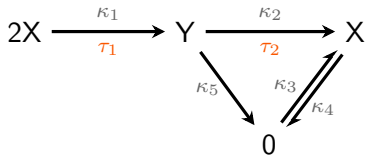


Figure 4.1: The delay mass-action system of Examples 4.1.3, 4.1.5 and 4.2.1.

**Example 4.1.3.** Consider the delay mass-action system in Figure 4.1. Its associated system of delay differential equations

$$\frac{d\boldsymbol{x}(t)}{dt} = \begin{pmatrix} \kappa_3 - \kappa_4 x(t) - 2\kappa_1[x(t)]^2 + \kappa_2 y(t-\tau_2) \\ -\kappa_5 y(t) + \kappa_1[x(t-\tau_1)]^2 - \kappa_2 y(t) \end{pmatrix}$$

has one positive steady state at

$$x^* = \left(\frac{\kappa_2+\kappa_5}{2\kappa_1(\kappa_2+2\kappa_5)}\right)\left(\sqrt{\kappa_4^2 + 4\kappa_1\kappa_3\left(\frac{\kappa_2+2\kappa_5}{\kappa_2+\kappa_5}\right)} - \kappa_4\right) \quad \text{and} \quad y^* = \frac{\kappa_1(x^*)^2}{\kappa_2+\kappa_5}.$$

In general, a delay mass-action system is non-linear. As is the case of non-linear ODEs, we study the local stability of a delay system by linearizing about a positive steady state $\boldsymbol{x}(t) \equiv \boldsymbol{x}^* \in \mathbb{R}^n_>$, assuming a solution of the form $\boldsymbol{x}(t) = \boldsymbol{x}^* + \boldsymbol{u}e^{\lambda t}$ where $\lambda \in \mathbb{C}$, and computing a characteristic equation, which is transcendental rather than polynomial. Where in the complex plane the roots of the characteristic equation are located can determine the asymptotic stability of the steady state $\boldsymbol{x}^*$.

Consider a single reaction $\boldsymbol{y} \to \boldsymbol{y}'$ with rate constant $\kappa = 1$ and delay $\tau \geq 0$. Let $\boldsymbol{x}_\tau(t) = \boldsymbol{x}(t-\tau)$. The associated delay system is

$$\frac{d\boldsymbol{x}(t)}{dt} = [\boldsymbol{x}_\tau(t)]^{\boldsymbol{y}}\boldsymbol{y}' - [\boldsymbol{x}(t)]^{\boldsymbol{y}}\boldsymbol{y}.$$

To linearize, consider a small perturbation from a positive steady state $\boldsymbol{x}^*$, i.e., $\boldsymbol{x}(t) =$

$\boldsymbol{x}^* + \boldsymbol{\delta x}(t)$, where $\boldsymbol{\delta x}(t)$ is a function on $[-\tau, 0]$. The linearized delay system is

$$\frac{d\boldsymbol{\delta x}(t)}{dt} = \underbrace{\left( \frac{\partial \boldsymbol{x}_\tau^{\boldsymbol{y}}}{\partial (x_\tau)_1} \boldsymbol{y}' \quad \dots \quad \frac{\partial \boldsymbol{x}_\tau^{\boldsymbol{y}}}{\partial (x_\tau)_n} \boldsymbol{y}' \right) \Bigg|_{\boldsymbol{x}_\tau(t) \equiv \boldsymbol{x}^*}}_{\mathbf{J}_\tau} \boldsymbol{x}_\tau(t) - \underbrace{\left( \frac{\partial \boldsymbol{x}^{\boldsymbol{y}}}{\partial x_1} \boldsymbol{y} \quad \dots \quad \frac{\partial \boldsymbol{x}^{\boldsymbol{y}}}{\partial x_n} \boldsymbol{y} \right) \Bigg|_{\boldsymbol{x}(t) \equiv \boldsymbol{x}^*}}_{\mathbf{J}_0} \boldsymbol{x}(t).$$

Assuming that $\boldsymbol{\delta x}(t) = \boldsymbol{u} e^{\lambda t}$, we arrive at

$$\lambda \boldsymbol{\delta x} = \frac{d\boldsymbol{\delta x}}{dt} = \underbrace{\left( e^{-\lambda \tau} \mathbf{J}_\tau - \mathbf{J}_0 \right)}_{\mathbf{J}_\lambda} \boldsymbol{\delta x}.$$

In other words, $\lambda \boldsymbol{u} = \mathbf{J}_\lambda \boldsymbol{u}$, which has a non-trivial solution $\boldsymbol{u}$ if and only if $\det(\mathbf{J}_\lambda - \lambda \mathbf{Id}) = 0$.

For a network with more than one reactions, we simply add the relevant terms. Let $(G, \boldsymbol{\kappa}, \boldsymbol{\tau})$ be a delay mass-action system and $\boldsymbol{x}^*$ a positive steady state. Its linearization is

$$\frac{d\boldsymbol{\delta x}(t)}{dt} = \sum_{r \in E} \kappa_r \left( \mathbf{J}_{\tau_r}(\boldsymbol{x}^*, \boldsymbol{\kappa}, \boldsymbol{\tau}) \boldsymbol{x}(t - \tau_r) - \mathbf{J}_r(\boldsymbol{x}^*, \boldsymbol{\kappa}) \boldsymbol{x}(t) \right), \tag{4.2}$$

where

$$\mathbf{J}_{\tau_r}(\boldsymbol{x}, \boldsymbol{\kappa}, \boldsymbol{\tau}) = \begin{pmatrix} \dfrac{\partial \boldsymbol{x}_{\tau_r}^{\boldsymbol{y}_r}}{\partial (x_{\tau_r})_1} \boldsymbol{y}_r' & \dots & \dfrac{\partial \boldsymbol{x}_{\tau_r}^{\boldsymbol{y}_r}}{\partial (x_{\tau_r})_n} \boldsymbol{y}_r' \end{pmatrix}$$

and

$$\mathbf{J}_r(\boldsymbol{x}, \boldsymbol{\kappa}) = \begin{pmatrix} \dfrac{\partial \boldsymbol{x}^{\boldsymbol{y}_r}}{\partial x_1} \boldsymbol{y}_r & \dots & \dfrac{\partial \boldsymbol{x}^{\boldsymbol{y}_r}}{\partial x_n} \boldsymbol{y}_r \end{pmatrix}.$$

Assume a solution of the form $\boldsymbol{x}(t) = \boldsymbol{x}^* + \boldsymbol{u} e^{\lambda t}$, so the linearized equation (4.2) is equivalent

to $\lambda \boldsymbol{u} = \mathbf{J}_\lambda(\boldsymbol{x}^*, \boldsymbol{\kappa}, \boldsymbol{\tau})\boldsymbol{u}$, where

$$\mathbf{J}_\lambda(\boldsymbol{x}, \boldsymbol{\kappa}, \boldsymbol{\tau}) = \sum_{r \in E} \kappa_r \begin{pmatrix} \partial_1 \boldsymbol{x}^{\boldsymbol{y}_r} \left(e^{-\lambda \tau_r} \boldsymbol{y}'_r - \boldsymbol{y}_r\right) & \dots & \partial_n \boldsymbol{x}^{\boldsymbol{y}_r} \left(e^{-\lambda \tau_r} \boldsymbol{y}'_r - \boldsymbol{y}_r\right) \end{pmatrix}, \tag{4.3}$$

with $\partial_i \boldsymbol{x}^{\boldsymbol{y}} = \frac{\partial \boldsymbol{x}^{\boldsymbol{y}}}{\partial x_i}\Big|_{\boldsymbol{x}^*} = \frac{\partial \boldsymbol{x}^{\boldsymbol{y}}_{\tau_r}}{\partial (x_{\tau_r})i}\Big|_{\boldsymbol{x}^*}$ for any $r \in E$. The linearized system has a non-trivial solution $\boldsymbol{u}$ if and only if

$$\det(\mathbf{J}_\lambda(\boldsymbol{x}^*, \boldsymbol{\kappa}, \boldsymbol{\tau}) - \lambda \mathbf{Id}) = 0, \tag{4.4}$$

which is the ***characteristic equation*** of the delay system (4.1).

**Remark 4.1.4.** When $\boldsymbol{\tau} \equiv \mathbf{0}$, the matrix $\mathbf{J}_\lambda$ of (4.3) reduces to the Jacobian matrix of the ODE counterpart:

$$\mathbf{J}(\boldsymbol{x}, \boldsymbol{\kappa}) = \sum_{r \in E} \kappa_r \begin{pmatrix} \partial_1 \boldsymbol{x}^{\boldsymbol{y}_r} \left(\boldsymbol{y}'_r - \boldsymbol{y}_r\right) & \dots & \partial_n \boldsymbol{x}^{\boldsymbol{y}_r} \left(\boldsymbol{y}'_r - \boldsymbol{y}_r\right) \end{pmatrix}. \tag{4.5}$$

**Example 4.1.5.** We continue with Example 4.1.3 and the system in Figure 4.1. The linearization of the delay model is

$$\frac{d\boldsymbol{\delta x}(t)}{dt} = \begin{pmatrix} -(4\kappa_1 x^* + \kappa_4)x(t) + \kappa_2 x(t - \tau_2) \\ -(\kappa_2 + \kappa_5)y(t) + 2\kappa_1 x^* x(t - \tau_1) \end{pmatrix}.$$

We also have

$$\mathbf{J}_\lambda(\boldsymbol{x}, \boldsymbol{\kappa}, \boldsymbol{\tau}) = \begin{pmatrix} -4\kappa_1 x - \kappa_4 & \kappa_2 e^{-\lambda \tau_2} \\ 2\kappa_1 x e^{-\lambda \tau_1} & -\kappa_2 - \kappa_5 \end{pmatrix},$$

whose characteristic equation is the *quasi-polynomial* [9] equation

$$0 = \lambda^2 + \lambda\left(4\kappa_1 x^* + \kappa_2 + \kappa_4 + \kappa_5\right) + \left(4\kappa_1 x^* + \kappa_4\right)\left(\kappa_2 + \kappa_5\right) - 2\kappa_1\kappa_2 x^* e^{-\lambda(\tau_1+\tau_2)}.$$

The characteristic equation is in general a polynomial of $\lambda$ and $\exp(-\lambda\tau_i)$, with coefficients that depend on $\boldsymbol{\kappa}$ and $\boldsymbol{x}^*$. In general, there can be infinitely many roots to the transcendental function, which is analytic on $\mathbb{C}$ [123].

As in the case of ODEs, where the roots of the characteristic equation are with respect to the left half of the complex plane provides information about local stability. A steady state $\boldsymbol{x}^* > \mathbf{0}$ of a delay mass-action system $(G, \boldsymbol{\kappa}, \boldsymbol{\tau})$ is ***asymptotically stable*** if every root of the characteristic equation (4.4) has negative real part; it is said to be ***unstable*** if the characteristic equation has a root with positive real part [123, Theorem 4.8].

We are interested in delay models that are asymptotically stable *independent of the delay parameters* and/or rate constants. The former is described by *absolute stability*, as opposed to *conditional stability*, when asymptotic stability depends on the delay parameters [20].

**Definition 4.1.6.** A mass-action system $(G, \boldsymbol{\kappa})$ is ***absolutely stable*** if for any positive steady state and any choice of delay parameters $\boldsymbol{\tau} \geq \mathbf{0}$, every root of the characteristic equation (4.4) of the delay system $(G, \boldsymbol{\kappa}, \boldsymbol{\tau})$ has negative real part.

**Definition 4.1.7.** A reaction network $G$ is ***delay stable*** if the mass-action system $(G, \boldsymbol{\kappa})$ is absolutely stable for any choice of rate constant $\boldsymbol{\kappa} > \mathbf{0}$. In other words, the delay system $(G, \boldsymbol{\kappa}, \boldsymbol{\tau})$ is asymptotically stable for all $\boldsymbol{\kappa} > \mathbf{0}$ and $\boldsymbol{\tau} \geq \mathbf{0}$.

## 4.2 Algebraic condition for absolute stability

In this section, we provide a sufficient algebraic condition for absolute stability of a delay mass-action system. Since the characteristic equation (4.4) is a transcendental equation, in principle with infinitely many roots, we would like to analyze polynomial equations instead. In

Theorem 4.2.3, we show that if the Jacobian matrix is non-singular and if the principal minors of a certain matrix, which does not involve the delay parameters, are non-positive, then all the roots of the characteristic equation have negative real parts, thus ensuring the asymptotic stability of the delay mass-action system. The result of this section is published in [42].

The ***modified Jacobian matrix*** of a mass-action system $(G, \boldsymbol{\kappa})$ is the $n \times n$ matrix

$$\tilde{\mathbf{J}}(\boldsymbol{x}, \boldsymbol{\kappa}) = \sum_{r \in E} \kappa_r \begin{pmatrix} \partial_1 \boldsymbol{x}^{\boldsymbol{y}_r} \left( \boldsymbol{y}'_r + \tilde{\boldsymbol{y}}_r^{(1)} \right) & \dots & \partial_n \boldsymbol{x}^{\boldsymbol{y}_r} \left( \boldsymbol{y}'_r + \tilde{\boldsymbol{y}}_r^{(n)} \right) \end{pmatrix}, \tag{4.6}$$

where $\tilde{\boldsymbol{y}}^{(j)} = (y_1, \dots, -y_j, \dots y_n)^\top$ is the vector $\boldsymbol{y}$ with a change of sign of its $j$th component. The matrix $\tilde{\mathbf{J}}$ is reminiscent of the Jacobian matrix $\mathbf{J}$ in (4.5); in the $j$th column, we replace each reaction vector $\boldsymbol{y}'_r - \boldsymbol{y}_r$ with $\boldsymbol{y}'_r + \boldsymbol{y}_r^{(j)}$.

**Example 4.2.1.** We continue with Examples 4.1.3 and 4.1.5, i.e., the system shown in Figure 4.1. The modified Jacobian matrix

$$\tilde{\mathbf{J}}(\boldsymbol{x}, \boldsymbol{\kappa}) = \mathbf{J}(\boldsymbol{x}, \boldsymbol{\kappa}) = \begin{pmatrix} -4\kappa_1 x - \kappa_4 & \kappa_2 \\ 2\kappa_1 x & -\kappa_2 - \kappa_5 \end{pmatrix}$$

is identical to the Jacobian matrix of the ODE counterpart. This is true in general if the network contains no *one-step catalysis* reaction. A one-step catalysis is when the same species appears as the reactant and as the product. Delay systems with no one-step catalysis is the focus of Section 4.5. The principal minors of $-\tilde{\mathbf{J}}(\boldsymbol{x}, \boldsymbol{\kappa})$ are $\det(-\tilde{\mathbf{J}}_{[1]}) = 4\kappa_1 x + \kappa_4 > 0$, and $\det(-\tilde{\mathbf{J}}_{[2]}) = \kappa_2 + \kappa_5 > 0$, and

$$\det(-\tilde{\mathbf{J}}) = 2\kappa_1 x(\kappa_2 + 2\kappa_5) + \kappa_4(\kappa_2 + \kappa_5) > 0.$$

It will follow from Theorem 4.2.3 and Corollary 4.2.4 that the reaction network in Figure 4.1 is delay stable, i.e., for any choice of rate constants $\boldsymbol{\kappa} > \mathbf{0}$ and delay parameters $\boldsymbol{\tau} \geq \mathbf{0}$, any positive steady state of the delay mass-action system $(G, \boldsymbol{\kappa}, \boldsymbol{\tau})$ is asymptotically stable.

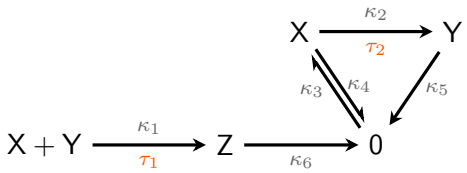


Figure 4.2: The delay mass-action system of Examples 4.2.2 and 4.2.6.

**Example 4.2.2.** Consider the delay mass-action system in Figure 4.2, whose associated delay system is

$$\frac{d\boldsymbol{x}}{dt} = \begin{pmatrix} \kappa_3 - \kappa_4 x - \kappa_1 xy - \kappa_2 x \\ -\kappa_5 y - \kappa_1 xy + \kappa_2 x_{\tau_2} \\ -\kappa_6 z + \kappa_1 x_{\tau_1} y_{\tau_1} \end{pmatrix},$$

where $x_{\tau_i}(t) = x(t-\tau_i)$ and $y_{\tau_i}(t) = y(t-\tau_i)$. The system has one positive steady state $(x^*, y^*, z^*)^\top$. The Jacobian matrix of the ODE model is

$$\mathbf{J}(\boldsymbol{x}, \boldsymbol{\kappa}) = \begin{pmatrix} -\kappa_1 y - \kappa_2 - \kappa_4 & -\kappa_1 x & 0 \\ -\kappa_1 y + \kappa_2 & -\kappa_1 x - \kappa_5 & 0 \\ \kappa_1 y & \kappa_1 x & -\kappa_6 \end{pmatrix},$$

and with the changes highlighted, the modified Jacobian matrix is

$$\tilde{\mathbf{J}}(\boldsymbol{x}, \boldsymbol{\kappa}) = \begin{pmatrix} -\kappa_1 y - \kappa_2 - \kappa_4 & +\kappa_1 x & 0 \\ +\kappa_1 y + \kappa_2 & -\kappa_1 x - \kappa_5 & 0 \\ \kappa_1 y & \kappa_1 x & -\kappa_6 \end{pmatrix}.$$

The characteristic equation can quickly get complicated:

$$\begin{aligned} 0 = e^{-\lambda\tau_2}\left(\lambda\kappa_1\kappa_2 x^* + \kappa_1\kappa_2\kappa_6 x^*\right) + \lambda^3 + \lambda^2\left(\kappa_1(x^*+y^*) + \kappa_2 + \kappa_4 + \kappa_5 + \kappa_6\right) \\ + \lambda\left((\kappa_1 y^* + \kappa_2 + \kappa_4)(\kappa_1 x^* + \kappa_5) - \kappa_1^2 x^* y^* + \kappa_6(\kappa_1(x^*+y^*) + \kappa_2 + \kappa_4 + \kappa_5)\right) \\ + \left(\kappa_6(\kappa_1 y^* + \kappa_2 + \kappa_4)(\kappa_1 x^* + \kappa_5) - \kappa_1^2\kappa_6 x^* y^*\right). \end{aligned}$$

Generally, the characteristic equation is of the form $0 = P(\lambda) + Q(\lambda, e^{-\lambda\tau_i})$, where $P$ and $Q$ are polynomials with coefficients dependent on $\boldsymbol{\kappa}$ and $\boldsymbol{x}^*$.

The theorem below is inspired by [75, Lemma 1], where the off-diagonal terms are dominated by the diagonal ones. Delay terms that appear off-diagonal in $\mathbf{J}_\lambda$ are intimately related to reactions which consume and produce the same species. A reaction $\boldsymbol{y} \to \boldsymbol{y}'$ is said to be ***autocatalytic*** if a chemical species is a reactant as well as a product, and there is a net production of the species; more precisely $\operatorname{supp}(\boldsymbol{y}) \cap \operatorname{supp}(\boldsymbol{y}') \neq \emptyset$, and $y'_p > y_p$ for all $p \in \operatorname{supp}(\boldsymbol{y}) \cap \operatorname{supp}(\boldsymbol{y}')$[1]. We are interested in ***non-autocatalytic networks***, i.e., networks with no autocatalytic reactions. In particular, for any reaction $\boldsymbol{y} \to \boldsymbol{y}'$ in our network and any $p \in \operatorname{supp}(\boldsymbol{y}) \cap \operatorname{supp}(\boldsymbol{y}')$, we have $y'_p \leq y_p$.

Note that $\det \mathbf{J} \neq 0$ is an assumption, a consequence of which is that the network is full rank, i.e., $S = \mathbb{R}^n$ and the system has no conservation relation. The proof uses Gershgorin Circle Theorem, which claims that the spectrum of a matrix lies in disks in $\mathbb{C}$ that are centred on the diagonal value with radius given by $\ell^1$-norm of the rows except the diagonal term. Two matrix properties are used. If all the principal minors are non-negative, we say this matrix is a ***$P_0$-matrix*** [65, 80]. A matrix is ***reducible*** if it can be put into block upper triangular form by simultaneous row and column permutations; otherwise it is ***irreducible***.

**Theorem 4.2.3.** *Let $G$ be a non-autocatalytic network. For any $\boldsymbol{\kappa} > \mathbf{0}$ and $\boldsymbol{\tau} \geq \mathbf{0}$, let $(G, \boldsymbol{\kappa}, \boldsymbol{\tau})$ be the delay mass action system and $\boldsymbol{x}^* > \mathbf{0}$ be a positive steady state. Let $\mathbf{J}_\lambda$, $\mathbf{J}$, and $\tilde{\mathbf{J}}$ be the matrices defined in* (4.3), (4.5), *and* (4.6) *respectively, evaluated at $\boldsymbol{x}^* > \mathbf{0}$, $\boldsymbol{\kappa}$, and $\boldsymbol{\tau}$. Suppose that $\det \mathbf{J} \neq 0$, $[-\tilde{\mathbf{J}}]_{pp} > 0$ for all $1 \leq p \leq n$ and $-\tilde{\mathbf{J}}$ is a $P_0$-matrix. Then every root of the characteristic equation $\det(\mathbf{J}_\lambda - \lambda \mathbf{Id}) = 0$ has negative real part. In particular, the mass-action system $(G, \boldsymbol{\kappa})$ is absolutely stable.*

*Proof.* Any root $\lambda \in \mathbb{C}$ of the characteristic equation (4.4) is not zero because $\mathbf{J}_\lambda$ reduces to

[1] For a comparison, a one-step catalysis does not require a net production of the species, only that $\operatorname{supp}(\boldsymbol{y}) \cap \operatorname{supp}(\boldsymbol{y}') \neq \emptyset$. In particular, an autocatalytic reaction is a one-step catalysis, while the converse may not be true.

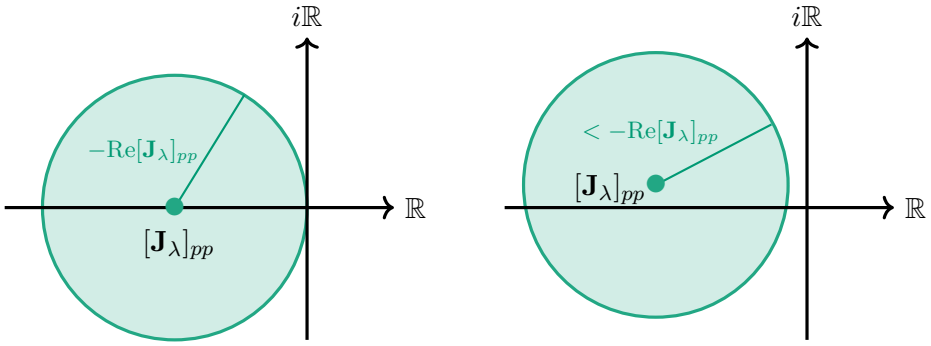


(a) A Gershgorin disk of first case, centred at $[\mathbf{J}_\lambda]_{pp} < 0$ with radius $R_p \leq -\mathrm{Re}[\mathbf{J}_\lambda]_{pp}$.

(b) A Gershgorin disk of second case, centred at $[\mathbf{J}_\lambda]_{pp}$ with $\mathrm{Re}[\mathbf{J}_\lambda]_{pp} < 0$ and has radius $R_p < -\mathrm{Re}[\mathbf{J}_\lambda]_{pp}$.

Figure 4.3: Two types of Gershgorin disks in the proof of Theorem 4.2.3. Any (non-zero) root of the characteristic equation (4.4) always has negative real part.

the non-singular matrix $\mathbf{J}$ when $\lambda = 0$. Suppose for a contradiction that the characteristic equation $\det(\mathbf{J}_\lambda - \lambda \mathbf{Id}) = 0$ has a root $\lambda$ with $\mathrm{Re}(\lambda) \geq 0$. This root is an eigenvalue of $\mathbf{J}_\lambda$. Note that $|e^{-\lambda \tau_r}| \leq 1$. Comparing the off-diagonal terms for $p \neq q$,

$$[\mathbf{J}_\lambda]_{pq} = \sum_{r \in E} \kappa_r \partial_q \boldsymbol{x}^{\boldsymbol{y}_r} \left[ y'_{rp} e^{-\lambda \tau_r} - y_{rp} \right] \quad \text{and} \quad [\tilde{\mathbf{J}}]_{pq} = \sum_{r \in E} \kappa_r \partial_q \boldsymbol{x}^{\boldsymbol{y}_r} \left[ y'_{rp} + y_{rp} \right],$$

we see that $|[\mathbf{J}_\lambda]_{pq}| \leq [\tilde{\mathbf{J}}]_{pq}$, so $[\tilde{\mathbf{J}}]_{pq} \neq 0$ if $[\mathbf{J}_\lambda]_{pq} \neq 0$. Suppose for now that $\tilde{\mathbf{J}}$ is irreducible. Because $-\tilde{\mathbf{J}}$ is an irreducible $P_0$-matrix, there exists a vector $\boldsymbol{v} > \mathbf{0}$ such that $\tilde{\mathbf{J}}\boldsymbol{v} \leq \mathbf{0}$ [65, Theorem 5.8]. In other words, for $p = 1, 2, \ldots, n$, we have

$$[\tilde{\mathbf{J}}]_{pp} v_p + \sum_{q \neq p} [\tilde{\mathbf{J}}]_{pq} v_q \leq 0.$$

Let $\mathbf{D} = \mathrm{diag}(v_1, v_2, \ldots, v_n)$ and consider the matrix $\mathbf{D}^{-1}\mathbf{J}_\lambda\mathbf{D}$, which shares the same eigenvalues as $\mathbf{J}_\lambda$. To apply the Gershgorin Theorem, we look at the disks $B_p$ centred at $[\mathbf{J}_\lambda]_{pp}$ with radius $R_p = v_p^{-1} \sum_{q \neq p} |[\mathbf{J}_\lambda]_{pq}| \, v_q$. For each $p = 1, 2, \ldots, n$, there are two types of disks, as illustrated in Figure 4.3.

The first case concerns $[\mathbf{J}_\lambda]_{pp} \in \mathbb{R}$. More precisely, suppose for every reaction $\boldsymbol{y}_r \to \boldsymbol{y}'_r$ such that $y'_{rp} \neq 0$, we have $e^{-\lambda\tau_r} \in \mathbb{R}$. Necessarily $e^{-\lambda\tau_r} \leq 0$, and

$$[\mathbf{J}_\lambda]_{pp} = \sum_{r\in E} \kappa_r \partial_p \boldsymbol{x}^{\boldsymbol{y}_r} \left[ y'_{rp} e^{-\lambda\tau_r} - y_{rp} \right] \leq \sum_{r\in E} \kappa_r \partial_p \boldsymbol{x}^{\boldsymbol{y}_r} \left[ y'_{rp} - y_{rp} \right] = [\tilde{\mathbf{J}}]_{pp} < 0,$$

where the last inequality follows from our hypothesis on the diagonal of $\tilde{\mathbf{J}}$. Gathering the inequalities thus far, we see that

$$R_p = v_p^{-1} \sum_{q\neq p} |[\mathbf{J}_\lambda]_{pq}|\, v_q \leq v_p^{-1} \sum_{q\neq p} [\tilde{\mathbf{J}}]_{pq} v_q \leq -[\tilde{\mathbf{J}}]_{pp} \leq -[\mathbf{J}_\lambda]_{pp} = -\mathrm{Re}[\mathbf{J}_\lambda]_{pp}.$$

Therefore, the disk $B_p$ is like that of Figure 4.3(a) with centre $[\mathbf{J}_\lambda]_{pp} < 0$ and radius $R_p \leq -\mathrm{Re}[\mathbf{J}_\lambda]_{pp}$. Note that $B_p$ lies in the strict left-half of the complex plane, with the exception of $\{0\}$.

The second case concerns $[\mathbf{J}_\lambda]_{pp} \notin \mathbb{R}$. More precisely, suppose there is at least one reaction $\boldsymbol{y}_r \to \boldsymbol{y}'_r$ in the network for which $y'_{rp} \neq 0$ and $e^{-\lambda\tau_r} \notin \mathbb{R}$, where $\tau_r$ is its delay parameter. For each such reaction,

$$e^{-\lambda\tau_r} = e^{-\mathrm{Re}(\lambda)\tau_r} \left[ \cos(\mathrm{Im}(\lambda)\tau_r) - i \sin(\mathrm{Im}(\lambda)\tau_r) \right],$$

where $\sin(\mathrm{Im}(\lambda)\tau_r) \neq 0$, and hence $\cos(\mathrm{Im}(\lambda)\tau_r) < 1$. It follows that $y'_{rp}\mathrm{Re}(e^{-\lambda\tau_r}) < y'_{rp}$, and

$$\mathrm{Re}[\mathbf{J}_\lambda]_{pp} = \sum_{r\in E} \kappa_r \partial_p \boldsymbol{x}^{\boldsymbol{y}_r} \left[ y'_{rp}\mathrm{Re}(e^{-\lambda\tau_r}) - y_{rp} \right] < \sum_{r\in E} \kappa_r \partial_p \boldsymbol{x}^{\boldsymbol{y}_r} \left[ y'_{rp} - y_{rp} \right] = [\tilde{\mathbf{J}}]_{pp} < 0.$$

From

$$\mathrm{Re}[\mathbf{J}_\lambda]_{pp} v_p + \sum_{q\neq p} |[\mathbf{J}_\lambda]_{pq}|\, v_q < [\tilde{\mathbf{J}}]_{pp} v_p + \sum_{q\neq p} [\tilde{\mathbf{J}}]_{pq} v_q \leq 0, \tag{4.7}$$

we find that

$$R_p = v_p^{-1} \sum_{q \neq p} |[\mathbf{J}_\lambda]_{pq}| \, v_q < -\mathrm{Re}[\mathbf{J}_\lambda]_{pp}.$$

The disk $B_p$ looks like that of Figure 4.3(b), whose centre $[\mathbf{J}_\lambda]_{pp}$ lies in the left-half plane with radius $R_p < -\mathrm{Re}[\mathbf{J}_\lambda]_{pp}$. Note that $B_p$ does not intersect the imaginary axis.

Consequently, for $p = 1, 2, \ldots, n$, any non-zero element in the disk $B_p$ with centre $[\mathbf{J}_\lambda]_{pp}$ and radius $R_p = v_p^{-1} \sum_{q \neq p} |[\mathbf{J}_\lambda]_{pq}| \, v_q$ has negative real part. By the Gershgorin Theorem, the eigenvalues of $\mathbf{D}^{-1}\mathbf{J}_\lambda\mathbf{D}$ are contained in the union of the disks $B_p$, so any non-zero eigenvalue of $\mathbf{J}_\lambda$ has negative real part. This contradicts our assumption that $\mathrm{Re}(\lambda) \geq 0$.

Now suppose that $\tilde{\mathbf{J}}$ is reducible. Up to a permutation of basis, we may assume that $\tilde{\mathbf{J}}$ is an upper block triangular matrix with irreducible blocks along the diagonal [75]. The principal minors of $\tilde{\mathbf{J}}$ are unchanged. For every off-diagonal entry, $[\tilde{\mathbf{J}}]_{pq} = 0$ implies $[\mathbf{J}_\lambda]_{pq} = 0$, so each irreducible diagonal block of $\tilde{\mathbf{J}}$ corresponds to a (possibly reducible) diagonal block of $\mathbf{J}_\lambda$. So $\det(\mathbf{J}_\lambda - \lambda\mathbf{Id})$ is the product of $\det(\mathbf{M}_j - \lambda\mathbf{Id})$, where each $\mathbf{M}_j$ is a diagonal block of $\mathbf{J}_\lambda$ corresponding to an irreducible diagonal block of $\tilde{\mathbf{J}}$. Since $\lambda$ is an eigenvalue of $\mathbf{J}_\lambda$, it is an eigenvalue of some $\mathbf{M}_j$. Now the argument above can be applied to the corresponding irreducible $P_0$-block of $\tilde{\mathbf{J}}$. Because $\mathbf{J} = \mathbf{J}(\boldsymbol{x}^*, \boldsymbol{\kappa})$ and $\tilde{\mathbf{J}} = \tilde{\mathbf{J}}(\boldsymbol{x}^*, \boldsymbol{\kappa})$ are independent of the delay parameters $\boldsymbol{\tau}$, absolute stability follows. □

Delay stability — linear stability independent of delay parameters and rate constants — follows from Theorem 4.2.3 when the hypotheses of the theorem holds for all $\boldsymbol{\kappa}$ and $\boldsymbol{x}^*$. In Section 4.5 we give a graph-theoretic condition sufficient for delay stability.

**Corollary 4.2.4.** *Let $G$ be a non-autocatalytic network. Let $\mathbf{J}$ and $\tilde{\mathbf{J}}$ be the matrices defined in* (4.5) *and* (4.6) *respectively, as functions of $\boldsymbol{\kappa} > \mathbf{0}$ and $\boldsymbol{x} > \mathbf{0}$. Suppose that* $\det(\mathbf{J}) \neq 0$, $[\tilde{\mathbf{J}}]_{pp} < 0$ *for all* $1 \leq p \leq n$ *and $-\tilde{\mathbf{J}}$ is a $P_0$-matrix for all $\boldsymbol{\kappa}$ and any steady state $\boldsymbol{x}$ of the mass-action system $(G, \boldsymbol{\kappa})$. Then $G$ is delay stable.*

**Remark 4.2.5.** Although Theorem 4.2.3 and Corollary 4.2.4 are stated explicitly for mass-action systems, the results hold for more general kinetics under mild assumptions. More precisely, the results hold when the rate function $\nu(\boldsymbol{x})$ for any reaction $\boldsymbol{y} \to \boldsymbol{y}'$ is non-decreasing, i.e., $\partial_p \nu \geq 0$ for all $p$, and monotically depends on the reactant species, i.e., $\partial_p \nu > 0$ whenever $p \in \operatorname{supp}(\boldsymbol{y}) = \{i : \ y_i \neq 0\}$. The difference in the proof lies with the strict inequality in (4.7).

**Example 4.2.6.** We apply Corollary 4.2.4 to Example 4.2.2 and the system in Figure 4.2. The network has no autocatalytic reaction, and

$$\det(\mathbf{J}) = -\kappa_6 \left[\kappa_1\kappa_5 y + 2\kappa_1\kappa_2 x + (\kappa_2 + \kappa_4)\kappa_5\right] \neq 0.$$

It is clear from the expression of the modified Jacobian matrix $\tilde{\mathbf{J}}(\boldsymbol{x}, \boldsymbol{\kappa})$ in Example 4.2.2 that the $1 \times 1$ and $2 \times 2$ principal minors of $-\tilde{\mathbf{J}}$ are always strictly positive. Moreover,

$$\det(-\tilde{\mathbf{J}}) = \kappa_6 \left[\kappa_1\kappa_4 x + \kappa_1\kappa_5 y + \kappa_5(\kappa_2 + \kappa_4)\right] > 0$$

for any $\boldsymbol{x} > \mathbf{0}$ and $\boldsymbol{\kappa} > \mathbf{0}$. Therefore $-\tilde{\mathbf{J}}$ is a $P_0$-matrix. By Corollary 4.2.4, the reaction network in Figure 4.2 is delay stable.

So far, we have reduced the difficult problem of analyzing the transcendental characteristic equation to more tenable polynomial equations that are the principal minors of the modified Jacobian matrix. The name of this matrix goes beyond the mere fact that we modified some terms in the Jacobian matrix; we show that the matrix is the Jacobian matrix of a different mass-action system. The rest of the chapter is devoted to constructing this other reaction network and providing a graph-theoretic condition for when the modified Jacobian matrix is a $P_0$-matrix.

## 4.3 Modified Jacobian and its reaction network

In this section, we describe how to construct a mass-action system whose Jacobian matrix is the modified Jacobian matrix (4.6). For the purpose of communication, we refer to the

starting network as the "original network" and the newly constructed network as the "modified network". The precise language needed obscures the simplicity of the construction. We introduce the procedure via an example.

**Example 4.3.1.** The mass-action system

$$\mathsf{X} + \mathsf{Y} \underset{\kappa_2}{\overset{\kappa_1}{\rightleftharpoons}} 2\mathsf{Z}$$

$$\mathsf{X} + 2\mathsf{Y} + \mathsf{Z} \xrightarrow{\kappa_3} \mathsf{W} \xrightarrow{\kappa_4} 0$$

has

$$\tilde{\mathbf{J}}(\boldsymbol{x}, \boldsymbol{\kappa}) = \begin{pmatrix} -\kappa_1 y - \kappa_3 y^2 z & \kappa_1 x + 2\kappa_3 xyz & 2\kappa_2 z + \kappa_3 x y^2 & 0 \\ \kappa_1 y + 2\kappa_3 y^2 z & -\kappa_1 x - 4\kappa_3 xyz & 2\kappa_2 z + 2\kappa_3 x y^2 & 0 \\ 2\kappa_1 y + \kappa_3 y^2 z & 2\kappa_1 x + 2\kappa_3 xyz & -4\kappa_2 z - \kappa_3 x y^2 & 0 \\ \kappa_3 y^2 z & 2\kappa_3 xyz & \kappa_3 x y^2 & -\kappa_4 \end{pmatrix}$$

as its modified Jacobian matrix. In constructing our modified network, we do not change the reactions involving less than two reactant species. For any reaction involving two or more reactant species, we create new reactions where the reactant species are migrated to the product side; for example, the reaction $\mathsf{X} + \mathsf{Y} \to 2\mathsf{Z}$ splits into two reactions: $\mathsf{X} \to 2\mathsf{Z} + \mathsf{Y}$ and $\mathsf{Y} \to 2\mathsf{Z} + \mathsf{X}$.

Fix a positive state $\boldsymbol{x}^* = (x^*, y^*, z^*, w^*)^\top$. The modified mass-action system $(\widetilde{G}, \tilde{\boldsymbol{\kappa}})$ contains the reactions

$$\mathsf{W} \xrightarrow{\kappa_4} 0 \qquad \mathsf{X} \xrightarrow{\kappa_1 y^*} 2\mathsf{Z} + \mathsf{Y} \qquad \mathsf{X} \xrightarrow{\kappa_3 (y^*)^2 z^*} \mathsf{W} + 2\mathsf{Y} + \mathsf{Z}$$

$$2\mathsf{Y} \xrightarrow{\kappa_3 x^* z^*} \mathsf{W} + \mathsf{X} + \mathsf{Z}$$

$$2\mathsf{Z} \xrightarrow{\kappa_2} \mathsf{X} + \mathsf{Y} \qquad \mathsf{Y} \xrightarrow{\kappa_1 x^*} 2\mathsf{Z} + \mathsf{X} \qquad \mathsf{Z} \xrightarrow{\kappa_3 x^* (y^*)^2} \mathsf{W} + \mathsf{X} + 2\mathsf{Y}$$

and whose Jacobian matrix is

$$\mathbf{J}(\boldsymbol{x};\tilde{\boldsymbol{\kappa}}(\boldsymbol{\kappa},\boldsymbol{x}^*)) = \begin{pmatrix} -\kappa_1 y^* - \kappa_3 (y^*)^2 z^* & \kappa_1 x^* + 2\kappa_3 x^* z^* y & 2\kappa_2 z + \kappa_3 x^* (y^*)^2 & 0 \\ \kappa_1 y^* + 2\kappa_3 (y^*)^2 z^* & -\kappa_1 x^* - 4\kappa_3 x^* z^* y & 2\kappa_2 z + 2\kappa_3 x^* (y^*)^2 & 0 \\ 2\kappa_1 y^* + \kappa_3 (y^*)^2 z^* & 2\kappa_1 x^* + 2\kappa_3 x^* z^* y & -4\kappa_2 z - \kappa_3 x^* (y^*)^2 & 0 \\ \kappa_3 (y^*)^2 z^* & 2\kappa_3 x^* z^* y & \kappa_3 x^* (y^*)^2 & -\kappa_4 \end{pmatrix},$$

which depends on $\boldsymbol{x}^* = (x^*, y^*, z^*, w^*)^\top$ as well as $\boldsymbol{x} = (x, y, z, w)^\top$. In particular, $\tilde{\mathbf{J}}(\boldsymbol{x}^*, \boldsymbol{\kappa}) = \mathbf{J}(\boldsymbol{x}^*; \tilde{\boldsymbol{\kappa}}(\boldsymbol{\kappa}, \boldsymbol{x}^*))$.

It is worth emphasizing that the modified Jacobian matrix $\tilde{\mathbf{J}}(\boldsymbol{x}, \boldsymbol{\kappa})$ happens to be the Jacobian matrix of another mass-action system, with carefully chosen rate constants and at a specific state. The two mass-action systems do not necessarily share the same set of steady states. There are generally more reactions in the modified network, and more importantly, its rate constants depend on a chosen state of the original system.

For the general procedure to construct the modified network, consider a mass-action system $(G, \boldsymbol{\kappa})$ consisting of a single reaction:

$$a_1\mathsf{X} + a_2\mathsf{Y} + a_3\mathsf{Z} \xrightarrow{\kappa} b_1\mathsf{X} + b_2\mathsf{Y} + b_3\mathsf{Z} + b_4\mathsf{W}$$

with $a_1$, $a_2$, $a_3 > 0$ and $b_1, \ldots, b_4 \geq 0$. Fix a positive state $\boldsymbol{x}^*$. Define the modified mass-action system $(\widetilde{G}, \tilde{\boldsymbol{\kappa}})$ with the reactions

$$a_1\mathsf{X} \xrightarrow{\tilde{\kappa}_1} b_1\mathsf{X} + (a_2 + b_2)\mathsf{Y} + (a_3 + b_3)\mathsf{Z} + b_4\mathsf{W}$$

$$a_2\mathsf{Y} \xrightarrow{\tilde{\kappa}_2} (a_1 + b_1)\mathsf{X} + b_2\mathsf{Y} + (a_3 + b_3)\mathsf{Z} + b_4\mathsf{W}$$

$$a_3\mathsf{Z} \xrightarrow{\tilde{\kappa}_3} (a_1 + b_1)\mathsf{X} + (a_2 + b_2)\mathsf{Y} + b_3\mathsf{Z} + b_4\mathsf{W}$$

where $\tilde{\kappa}_1 = \kappa (y^*)^{a_2} (z^*)^{a_3}$, $\tilde{\kappa}_2 = \kappa (x^*)^{a_1} (z^*)^{a_3}$ and $\tilde{\kappa}_3 = \kappa (x^*)^{a_1} (y^*)^{a_2}$.

The matrix $\mathbf{J}(\boldsymbol{x};\tilde{\boldsymbol{\kappa}}(\boldsymbol{\kappa},\boldsymbol{x}^*))$ has contributions from three reactions, each filling a column:

$$\mathbf{J}(\boldsymbol{x};\tilde{\boldsymbol{\kappa}}(\boldsymbol{\kappa},\boldsymbol{x}^*)) = \begin{pmatrix} \tilde{\kappa}_1\partial_1 x^{a_1}(b_1-a_1) & \tilde{\kappa}_2\partial_2 y^{a_2}(b_2+a_2) & \tilde{\kappa}_3\partial_3 z^{a_3}(b_3+a_3) & 0 \\ \tilde{\kappa}_1\partial_1 x^{a_1}(b_1+a_1) & \tilde{\kappa}_2\partial_2 y^{a_2}(b_2-a_2) & \tilde{\kappa}_3\partial_3 z^{a_3}(b_3+a_3) & 0 \\ \tilde{\kappa}_1\partial_1 x^{a_1}(b_1+a_1) & \tilde{\kappa}_2\partial_2 y^{a_2}(b_2+a_2) & \tilde{\kappa}_3\partial_3 z^{a_3}(b_3-a_3) & 0 \\ \tilde{\kappa}_1\partial_1 x^{a_1}(b_4) & \tilde{\kappa}_2\partial_2 y^{a_2}(b_4) & \tilde{\kappa}_3\partial_3 z^{a_3}(b_4) & 0 \end{pmatrix}.$$

In each column, there is a sign change off-diagonal, just as one expects in the modified Jacobian matrix $\tilde{\mathbf{J}}$ of the network $G$. Moreover, the coefficient, say in first column, is

$$\tilde{\kappa}_1\partial_1 x^{a_1} = \kappa a_1 x^{a_1-1}(y^*)^{a_2}(z^*)^{a_3}.$$

Thus, when $\boldsymbol{x}=\boldsymbol{x}^*$, the modified Jacobian matrix $\tilde{\mathbf{J}}(\boldsymbol{x}^*,\boldsymbol{\kappa})$ is exactly $\mathbf{J}(\boldsymbol{x}^*;\tilde{\boldsymbol{\kappa}}(\boldsymbol{\kappa},\boldsymbol{x}^*))$.

The construction above generalizes to reactions involving even more species. What is remarkable is that the resulting modified network does not depend on the choice of rate constants and the positive state. We now formally state the construction for a general reaction network. Let $\hat{\mathbf{e}}_i$ be the $i$th standard basis vector of $\mathbb{R}^n$.

**Definition 4.3.2.** Let $(G,\boldsymbol{\kappa})$ be a mass-action system, and fix a positive state $\boldsymbol{x}^*$. Let $\tilde{E}$ be the set of the following reactions, with rate constants $\tilde{\boldsymbol{\kappa}}$ as specified:

(a) any reaction $\boldsymbol{y}\to\boldsymbol{y}'\in E$ with $|\operatorname{supp}(\boldsymbol{y})|\leq 1$, with rate constant $\kappa_{\boldsymbol{y}\to\boldsymbol{y}'}$, and

(b) for any $\boldsymbol{y}\to\boldsymbol{y}'\in E$ with $|\operatorname{supp}(\boldsymbol{y})|\geq 2$ and any $p\in\operatorname{supp}(\boldsymbol{y})$, the reactions

$$y_p\hat{\mathbf{e}}_p \to \boldsymbol{y}'+\boldsymbol{y}-y_p\hat{\mathbf{e}}_p,$$

with rate constant $\kappa_{\boldsymbol{y}\to\boldsymbol{y}'}(\boldsymbol{x}^*)^{\boldsymbol{y}}/(x_p^*)^{y_p}$.

Let $\tilde{V}$ be the set of source and target complexes of the reactions in $\tilde{E}$. Then $\widetilde{G}=(\tilde{V},\tilde{E})$ is the ***modified network*** of $G$ and $(\widetilde{G},\tilde{\boldsymbol{\kappa}})$ is the ***modified mass-action system*** at $\boldsymbol{x}^*$.

**Proposition 4.3.3.** *Let* $(G, \boldsymbol{\kappa}, \boldsymbol{\tau})$ *be a delay mass-action system, and* $\tilde{\mathbf{J}}$ *be the modified Jacobian matrix* (4.6) *evaluated at some positive state* $\boldsymbol{x}^*$*. Let* $(\widetilde{G}, \tilde{\boldsymbol{\kappa}})$ *be the modified mass-action system at* $\boldsymbol{x}^*$*. Then* $\tilde{\mathbf{J}}$ *is the Jacobian matrix of* $(\widetilde{G}, \tilde{\boldsymbol{\kappa}})$ *evaluated at* $\boldsymbol{x}^*$*.*

The proof of this proposition follows by treating each reaction as in the sample calculation above, and noting that the Jacobian matrix is linear with respect to reactions.

## 4.4 The directed species-reaction (DSR) graph

The aim of this section is to introduce the *directed species-reaction graph* (DSR graph) [33], and in Section 4.5 we provide a condition on the DSR graphs of the original and modified networks that is sufficient to conclude delay stability.

The DSR graph, and its closely related cousin the *species-reaction graph* were used to study *injectivity* of a reaction network, i.e., the negative Jacobian is positive for any positive rate constants and at any positive state [32, 33, 36, 37]. In particular, injectivity can be used to rule out the capacity for *multistationarity*, since an injective network cannot admit multiple positive steady states for any choice of rate constants.

The DSR graph can also be used to study stability of matrices [6, 7]. A $n \times m$ matrix $\mathbf{M}$ is naturally associated to a bipartite graph with $n + m$ vertices, where an edge connects vertices $i$ and $j$ if and only if $[\mathbf{M}]_{ij} \neq 0$. Sign information can also be recorded as labels on the edges. Each cycle in the graph corresponds to a minor expansion. For example, a cycle $\langle i, j, k, \ell \rangle$ is associated to the minor with rows $i$, $k$ and columns $j$ and $\ell$. There are other variants of the DSR graph, including Petri nets from computer science and Volpert's graph for chemical reactions. We focus on a version that is a hybrid of what is defined in [37] and [33].

In the previous section, we have considered non-autocatalytic networks, i.e., there is no *net* production of a chemical species involved both as a reactant and a product. In this section, we further restrict ourselves to networks with *no* ***one-step catalysis***. A reaction is a one-step catalysis if a species appears as a reactant as well as a product. Hence, for a network

with no one-step catalysis, we have $\mathrm{supp}(\boldsymbol{y}) \cap \mathrm{supp}(\boldsymbol{y}') = \emptyset$ for any reaction $\boldsymbol{y} \to \boldsymbol{y}'$.

In this more restrictive setting, the DSR graph takes on a simpler form. Here, we give a definition of the directed species-reaction graph that is sufficient for our purpose. We first illustrate how a DSR graph is drawn for a given network.

**Example 4.4.1.** Consider the reaction network

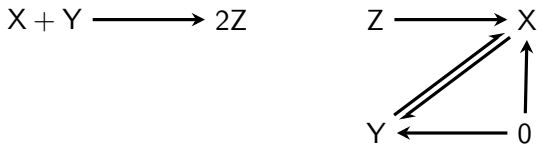


with three species and five edges, one of which is a reversible pair. Two reactions ($0 \to X$ and $0 \to Y$) are inflows and will not appear in DSR graph. Its DSR graph, shown in Figure 4.4, contains three species node and three reaction nodes. For the reaction $X + Y \to 2Z$, the source species X and Y are connected to the reaction node by undirected edges, which are labelled with their *stoichiometric coefficients* (1 and 1 respectively). The product species Z receives an incoming edge from the reaction node, labelled with its stoichiometric coefficient 2. For a reversible reaction like that of $X \rightleftharpoons Y$, the edges connecting the reaction node and the corresponding species nodes are undirected. In a DSR graph, an undirected edge should be understood as bidirectional.

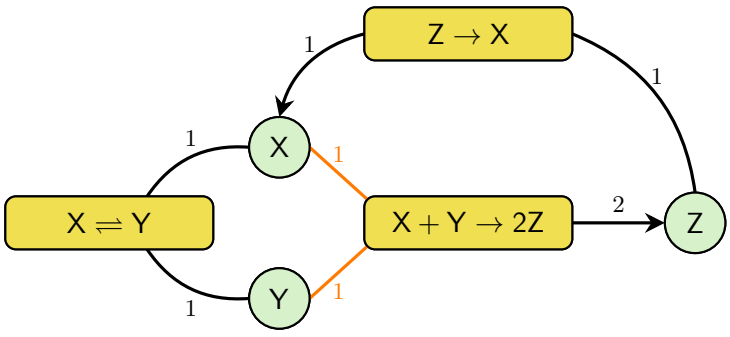


Figure 4.4: The DSR graph of Examples 4.4.1 and 4.4.5. The edges (orange) connecting the S-nodes X and Y to the R-node of the bispecies reaction is a *c-pair* (Definition 4.4.4).

Let $G = (V, E)$ be a network with $n$ species and no one-step catalysis. Let $E^*$ denote the subset of reactions that are neither (generalized) inflows nor outflows[2], with the caveat that any reversible pair of reactions count as one element. In other words,

$$E^* = \Big\{ \{\boldsymbol{y}, \boldsymbol{y}'\} \,:\, \boldsymbol{y},\, \boldsymbol{y}' \neq \mathbf{0}, \text{ and either } \boldsymbol{y} \to \boldsymbol{y}' \text{ or } \boldsymbol{y}' \to \boldsymbol{y} \in E \Big\}.$$

The DSR graph of $G$ then consists of $n$ S-nodes, one for each species, and $|E^*|$ R-nodes, one for each element of $E^*$.

**Definition 4.4.2.** A ***directed species-reaction graph*** (***DSR-graph***) $\mathfrak{D} = (\mathcal{V}_S, \mathcal{V}_R, \mathcal{E}, \sigma)$ is a bipartite graph $(\mathcal{V}_S, \mathcal{V}_R, \mathcal{E})$ with a map $\sigma \colon \mathcal{E} \to \mathbb{R}_>$. Vertices in $\mathcal{V}_S$ are ***S-nodes*** (***species nodes***), while those in $\mathcal{V}_R$ are ***R-nodes*** (***reaction nodes***). Each edge in $\mathcal{E}$, either oriented or unoriented, is assigned a ***stoichiometric coefficient*** by the map $\sigma$.

To simplify the language, we refer to a S-node as if it is the species, and a R-node as if it is the relevant reaction. For example, an R-node $\mathsf{R}$ is irreversible if the corresponding reaction in the network is irreversible. Any edge in the DSR graph will be denoted by the ordered pair in $\mathcal{V}_S \times \mathcal{V}_R$; whether it is oriented or not will be explicitly stated.

An edge connects a S-node $\mathsf{X}_i$ and a R-node $\mathsf{R}$ if and only if $\mathsf{X}_i$ participates as a reactant or product species in the reaction (pair) $\mathsf{R}$. The edge is oriented from $\mathsf{R}$ to $\mathsf{X}_i$ if $\mathsf{R}$ is an irreversible reaction and $\mathsf{X}_i$ is a product; otherwise it is unoriented. Finally, suppose the species $\mathsf{X}_i$ participates in a reaction corresponding to $\mathsf{R} = \{\boldsymbol{y}, \boldsymbol{y}'\}$ (either $\boldsymbol{y} \to \boldsymbol{y}'$ or $\boldsymbol{y} \rightleftharpoons \boldsymbol{y}'$), the stoichiometric coefficient of the edge $(\mathsf{X}_i, \mathsf{R})$ is the non-zero coefficient $y_i + y_i' = \max\{y_i,\, y_i'\}$.

**Remark 4.4.3.** DSR graph is defined for more general reaction networks. If the network has a one-step catalysis, its DSR graph is a multigraph [33, 37]. For example, the DSR graph of the reaction $\mathsf{X} + \mathsf{Y} \to 2\mathsf{X}$ has two edges between the S-node $\mathsf{X}$ and the R-node, one of which is unoriented and assigned a stoichiometric coefficient 1, while the other is oriented and assigned a coefficient 2. In this work, we avoid any one-step catalysis.

[2] By generalized inflows and outflows, we mean reactions of the form $a\mathsf{X} \to \mathsf{0}$ or $\mathsf{0} \to a\mathsf{X}$ for some $a > 0$.

The aim is to deduce information about the determinant of the Jacobian matrix from the DSR graph [32, 33, 37]. Cycles in the DSR graph are of interest to us. A subset of edges defines a subgraph of the DSR graph. A *path* is an open simple walk compatible with any edge orientation (whenever present), and a *cycle* is a closed simple walk compatible with any edge orientation. If $C_1$ and $C_2$ are two cycles, the intersection $C_1 \cap C_2$ is non-empty if there is at least one edge in $C_1 \cap C_2$, and the orientation (whenever present) of every edge is consistent with that of $C_1$ and also that of $C_2$.

**Definition 4.4.4.** Let $\mathfrak{D} = (\mathcal{V}_S, \mathcal{V}_R, \mathcal{E}, \sigma)$ be the DSR graph of a reaction network with no one-step catalysis.

(a) A ***c-pair*** (***complex-pair***) is a pair of edges adjacent to a R-node such that the two adjacent species are reactants in the same reaction.

(b) A cycle is an ***e-cycle*** (***even-cycle***) if it contains an even number of c-pairs.

(c) A cycle is an ***o-cycle*** (***odd-cycle***) if it contains an odd number of c-pairs.

(d) Alternatingly multiply and divide the stoichiometric coefficients along a cycle. If the result is equal to 1, then the cycle is an ***s-cycle***.

(e) Two cycles $C_1$ and $C_2$ have an ***S-to-R intersection*** if $C_1 \cap C_2$ consists of paths that start at an S-node and terminate at an R-node. We say $\mathfrak{D}$ ***has an S-to-R intersection*** if there exist two cycles in $\mathfrak{D}$ with an S-to-R intersection.

**Example 4.4.5.** We revisit the DSR graph in Figure 4.4. The highlighted (orange) edges connecting the S-nodes $\mathsf{X}$ and $\mathsf{Y}$, to the R-node of the irreversible bispecies reaction, form a c-pair. There are three cycles in the DSR graph: the left-most cycle $C_1$ contains only the S-nodes $\mathsf{X}$ and $\mathsf{Y}$; the upper-right cycle $C_2$ contains only the S-nodes $\mathsf{X}$ and $\mathsf{Z}$; and running along the outer edges of the graph, $C_3$ contains all three S-nodes. The left-most cycle $C_1$ passing through only $\mathsf{X}$ and $\mathsf{Y}$ is a s-cycle and an o-cycle, since all stoichiometric coefficients are 1 and $C_1$ contains the c-pair. The cycle $C_2$ passing through only $\mathsf{X}$ and $\mathsf{Z}$ is *not* a s-cycle,

but it is an e-cycle. The cycle $C_3$ passing through all S-nodes is an e-cycle but not a s-cycle. Finally, $C_1$ and $C_2$ have a S-to-R intersection, since $C_1 \cap C_2$ is half of the c-pair inheriting the orientations of the two cycles. Similarly, $C_1$ and $C_3$ have a S-to-R intersection. However, $C_2$ and $C_3$ do not have a S-to-R intersection even though $C_2 \cap C_3 \neq \emptyset$.

Cycles in the DSR graph are intimately connected to the principal minors of the Jacobian matrix [6, 7, 32, 33, 37].

**Theorem 4.4.6.** *Let $G$ be a network with no one-step catalysis, and there is an outflow for every species. Suppose its DSR graph satisfies the following conditions:*

(a) *all cycles are o-cycles or s-cycles, and*

(b) *no two e-cycles have a S-to-R intersection.*

*Then the negative Jacobian matrix $-\mathbf{J}$ of the mass-action system $(G, \boldsymbol{\kappa})$ is a $P_0$-matrix for any $\boldsymbol{\kappa}$ and $\boldsymbol{x} > \mathbf{0}$. Moreover,* $\det(-\mathbf{J}) > 0$.

More is true than what we have stated here. Not only are the principal minors of $-\mathbf{J}$ non-negative, but that each of them are positive combinations of monomials in $\boldsymbol{\kappa}$ and $\boldsymbol{x}^*$ [36].

In Section 4.2, we gave an algebraic condition for delay stability based on the modified Jacobian matrix $\tilde{\mathbf{J}}$. We then related $\tilde{\mathbf{J}}$ to the Jacobian matrix of a different mass-action system in Proposition 4.3.3. Therefore, by Theorem 4.4.6 delay stability follows if the modified mass-action system has a DSR graph that satisfies the above graph theoretic conditions.

Furthermore, our construction of the modified network always results in reactions involving at most one reactant species, so there is *no* c-pair in the DSR graph of the modified network, and all cycles are e-cycles. This simplifies Theorem 4.4.6.

**Corollary 4.4.7.** *Let $G$ be a network with no one-step catalysis, and there is an outflow for every species. For any choice of rate constants $\boldsymbol{\kappa} > \mathbf{0}$, let $(G, \boldsymbol{\kappa})$ denote the mass-action system,*

*and let* $(\widetilde{G}, \tilde{\boldsymbol{\kappa}})$ *be its modified mass-action system at any positive state* $\boldsymbol{x}^* > \mathbf{0}$*, with Jacobian matrix* $\tilde{\mathbf{J}}$*. Suppose the DSR graph* $\tilde{\mathfrak{D}}$ *of* $\tilde{G}$ *satisfies the following conditions:*

(a) *all cycles are s-cycles, and*

(b) *there is no S-to-R intersection.*

*Then* $-\tilde{\mathbf{J}}$ *is a* $P_0$*-matrix, and* $\det(-\tilde{\mathbf{J}}) > 0$*.*

## 4.5 DSR-graph condition for delay stability

In this section, we relate the DSR graphs of a reaction network and that of the modified network. In general, the modified network has many more reactions than the original, and its DSR graph contains more nodes and cycles. Moreover, the modified network is an artifact of the proof of Theorem 4.2.3; it may not have any biological relevance. The aim is to deduce delay stability based on the structure of the DSR graph of the original network instead of that of the modified network.

For the main result of this section, we require four assumptions on the network.

**(N1)** Every species has a generalized outflow, i.e., $a_i\mathsf{X}_i \to 0$ for some $a_i > 0$ is a reaction.

**(N2)** The network has no one-step catalysis, i.e., $\operatorname{supp}(\boldsymbol{y}) \cap \operatorname{supp}(\boldsymbol{y}') = \emptyset$ for any reaction $\boldsymbol{y} \to \boldsymbol{y}'$.

**(N3)** Every reaction has at most two different reactant species, i.e., $|\operatorname{supp}(\boldsymbol{y})| \leq 2$ for any reaction $\boldsymbol{y} \to \boldsymbol{y}'$.

**(N4)** Any bispecies reaction is irreversible.

Many reasonable biochemical systems satisfy **(N1)** and **(N3)**. Condition **(N1)** typically reflects the natural degradation of molecules. Condition **(N3)** is similar to, but more relaxed than, the common assumption that a reaction requiring three participating molecules is a rare

event and can be safely neglected from the model.

The remainder of this section is structured as follows. First we state the main results; then apply them to several networks. Next we illustrate by way of examples the difference between the DSR graphs of the original and modified networks. Finally we state and prove a series of lemmas, leading to a proof of the main theorem. We have chosen to structure the section this way because the last proof is technical and not particularly enlightening, and the reader may feel justified to skip the proof if so desired.

**Definition 4.5.1.** Let $\mathsf{R}$ be a R-node of an irreversible reaction involving two reactant species. Let $\mathsf{X}$ be a S-node corresponding to one of the *product* species of the reaction. The edge $(\mathsf{X}, \mathsf{R})$ in $\mathfrak{D}$ is a ***bispecies production edge***.

To conclude delay stability, we would like to avoid cycles with bispecies production edges. Such a cycle can be interpreted as a feedback loop. For example, the reaction network

$$\mathsf{X} + \mathsf{Y} \longrightarrow \mathsf{Z} \longrightarrow \mathsf{X}$$

whose DSR graph, shown in Figure 4.10(a) has a cycle with a bispecies production edge. This cycle points out that the product $\mathsf{Z}$ of a bispecies reaction is eventually used to feed the production of reactant $\mathsf{X}$. The main results of this section are the following.

**Theorem 4.5.2.** *Let $G$ be a reaction network satisfying conditions **(N2)**–**(N4)**. For any vector of rate constants $\boldsymbol{\kappa} > \mathbf{0}$, let $(G, \boldsymbol{\kappa})$ denote the mass-action system, and let $(\widetilde{G}, \tilde{\boldsymbol{\kappa}})$ be its modified mass-action system at any positive state. In the DSR graph $\tilde{\mathfrak{D}}$ of the network $\tilde{G}$,*

(i) *all cycles are s-cycles, and*

(ii) *there is no S-to-R intersection,*

*if and only if in the DSR graph $\mathfrak{D}$ of the network $G$,*

(a) *no cycle contains a bispecies production edge;*

(b) *all cycles are s-cycles, and*

(c) *there is no S-to-R intersection.*

**Theorem 4.5.3.** *Let $G$ be a reaction network satisfying conditions **(N1)**–**(N4)**. Suppose $\mathfrak{D}$, the DSR graph of $G$, satisfies the following:*

(a) *no cycle contains a bispecies production edge;*

(b) *all cycles are s-cycles, and*

(c) *there is no S-to-R intersection.*

*Then $G$ is delay stable, i.e., for any rate constants $\boldsymbol{\kappa} > \mathbf{0}$ and any delay parameters $\boldsymbol{\tau} \geq \mathbf{0}$, any positive steady state of the delay mass-action system $(G, \boldsymbol{\kappa}, \boldsymbol{\tau})$ is asymptotically stable.*

*Proof.* Let $G$ be a reaction network satisfying **(N1)**–**(N4)**, and suppose its DSR graph $\mathfrak{D}$ satisfies (a)–(c) of Theorem 4.5.3. Let $\tilde{G}$ be the modified network as in Definition 4.3.2, and $\tilde{\mathfrak{D}}$ be its DSR graph. By Theorem 4.5.2, all cycles in $\tilde{\mathfrak{D}}$ are s-cycles, and $\tilde{\mathfrak{D}}$ has no S-to-R intersection. By Corollary 4.4.7, its Jacobian matrix $-\tilde{\mathbf{J}}$ is a $P_0$-matrix, independent of the choice of rate constant $\boldsymbol{\kappa} > \mathbf{0}$ and the positive state. Proposition 4.3.3 says that $\tilde{\mathbf{J}}$ is the modified Jacobian matrix of the delay mass-action system $(G, \boldsymbol{\kappa}, \boldsymbol{\tau})$.

It remains to be shown — independent of $\boldsymbol{\kappa} > \mathbf{0}$, $\boldsymbol{x} > \mathbf{0}$ — that $[\tilde{\mathbf{J}}]_{pp} < 0$ for all $1 \leq p \leq n$ and $\det(\mathbf{J}) \neq 0$, where $\mathbf{J}$ is the Jacobian matrix of the mass-action system $(G, \boldsymbol{\kappa})$. Condition **(N1)** — that every species has an outflow reaction — guarantees that $[\tilde{\mathbf{J}}]_{pp} = [\mathbf{J}]_{pp} < 0$. Finally, the conditions on the DSR graph of $G$ also ensures that $\mathbf{J}$ itself is a $P_0$-matrix and that $\det(-\mathbf{J}) > 0$ by Theorem 4.4.6. Therefore, delay stability of $G$ follows from Corollary 4.2.4. □

Since the proof of Theorem 4.5.2 is very technical and does not shed light on the underlying structure on the DSR graph, it suffices to say that (i) the s-cycles of $\mathfrak{D}$ and $\tilde{\mathfrak{D}}$

are related (Lemma 4.5.8 and Proposition 4.5.11); (ii) there is a S-to-R intersection in $\tilde{\mathfrak{D}}$ if and only if either there is one in $\mathfrak{D}$ or there is a cycle containing a bispecies production edge (Proposition 4.5.12). So instead, we explore several examples applying Theorem 4.5.3 before proving Theorem 4.5.2.

Several physical and biochemical processes are believed to follow a *nucleation-propagation mechanism*, from crystallization in solution, polymerization reactions including micelles formation [27, 105], and DNA double-helix formation [101, 104, 114]. Under this mechanism, nucleation, whereby the process is initiated, is the rate determining step, followed by the faster propagation step that takes the process to completion or termination.

**Example 4.5.4.** A DNA helix comprises of two complementary single-stranded DNA. During the nucleation step, several base pairs must find their partners in the complementary strand. However, once that happens, the two strands zip together like a zipper; this is the propagation step [24, Chapter 23].

As a toy model of duplex formation, consider two single-stranded DNA ($\mathsf{S}$) forming a duplex ($\mathsf{D}$) reversibly with some time delays. Reality is of course much more complicated; we are neglecting that the single-stranded DNA should be complementary, not identical. Moreover, in DNA replication, usually one strand forms a template, and the other strand is built from individual nucleotides. Finally, we are also neglecting the physical process whereby the double-stranded DNA twists to form a helix, and the thermodynamics when long sequences are involved. In this toy model, we assume that the delay parameters are proportional to the length of the DNA sequence. Moreover, we include the degradation of $\mathsf{D}$, and the synthesis and degradation of $\mathsf{S}$.

The delay mass-action system under consideration

$$2\mathsf{S} \underset{\kappa_2,\ \tau_2}{\overset{\kappa_1,\ \tau_1}{\rightleftharpoons}} \mathsf{D} \xrightarrow{\kappa_D} 0 \underset{\kappa_{S-}}{\overset{\kappa_{S+}}{\rightleftharpoons}} \mathsf{S}$$

satisfies conditions **(N1)**–**(N4)**. By an abuse of notation, let $\mathsf{S}$ and $\mathsf{D}$ be the concentration

variables of the single-stranded and double-stranded DNA respectively. The associated system of delay equations

$$\frac{d\mathsf{S}(t)}{dt} = \kappa_{S+} - \kappa_{S-}\mathsf{S}(t) - 2\kappa_1[\mathsf{S}(t)]^2 + 2\kappa_2\mathsf{D}(t-\tau_2)$$
$$\frac{d\mathsf{D}(t)}{dt} = -\kappa_D\mathsf{D}(t) + \kappa_1[\mathsf{S}(t-\tau_1)]^2 - \kappa_2\mathsf{D}(t)$$

has a single positive steady state for any choice of rate constants. These are given by

$$\frac{\kappa_1\mathsf{S}^2}{\kappa_2+\kappa_D} = \mathsf{D} = \frac{\kappa_{S+}-\kappa_{S-}\mathsf{S}}{2\kappa_D}.$$

The resulting quadratic equation $2\kappa_1\kappa_D\mathsf{S}^2 + \kappa_{S-}(\kappa_2+\kappa_D)\mathsf{S} - \kappa_{S+}(\kappa_2+\kappa_D) = 0$ always has a positive root and a negative root, leading to a unique positive steady state.

The characteristic equation (4.4) of the delay system is

$$\begin{aligned} 0 &= \det\begin{pmatrix} -\kappa_S - 4\kappa_1\mathsf{S} - \lambda & 2\kappa_2 e^{-\lambda\tau_2} \\ 2\kappa_1\mathsf{S}e^{-\lambda\tau_1} & -2\kappa_2 - \kappa_D - \lambda \end{pmatrix} \\ &= \lambda^2 + \lambda\left(4\kappa_1\mathsf{S} + \kappa_{S-} + 2\kappa_2 + \kappa_D\right) \\ &\quad + \left(4\kappa_1\mathsf{S} + \kappa_{S-}\right)\left(2\kappa_2 + \kappa_D\right) - 4\kappa_1\kappa_2\mathsf{S}e^{-\lambda(\tau_1+\tau_2)}. \end{aligned}$$

Of course, one can check the criteria of Theorem 4.2.3 or Corollary 4.2.4, which is not difficult since the modified Jacobian matrix (which also happens to be the Jacobian matrix)

$$\tilde{\mathbf{J}} = \begin{pmatrix} -\kappa_S - 4\kappa_1\mathsf{S} & 2\kappa_2 \\ 2\kappa_1\mathsf{S} & -2\kappa_2 - \kappa_D \end{pmatrix}$$

is only a $2 \times 2$ matrix. However, we look instead at its DSR graph, shown in Figure 4.5. The DSR graph has no cycle, so conditions (a)–(c) of Theorem 4.5.3 are trivially satisfied. Therefore, the network corresponding to duplex formation is delay stable, i.e., asymptotically stable for any choice of rate constants and delay parameters.

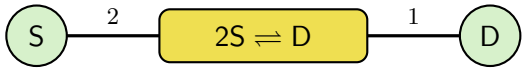


Figure 4.5: The DSR graph of Example 4.5.4 has no cycle. Thus, the toy model for the formation of double-stranded helix via the nucleation-propagation mechanism is delay stable.

We now return to a discussion leading up to a proof of Theorem 4.5.2. One can imagine if the reaction network $G$ has only one bispecies reaction, then $G$ differs from its modified network $\tilde{G}$ only by the relevant reaction (two reactions from the view of $\tilde{G}$), and their respective DSR graphs differ only near the relevant R-node(s).

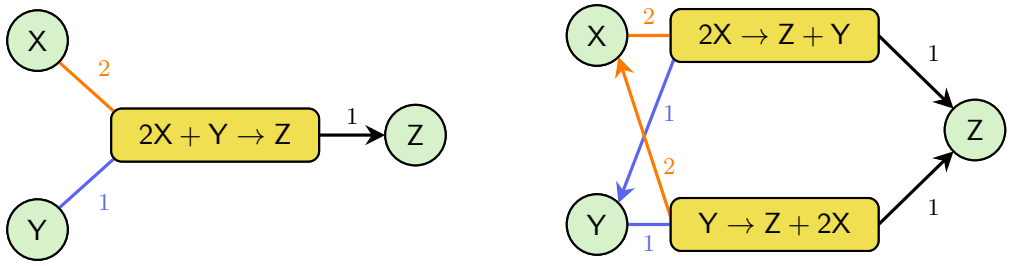


(a) (b)

Figure 4.6: The DSR graphs of (a) the original network $\{2X + Y \to Z\}$ and (b) its modified network from Example 4.5.5.

**Example 4.5.5.** Consider the reaction network consisting of a single reaction

$$2X + Y \longrightarrow Z$$

whose DSR graph $\mathfrak{D}$ is shown in Figure 4.6(a). Independent of the choice of rate constants and positive state, the modified network consisting of two reactions

$$2X \longrightarrow Z + Y$$

$$Y \longrightarrow Z + 2X$$

has the DSR graph $\tilde{\mathfrak{D}}$ in Figure 4.6(b). The edges are coloured in the figure to show correspondence with those in Figure 4.6(a). Each R-node in $\tilde{\mathfrak{D}}$ has degree 3, and its adjacent edges have the same set of stoichiometric coefficients. A s-cycle is present in $\tilde{\mathfrak{D}}$ even though $\mathfrak{D}$ has no cycle.

On the DSR graphs in Figure 4.6, we define a graph homomorphism $\Phi\colon \tilde{\mathfrak{D}} \to \mathfrak{D}$. It acts as the identity on the S-nodes, and maps the two R-nodes in $\tilde{\mathfrak{D}}$ to the R-node in $\mathfrak{D}$. So $\Phi$ maps any edge of $\tilde{\mathfrak{D}}$ correspondingly (edges colour-coded as such in Figure 4.6). Note that the stoichiometric coefficient of any edge is preserved by $\Phi$. Finally, note that an oriented edge in $\tilde{\mathfrak{D}}$ may become unoriented in $\mathfrak{D}$ under the graph homomorphism $\Phi$.

Regarding the DSR graphs of a reaction network and its modified network, it is not difficult to imagine all the actions happening around a R-node that involves two reactant species, which we call a ***bispecies R-node***.

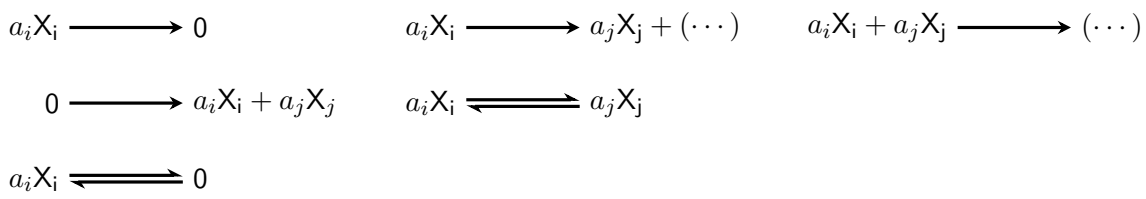


Figure 4.7: A reaction network satisfying conditions **(N2)**–**(N4)** can only admit reactions of these form. In each case, $i \neq j$ and $a_i$, $a_j > 0$. By $(\cdots)$, we allow any combination of species except for $\mathsf{X}_i$ and $\mathsf{X}_j$.

In what follows, we start with a reaction network satisfying conditions **(N2)**–**(N4)**. The only reactions allowed are those of the forms in Figure 4.7. By definition, the three left-most reactions in Figure 4.7 are omitted from $\mathcal{V}_R$ in the DSR graph. As a result, $\mathcal{V}_R$ only contain R-nodes corresponding to reactions in the latter two columns in Figure 4.7.

**Remark 4.5.6.** In how we defined the modified network in Definition 4.3.2, an awkward scenario can occur. If we start with the reaction network $G$

$$\mathsf{X}+\mathsf{Y} \longrightarrow 0 \qquad\qquad \mathsf{X} \longrightarrow \mathsf{Y}$$

then the modified network $\tilde{G}$ consisting of

$$\begin{array}{l} \mathsf{X} \longrightarrow \mathsf{Y} \\ \mathsf{Y} \longrightarrow \mathsf{X} \end{array} \qquad\qquad \mathsf{X} \longrightarrow \mathsf{Y}$$

awkwardly has a reaction repeated! Technically, the set of R-nodes $E^*$ will only have one copy of the reaction $\mathsf{X} \to \mathsf{Y}$; however, for the rest of this section, we ensure that both R-nodes are included in the DSR graph. See Figure 4.8 for the DSR graphs of $G$ and $\tilde{G}$. This is to ensure that cycles are not lost in going from the modified DSR graph to the original DSR graph.

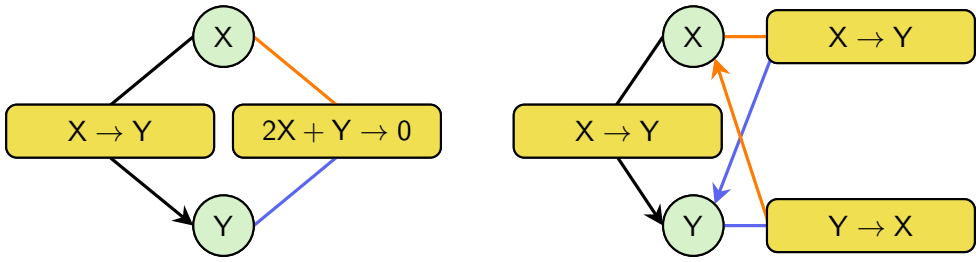


(a) (b)

Figure 4.8: The DSR graphs of (a) the original network and (b) the modified network from Remark 4.5.6. Duplicated R-nodes *can* arise and should be kept.

We now define a graph homomorphism from the modified DSR graph to the original, smaller DSR graph.

**Definition 4.5.7.** Let $\mathfrak{D} = (\mathcal{V}_S, \mathcal{V}_R, \mathcal{E}, \sigma)$ be the DSR graph of a reaction network satisfying **(N2)**–**(N4)**, and $\tilde{\mathfrak{D}} = (\mathcal{V}_S, \tilde{\mathcal{V}}_R, \tilde{\mathcal{E}}, \tilde{\sigma})$ the DSR graph of the modified network. Define a graph homomorphism $\Phi\colon \mathcal{V}_S \cup \tilde{\mathcal{V}}_R \to \mathcal{V}_S \cup \mathcal{V}_R$ by $\Phi(\mathsf{X}) = \mathsf{X}$ for any $\mathsf{X} \in \mathcal{V}_S$. For any $\tilde{\mathsf{R}} \in \tilde{\mathcal{V}}_R$ that is *not* a bispecies reaction, there is a unique $\mathsf{R} \in \mathcal{V}_R$ associated to it by the construction in Definition 4.3.2; let $\Phi(\tilde{\mathsf{R}}) = \mathsf{R}$. Finally, any bispecies R-node $\mathsf{R} \in \mathcal{V}_R$ is naturally associated to two R-nodes $\tilde{\mathsf{R}}_1$, $\tilde{\mathsf{R}}_2 \in \tilde{\mathcal{V}}_R$, so let $\Phi(\tilde{\mathsf{R}}_i) = \mathsf{R}$.

We claim that $\Phi$ is a graph homomorphism. First, consider an edge $(\mathsf{X}, \tilde{\mathsf{R}}) \in \tilde{\mathfrak{D}}$, where

$\Phi(\tilde{\mathsf{R}})$ is *not* a bispecies R-node. The map $\Phi$ acts as the identity on these vertices. If the edge is unoriented, either the reaction is reversible, or $\mathsf{X}$ is a reactant species in an irreversible reaction. Thus $(\mathsf{X}, \Phi(\tilde{\mathsf{R}})) \in \mathfrak{D}$ is unoriented. If the edge is oriented, necessarily the reaction is irreversible and $\mathsf{X}$ is a product species; hence the resulting edge is also oriented.

Now consider an edge $(\mathsf{X}, \tilde{\mathsf{R}}) \in \tilde{\mathfrak{D}}$, where $\Phi(\tilde{\mathsf{R}})$ is a bispecies R-node. If the edge is unoriented, then $\mathsf{X}$ is a reactant species in the bispecies reaction. Hence $(\mathsf{X}, \Phi(\tilde{\mathsf{R}})) \in \mathfrak{D}$ is also unoriented. However, if the edge in $\tilde{\mathfrak{D}}$ is oriented, the species $\mathsf{X}$ is either a product in the bispecies reaction (in which case $(\mathsf{X}, \Phi(\tilde{\mathsf{R}}))$ is also oriented), or $\mathsf{X}$ is a reactant in the bispecies reaction (in which case $(\mathsf{X}, \Phi(\tilde{\mathsf{R}}))$ is unoriented). Regardless, the directions of the edges are consistent under $\Phi$.

Therefore, $\Phi$ is a graph homomorphism. By an abuse of notation, we let $\Phi\colon \tilde{\mathfrak{D}} \to \mathfrak{D}$, and allow $\Phi$ to act on both vertices and edges of $\tilde{\mathfrak{D}}$. We start with a simple observation.

**Lemma 4.5.8.** *The map $\Phi$ preserves stoichiometric coefficients, i.e., $\sigma \circ \Phi = \tilde{\sigma}$.*

*Proof.* This follows from the construction in Definition 4.3.2; reactant species are always moved together with their stoichiometric coefficients. □

**Remark 4.5.9.** Let $\tilde{C} \subseteq \tilde{\mathfrak{D}}$ be a cycle that gets mapped to a c-pair under $\Phi$. As Figure 4.6(b) clearly illustrates, the edges adjacent to any S-node in $\tilde{C}$ shares the same stoichiometric coefficient. Therefore, then $\tilde{C}$ is a s-cycle.

In the following lemma, we show that if no cycle in $\mathfrak{D}$ contains a bispecies production edge, then there is a one-to-one correspondence between the cycles in $\tilde{\mathfrak{D}}$ and the set of cycles and c-pairs in $\mathfrak{D}$. By ruling out bispecies production edges, the R-nodes in $\tilde{\mathfrak{D}}$ associated to a bispecies reaction can only be adjacent to its reactant S-nodes in any cycle.

**Lemma 4.5.10.** *Suppose also that no cycle in $\mathfrak{D}$ contains a bispecies production edge. If $\tilde{C} \subseteq \tilde{\mathfrak{D}}$ is a cycle, then $\Phi(\tilde{C})$ is either a cycle or a c-pair in $\mathfrak{D}$. If $\Phi(\tilde{C})$ is a cycle, then $\Phi$*

*acts bijectively on $\tilde{C}$. Then for any cycle $C \subseteq \mathfrak{D}$, there exists a unique cycle $\tilde{C} \subseteq \tilde{\mathfrak{D}}$ such that $\Phi(\tilde{C}) = C$. In other words, there is a one-to-one correspondence between the set of cycles in $\tilde{\mathfrak{D}}$, and the set of cycles and c-pairs in $\mathfrak{D}$.*

*Proof.* Restrict the map $\Phi$ to the cycle $\tilde{C} \subseteq \tilde{\mathfrak{D}}$. If $\Phi$ is one-to-one (on the vertices of $\tilde{C}$), then $\Phi(\tilde{C})$ is a cycle. However, if $\Phi$ is not one-to-one, then there exist R-nodes $\tilde{\mathsf{R}})_i \neq \tilde{\mathsf{R}}_j$ in $\tilde{C}$ such that $\mathsf{R} = \Phi(\tilde{\mathsf{R}}_i) = \Phi(\tilde{\mathsf{R}}_j)$ is a bispecies R-node. Condition **(N3)** implies that there are two reactant S-nodes to $\mathsf{R}$, say $\mathsf{X}_i$ and $\mathsf{X}_j$. Figure 4.9(b) shows a similar setup. Note that $\tilde{\mathsf{R}}_i$ is adjacent to edges $(\mathsf{X}_i, \tilde{\mathsf{R}}_i)$, $(\mathsf{X}_j, \tilde{\mathsf{R}}_i)$, and possibly oriented edges to some other species $\mathsf{X}_k$ (i.e., in the preimage of the bispecies production edge). Because no cycle in $\mathfrak{D}$ contains a bispecies production edge, $\Phi(\tilde{C})$ cannot contain an oriented edge like $(\mathsf{X}_k, \Phi(\tilde{\mathsf{R}}_i))$. Therefore, $\tilde{C}$ cannot contain edges like $(\mathsf{X}_k, \tilde{\mathsf{R}}_i)$ or $(\mathsf{X}_k, \tilde{\mathsf{R}}_j)$. Because each of $\tilde{\mathsf{R}}_i$ and $\tilde{\mathsf{R}}_j$ has only one incoming (unoriented) edge, it must be the case that $\tilde{C} = \left\langle \mathsf{X}_i, \tilde{\mathsf{R}}_i, \mathsf{X}_j, \tilde{\mathsf{R}}_j \right\rangle$, so $\Phi(\tilde{C})$ is a c-pair.

Conversely, let $C \subseteq \mathfrak{D}$ be a cycle. If $C$ does not contain any bispecies R-nodes, then because $\Phi$ acts bijectively on the cycle, $\Phi^{-1}(C) \subseteq \tilde{\mathfrak{D}}$ is the unique cycle mapping to $C$. Suppose however, that $C$ contains a bispecies R-node; we claim that there is a unique cycle in $\tilde{\mathfrak{D}}$ that gets mapped to $C$, as illustrated in Figure 4.9. For now, assume there is exactly one bispecies R-node $\mathsf{R}$. Let the cycle $C$ be $\langle v_\ell = v_0, v_1, v_2, \ldots, v_{\ell-1} \rangle$, where $v_1 = \mathsf{R}$ is the bispecies R-node, with reactant species S-nodes $v_0 = \mathsf{X}_i$ and $v_2 = \mathsf{X}_j$. For $k \neq 1$, the vertex $v_k$ has a unique preimage under $\Phi$. However, the preimage of $v_1$ consists of two R-nodes: $\tilde{\mathsf{R}}_i$ for the modified reaction where $\mathsf{X}_i$ is the reactant, and $\tilde{\mathsf{R}}_j$ for the reaction where $\mathsf{X}_j$ is the reactant. Then $\Phi$ maps the cycle $\left\langle v_\ell = v_0, \tilde{\mathsf{R}}_i, v_2, \ldots, v_{\ell-1} \right\rangle \subseteq \tilde{\mathfrak{D}}$ uniquely to $C$.

If $C$ contains multiple bispecies R-node, a similar argument can be made locally at each bispecies R-node. Suppose $v_k = \mathsf{R}$ is a bispecies R-node, then $v_{k-1}$ and $v_{k+1}$ are S-nodes corresponding to the reactants of $\mathsf{R}$. Say $v_{k-1} = \mathsf{X}_i$ and $v_{k+1} = \mathsf{X}_j$. In the DSR graph $\mathfrak{D}$ of the modified network, $\mathsf{R}$ is associated to two R-nodes: $\tilde{\mathsf{R}}_i$ with reactant $\mathsf{X}_i$ and $\tilde{\mathsf{R}}_j$ another with reactant $\mathsf{X}_j$. Then for the segment $\langle v_{k-1}, v_k, v_{k+1} \rangle$ of the cycle, choose $\left\langle v_{k-1} = \mathsf{X}_i, \tilde{\mathsf{R}}_i, v_{k+1} = \mathsf{X}_j \right\rangle$ as its preimage under $\Phi$. □

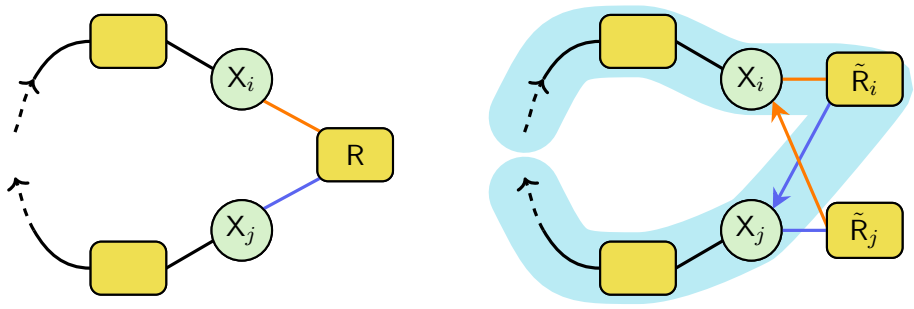


(a) (b)

Figure 4.9: If no cycle in $\mathfrak{D}$ contains a bispecies production edge, the preimage of a cycle in $\mathfrak{D}$ is a unique cycle in $\tilde{\mathfrak{D}}$. A cycle $C \subseteq \mathfrak{D}$ containing a bispecies R-node (a) is uniquely mapped from the cycle in (b). The edges adjacent to the R-node are coloured to emphasize the pairing in the DSR graphs, and arrows indicate direction of the cycle.

We are ready to approach the proof of Theorem 4.5.2. When no cycle contains a bispecies production edge, Proposition 4.5.11 relates the s-cycles of the DSR graphs, while Proposition 4.5.12 relates the S-to-R intersections. These two propositions together imply Theorem 4.5.2.

Note that in the following proposition, it is not necessary to assume that $\mathfrak{D}$ does not have a cycle with a bispecies product edge. With this assumption, the proof greatly simplifies.

**Proposition 4.5.11.** *Assumes that no cycle in $\mathfrak{D}$ contains a bispecies production edge. Then all cycles in $\mathfrak{D}$ are s-cycles if and only if all cycles in $\tilde{\mathfrak{D}}$ are s-cycles.*

*Proof.* Suppose all cycles in $\mathfrak{D}$ are s-cycles. Let $\tilde{C} \subseteq \tilde{\mathfrak{D}}$ be a cycle. Lemma 4.5.10 implies that $\Phi(\tilde{C})$ is either a cycle or a c-pair. Recall that $\Phi$ preserves the stoichiometric coefficients. Thus $\tilde{C}$ is a s-cycle by assumption in the former case and by Remark 4.5.9 in the latter.

Conversely, suppose all cycles in $\tilde{\mathfrak{D}}$ are s-cycles, and let $C \subseteq \mathfrak{D}$ be any cycle. By Lemma 4.5.10, $\Phi^{-1}(C)$ is a cycle, thus a s-cycle by assumption. Hence, its image $C$ is also a s-cycle. □

Finally, we reached our last proposition, and the subtle connection between the DSR

graphs of a network and its modified version. Figure 4.10 shows that if $\mathfrak{D}$ has a cycle with a bispecies production edge, then there is a S-to-R intersection in $\tilde{\mathfrak{D}}$.

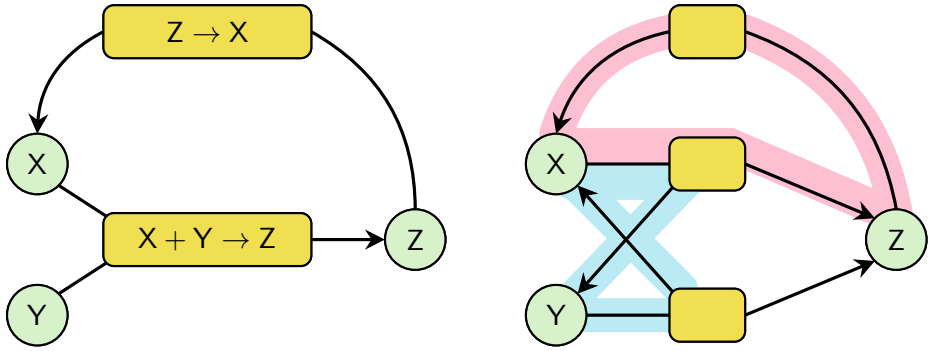


Figure 4.10: (a) The DSR graph of a network that has a cycle with a bispecies production edge. (b) The DSR graph of the modified network, which contains a S-to-R intersection. Two cycles are highlighted whose intersection is one edge.

**Proposition 4.5.12.** *There is a S-to-R intersection in $\tilde{\mathfrak{D}}$ if and only if there is either*

(a) *a S-to-R intersection in $\mathfrak{D}$, or*

(b) *a cycle in $\mathfrak{D}$ containing a bispecies production edge.*

*Proof.* First we prove that if $\mathfrak{D}$ has no S-to-R intersection and no cycles with a bispecies production edge, then $\tilde{\mathfrak{D}}$ cannot have a S-to-R intersection. Let $\tilde{C}_1 \neq \tilde{C}_2$ be two cycles in $\tilde{\mathfrak{D}}$ with at least one common R-node and a S-node; we need to show that $\tilde{C}_1 \cap \tilde{C}_2$ is *not* a S-to-R intersection. Without loss of generality, Lemma 4.5.10 implies we have three cases (Figure 4.11) to handle separately:

1. $\Phi(\tilde{C}_1)$ and $\Phi(\tilde{C}_2)$ are c-pairs;

2. $\Phi(\tilde{C}_1)$ is a cycle while $\Phi(\tilde{C}_2)$ is a c-pair;

3. $\Phi(\tilde{C}_1)$ and $\Phi(\tilde{C}_2)$ are both cycles.

In the case where $\Phi(\tilde{C}_1)$ and $\Phi(\tilde{C}_2)$ are c-pairs (Figure 4.11(a)), they must share the same R-node, which is a bispecies R-node in $\mathfrak{D}$. Since a bispecies R-node has exactly two incoming (unoriented in this case) edges, $\tilde{C}_1 = \tilde{C}_2$, which contradicts our assumption.

In the next case, the unique R-node of the c-pair $\Phi(\tilde{C}_2)$ is a bispecies R-node in the cycle $\Phi(\tilde{C}_1)$. Because the two edges in $\Phi(\tilde{C}_2)$ form part of the cycle, $\Phi(\tilde{C}_2)$ has the form of the partially shown cycle in Figure 4.11(b). The intersection $\tilde{C}_1 \cap \tilde{C}_2$ consists of exactly two edges in $\tilde{\mathfrak{D}}$ that get mapped to the c-pair. The intersection in $\tilde{\mathfrak{D}}$ is similar to the segment $\left\langle \mathsf{X}_i, \tilde{\mathsf{R}}_i, \mathsf{X}_j \right\rangle$ in Figure 4.9. Thus, $\tilde{C}_1 \cap \tilde{C}_2$ starts and ends at S-nodes, i.e., it is not a S-to-R intersection.

In the final case, $\Phi(\tilde{C}_1)$ and $\Phi(\tilde{C}_2)$ are cycles. Since no cycle in $\mathfrak{D}$ contains a bispecies production edge, $\Phi$ acts bijectively on the cycles $\tilde{C}_1$ and $\tilde{C}_2$, and $\Phi(\tilde{C}_1 \cap \tilde{C}_2) = \Phi(\tilde{C}_1) \cap \Phi(\tilde{C}_2)$. Because $\mathfrak{D}$ does not have any S-to-R intersection, $\tilde{C}_1 \cap \tilde{C}_2$ is not a S-to-R intersection.

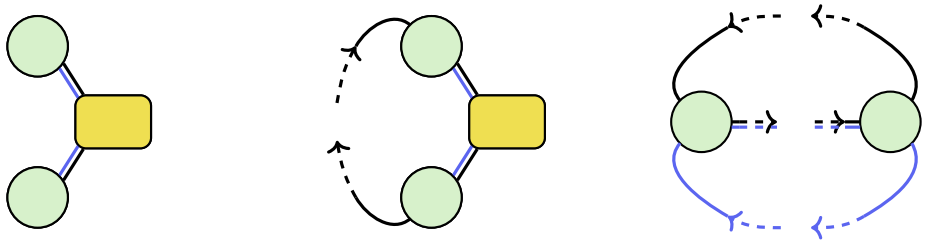

(a) (b) (c)

Figure 4.11: Preimages in $\tilde{\mathfrak{D}}$ of two cycles with at least one common node. The three cases to consider in the proof of Proposition 4.5.12: when (a) both $\Phi(\tilde{C}_i)$ are c-pairs, (b) one of them is a c-pair, and (c) neither is a c-pair. In (a) and (b), the intersection $\tilde{C}_1 \cap \tilde{C}_2$ is the preimage of the c-pair. In (c), because $\Phi(\tilde{C}_1)$ and $\Phi(\tilde{C}_2)$ are cycles on which $\Phi$ acts bijectively, $\Phi(\tilde{C}_1 \cap \tilde{C}_2) = \Phi(\tilde{C}_1) \cap \Phi(\tilde{C}_2)$.

Conversely, first suppose now that no cycle contains a bispecies production edge, but that there are two cycles $C_1 \neq C_2$ in $\mathfrak{D}$ whose intersection $C_1 \cap C_2$ is a S-to-R intersection. By Lemma 4.5.10, let $\tilde{C}_1$ and $\tilde{C}_2$ be the unique cycles mapped to $C_1$ and $C_2$ respectively. Since $\Phi$ acts bijectively on these cycles, we have $\Phi(\tilde{C}_1 \cap \tilde{C}_2) = C_1 \cap C_2$, a S-to-R intersection; therefore $\tilde{C}_1 \cap \tilde{C}_2$ is also a S-to-R intersection.

Now suppose that a cycle $C$ in $\mathfrak{D}$ contains a bispecies production edge $(\mathsf{X}_k, \mathsf{R})$ where $\mathsf{R}$ is the bispecies R-node, with reactant S-nodes $\mathsf{X}_i$ and $\mathsf{X}_j$. Figure 4.10 hints at the proof. Let $\tilde{C}^*$ be the s-cycle that is the preimage of the c-pair adjacent to $\mathsf{R}$; say $\tilde{C}^* = \left\langle \mathsf{X}_i, \tilde{\mathsf{R}}_i, \mathsf{X}_j, \tilde{\mathsf{R}}_j \right\rangle$. We will construct a cycle in $\tilde{\mathfrak{D}}$ whose intersection with $\tilde{C}^*$ is a S-to-R intersection. Let $C = \langle v_\ell = v_0, v_1, \ldots, v_{\ell-1} \rangle$, where $v_1 = \mathsf{R}$, $v_0 = \mathsf{X}_i$, and $v_2 = \mathsf{X}_k$. Then $\Phi$ maps the segment $\left\langle \mathsf{X}_i, \tilde{\mathsf{R}}_i, \mathsf{X}_k \right\rangle$ to the $\langle v_0, v_1, v_2 \rangle$ part of the cycle $C$. Note that the intersection of $\left\langle \mathsf{X}_i, \tilde{\mathsf{R}}_i, \mathsf{X}_k \right\rangle$ with $\tilde{C}^*$ is $(\mathsf{X}_k, \tilde{\mathsf{R}}_i)$, a S-to-R intersection. More precisely, whenever $v_k$ is a bispecies R-node, and $v_{k-1} = \mathsf{X}_i$, choose $\tilde{\mathsf{R}}_i$ from the preimage of $v_k$. The result is a cycle in $\tilde{\mathfrak{D}}$, whose intersection with $\tilde{C}^*$ is precisely $(\mathsf{X}_k, \tilde{\mathsf{R}}_i)$, a S-to-R intersection. □

### Proof of Theorem 4.5.2

Recall that we supposed $G$ satisfy conditions **(N2)**–**(N4)**; Theorem 4.5.2 claims that in the DSR graph $\tilde{\mathfrak{D}}$ of the network $\tilde{G}$,

(i) all cycles are s-cycles, and

(ii) there is no S-to-R intersection,

if and only if in the DSR graph $\mathfrak{D}$ of the network $G$,

(a) no cycle contains a bispecies production edge;

(b) all cycles are s-cycles, and

(c) there is no S-to-R intersection.

Proposition 4.5.12 claims (ii) is equivalent to (a) and (c). Assuming (a), Proposition 4.5.11 proves the equivalence of (i) and (b). Clearly, (a)–(c) implies (i)–(ii). Towards the other direction, (ii) implies (a) and (c). Hence, we may take (a) as an assumption, and conclude (b) from (i). □

### Logical relations of implications

Results have become more intertwined in this section; it is worth spelling out the logical implications.

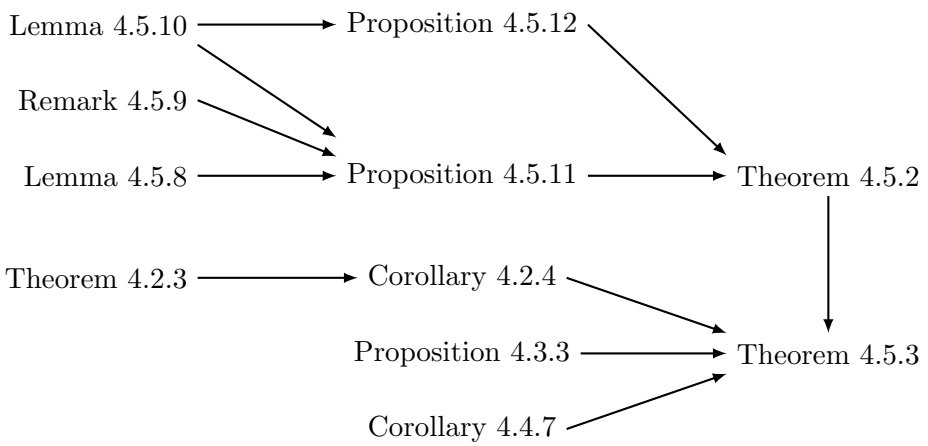

# Bibliography

[1] L. J. Allen, *An Introduction to Stochastic Processes with Applications to Biology*, CRC Press, 2010.

[2] D. F. Anderson, *A proof of the global attractor conjecture in the single linkage class case*, SIAM Journal on Applied Mathematics, 71 (2011), pp. 1487–1508.

[3] D. F. Anderson, *A short note on the lyapunov function for complex-balanced chemical reaction networks*, unpublished note, (2014). Available at `http://www.math.wisc.edu/~anderson/CRNT_Lyapunov.pdf`.

[4] D. F. Anderson, D. Cappelletti, J. Kim, and T. Nguyen, *Tier structure of strongly endotactic reaction networks*, Stochastic Processes and their Applications, 130 (2020), pp. 7218–7259.

[5] D. F. Anderson and T. Kurtz, *Stochastic Analysis of Biochemical Systems*, vol. 1.2 of Stochastics in Biological Systems, Springer International Publishing, 2015.

[6] M. Banaji, *Cycle Structure in SR and DSR Graphs: Implications for Multiple Equilibria and Stable Oscillation in Chemical Reaction Networks*, vol. 6900 of Lecture Notes in Computer Science, Springer, 2012, pp. 1–22.

[7] M. Banaji and C. Rutherford, *P-matrices and signed digraphs*, Discrete Mathematics, 311 (2011), pp. 295–301.

[8] H. T. Banks, D. Robbins, and K. L. Sutton, *Theoretical foundations for traditional and generalized sensitivity functions for nonlinear delay differential equations*, Mathematical Biosciences and Engineering, 10 (2013), pp. 1301–1333.

[9] R. Bellman and K. L. Cooke, *Differential-Difference Equations*, Academic Press, 1963.

[10] A. A. Berryman, *The orgins and evolution of predator-prey theory*, Ecology, 73 (1992), pp. 1530–1535.

[11] M. Birch, *Maximum likelihood in three-way contingency tables*, Journal of the Royal Statistical Society. Series B (Methodological), 25 (1963), pp. 220–233.

[12] M. Bodnar, *The nonnegativity of solutions of delay differential equations*, Applied Mathematics Letters, 13 (2000), pp. 91–95.

[13] L. Boltzmann, *Further Studies on the Thermal Equilibrium of Gas Molecules*, 1872, pp. 262–349, https://doi.org/10.1142/9781848161337_0015.

[14] L. Boltzmann, *Neuer beweis zweier sätze über das wärmegleich-gewicht unter mehratomigen gasmolekülen*, Sitzungsberichte der Kaiserlichen Akademie der Wissenschaften in Wien, 95 (1887), pp. 153–164.

[15] L. Boltzmann, *Gastheorie*, J. A. Barth, 1896.

[16] B. Boros, *Existence of positive steady states for weakly reversible mass-action systems*, SIAM Journal on Mathematical Analysis, 51 (2019), pp. 435–449.

[17] B. Boros and J. Hofbauer, *Permanence of weakly reversible mass-action systems with a single linkage class*, SIAM Journal on Applied Dynamical Systems, 19 (2020), pp. 352–365.

[18] B. Boros, J. Hofbauer, S. Müller, and G. Regensburger, *The center problem for the Lotka reactions with generalized mass-action kinetics*, Qualitative Theory of Dynamical Systems, 17 (2018), pp. 403–410.

[19] B. Boros, S. Müller, and G. Regensburger, *Complex-balanced equilibria of*

*generalized mass-action systems: Necessary conditions for linear stability*, Mathematical Biosciences and Engineering, 17 (2020), pp. 442–459.

[20] F. Brauer, *Absolute stability in delay equations*, Journal of Differential Equations, 69 (1987), pp. 185–191.

[21] F. Brauer and C. Castillo-Chavez, *Mathematical Models in Population Biology and Epidemiology*, vol. 40 of Texts in Applied Mathematics, Springer, 2001.

[22] J. D. Brunner and G. Craciun, *Robust persistence and permanence of polynomial and power law dynamical systems*, SIAM Journal on Applied Mathematics, 78 (2018), pp. 801–825.

[23] L. Brustenga i Moncusí, G. Craciun, and M.-S. Sorea, *Disguised toric dynamical systems*, ArXiv e-prints, (2020), `https://arxiv.org/abs/2006.01289`.

[24] C. R. Cantor and P. R. Schimmel, *Biophysical Chemistry: Part III. The Behavior of Biological Macromolecules*, W.H. Freeman and Company, 1980.

[25] A. Cayley, *A theorem on trees*, Quarterly Journal of Pure and Applied Mathematics, 23 (1889), pp. 376–378.

[26] S. Chaiken and D. J. Kleitman, *Matrix tree theorems*, Journal of Combinatorial Theory, Series A, 24 (1978), pp. 377–381.

[27] C.-S. Chern, *Emulsion polymerization mechanisms and kinetics*, Progress in Polymer Science, 31 (2006), pp. 443–486.

[28] B. L. Clarke, *Stoichiometric network analysis*, Cell Biophysics, 12 (1988), pp. 237–253.

[29] C. Conradi, E. Feliu, M. Mincheva, and C. Wiuf, *Identifying parameter regions for multistationarity*, PLOS Computational Biology, 13 (2017), pp. 1–25.

[30] G. Craciun, *Toric differential inclusions and a proof of the global attractor conjecture*, ArXiv e-prints, (2015), https://arxiv.org/abs/1501.02860.

[31] G. Craciun, *Polynomial dynamical systems, reaction networks, and toric differential inclusions*, SIAM Journal on Applied Algebra and Geometry, 3 (2019), pp. 87–106.

[32] G. Craciun and M. Banaji, *Graph-theoretic approaches to injectivity and multiple equilibria in systems of interacting elements*, Communications in Mathematical Sciences, 7 (2009), pp. 867–900.

[33] G. Craciun and M. Banaji, *Graph-theoretic criteria for injectivity and unique equilibria in general chemical reaction systems*, Advances in Applied Mathematics, 44 (2010), pp. 168–184.

[34] G. Craciun and A. Deshpande, *Endotactic networks and toric differential inclusions*, SIAM Journal on Applied Dynamical Systems, 19 (2020), pp. 1798–1822.

[35] G. Craciun, A. Dickenstein, A. Shiu, and B. Sturmfels, *Toric dynamical systems*, Journal of Symbolic Computation, 44 (2009), pp. 1551–1565.

[36] G. Craciun and M. Feinberg, *Multiple equilibria in complex chemical reaction networks: I. The injectivity property*, SIAM Journal on Applied Mathematics, 65 (2005), pp. 1526–1546.

[37] G. Craciun and M. Feinberg, *Multiple equilibria in complex chemical reaction networks: II. The species-reaction graph*, SIAM Journal on Applied Mathematics, 66 (2006), pp. 1321–1338.

[38] G. Craciun, L. D. Gracía-Puente, and F. Sottile, *Some geometrical aspects of control points for toric patches*, in Mathematical Methods for Curves and Surfaces, Springer, 2010, pp. 111–135.

[39] G. Craciun, J. Jin, and P. Y. Yu, *An efficient characterization of complex-balanced,*

*detailed-balanced, and weakly reversible systems*, SIAM Journal on Applied Mathematics, 80 (2020), pp. 183–205.

[40] G. Craciun, J. Jin, and P. Y. Yu, *Single-target networks*, ArXiv e-prints, (2020), https://arxiv.org/abs/2006.01192.

[41] G. Craciun, M. D. Johnston, G. Szederkényi, E. Tonello, J. Tóth, and P. Y. Yu, *Realizations of kinetic differential equations*, Mathematical Biosciences and Engineering, 17 (2020), pp. 862–892.

[42] G. Craciun, M. Mincheva, C. Pantea, and P. Y. Yu, *Delay stability of reaction systems*, Mathematical Biosciences, 326 (2020), p. 108387.

[43] G. Craciun, M. Mincheva, C. Pantea, and P. Y. Yu, *Delay stability of reaction systems II: Graph-theoretic condition*, (In preparation).

[44] G. Craciun, S. Müller, C. Pantea, and P. Y. Yu, *A generalization of birch's theorem and vertex-balanced steady states for generalized mass-action systems*, Mathematical Biosciences and Engineering, 16 (2019), pp. 8243–8267.

[45] G. Craciun, F. Nazarov, and C. Pantea, *Persistence and permanence of mass-action and power-law dynamical systems*, SIAM Journal on Applied Mathematics, 73 (2013), pp. 305–329.

[46] G. Craciun and C. Pantea, *Identifiability of chemical reaction networks*, Journal of Mathematical Chemistry, 44 (2008), pp. 244–259.

[47] H. de Jong, *Modeling and simulation of genetic regulatory systems: a literature review*, Journal of Computational Biology, 9 (2002), pp. 67–103.

[48] P. De Leenheer, *An elementary proof of a matrix tree theorem for directed graphs*, SIAM Review, 62 (2020), pp. 716–726.

[49] A. Dickenstein and M. Pérez Millán, *How far is complex balancing from detailed balancing?*, Bulletin of Mathematical Biology, 73 (2011), pp. 811–828.

[50] A. Dickenstein, M. Pérez Millán, A. Shiu, and X. Tang, *Multistationarity in structured reaction networks*, Bulletin of Mathematical Biology, 81 (2019), pp. 1527–1581.

[51] L. Edelstein-Keshet, *Mathematical Models in Biology*, Society for Industrial and Applied Mathematics, 2005, https://doi.org/10.1137/1.9780898719147.

[52] I. R. Epstein, *Differential delay equations in chemical kinetics: Some simple linear model systems*, Journal of Chemical Physics, 92 (1990), pp. 1702–1712.

[53] I. R. Epstein and Y. Luo, *Differential delay equations in chemical kinetics. Nonlinear models: The cross-shaped phase diagram and the oregonator*, Journal of Chemical Physics, 95 (1991), pp. 244–254.

[54] I. R. Epstein and J. A. Pojman, *An Introduction to Nonlinear Chemical Dynamics: Oscillations, Waves, Patterns, and Chaos*, Oxford University Press, 1998.

[55] J. H. Espenson, *Chemical Kinetics and Reaction Mechanisms*, McGraw-Hill, 2 ed., 1795.

[56] M. Feinberg, *Complex balancing in general kinetic systems*, Archive for Rational Mechanics and Analysis, 49 (1972), pp. 187–194.

[57] M. Feinberg, *Chemical reaction network structure and the stability of complex isothermal reactors–I. the deficiency zero and deficiency one theorems*, Chemical Engineering Science, 42 (1987), pp. 2229–2268.

[58] M. Feinberg, *Necessary and sufficient conditions for detailed balancing in mass action systems of arbitrary complexity*, Chemical Engineering Science, 44 (1989), pp. 1819–1827.

[59] M. Feinberg, *Foundations of Chemical Reaction Network Theory*, vol. 202 of Applied

Mathematical Sciences, Springer International Publishing, 2019.

[60] M. Feinberg and F. Horn, *Dynamics of open chemical systems and the algebraic structure of the underlying reaction network*, Chemical Engineering Science, 29 (1974), pp. 775–787.

[61] M. Feinberg and F. Horn, *Chemical mechanism structure and the coincidence of the stoichiometric and kinetic subspaces*, Archive for Rational Mechanics and Analysis, 66 (1977), pp. 89–97.

[62] E. Feliu, *On the role of algebra in models in molecular biology*, Journal of Mathematical Biology, 80 (2020), pp. 1159–1161.

[63] E. Feliu, D. Cappelletti, and C. Wiuf, *Node balanced steady states: Unifying and generalizing complex and detailed balanced steady states*, Mathematical Biosciences, 301 (2018), pp. 68–82.

[64] E. Feliu and C. Wiuf, *Finding the positive feedback loops underlying multi-stationarity*, BMC Systems Biology, 9 (2015).

[65] M. Fiedler and V. Pták, *On matrices with non-positive off-diagonal elements and positive principal minors*, Czechoslovak Mathematical Journal, 12 (1962), pp. 382–400.

[66] J. Gallier, *Notes on elementary spectral graph theory applications to graph clustering using normalized cuts*, ArXiv e-prints, (2013), `https://arxiv.org/abs/1311.2492`.

[67] K. Gatermann, *Counting Stable Solutions of Sparse Polynomial Systems in Chemistry*, Proceedings of an AMS-IMS-SIAM Joint Summer Research Conference on Symbolic Computation, 2000, pp. 53–70, `https://doi.org/10.1090/conm/286`.

[68] K. Gatermann and B. Huber, *A family of sparse polynomial systems arising in chemical reaction systems*, Journal of Symbolic Computation, 33 (2002), pp. 275–305.

[69] M. Gopalkrishnan, E. Miller, and A. Shiu, *A geometric approach to the global attractor conjecture*, SIAM Journal on Applied Dynamical Systems, 13 (2014), pp. 758–797.

[70] E. Gross, H. Harrington, N. Meshkat, and A. Shiu, *Joining and decomposing reaction networks*, Journal of Mathematical Biology, 80 (2020), pp. 1683–1731.

[71] E. Gross and C. Hill, *The steady-state degree and mixed volume of a chemical reaction network*, ArXiv e-prints, (2019), `https://arxiv.org/abs/1909.06652`.

[72] V. Guillemin and A. Pollack, *Differential Topology*, Prentice-Hall, 1974.

[73] J. Gunawardena, *Chemical reaction network theory for* in-silico *biologists*, unpublished note, (2003). Available at `http://vcp.med.harvard.edu/papers/crnt.pdf`.

[74] J. Gunawardena, *A linear framework for time-scale separation in nonlinear biochemical systems*, PLoS One, 7 (2012), p. e36321.

[75] J. Hofbauer and J. W.-H. So, *Diagonal dominance and harmless off-diagonal delays*, Proceedings of the American Mathematical Society, 128 (2000), pp. 2675–2682.

[76] F. Horn, *Necessary and sufficient conditions for complex balancing in chemical kinetics*, Archive for Rational Mechanics and Analysis, 49 (1972), pp. 172–186.

[77] F. Horn, *The dynamics of open reaction systems*, SIAM-AMS Proceedings, 8 (1974), pp. 125–137.

[78] F. Horn and R. Jackson, *General mass action kinetics*, Archive for Rational Mechanics and Analysis, 47 (1972), pp. 81–116.

[79] H. Jakubowski, *Kinetics of Simple and Enzyme-Catalyzed Reactions*, 2016 (accessed May 27, 2020), `https://employees.csbsju.edu/hjakubowski/classes/ch331/transkinetics/TK_6B0_Kin_Simple_Enz_Cat_Rx_Sections.html`.

[80] C. R. Johnson, *Second, third, and fourth order D-stability*, Journal of Research of the National Bureau of Standards, Section B: Mathematical Sciences, 78B (1974), pp. 11–13.

[81] K. A. Johnson and R. S. Goody, *The original Michaelis constant: Translation of the 1913 Michaelis–Menten paper*, Biochemistry, 50 (2011), pp. 8264–8269.

[82] M. D. Johnston, *Topics in Chemical Reaction Network Theory*, PhD thesis, University of Waterloo, 2011.

[83] M. D. Johnston, *Translated chemical reaction networks*, Bulletin of Mathematical Biology, 76 (2014), pp. 1081–1116.

[84] M. D. Johnston, S. Müller, and C. Pantea, *A deficiency-based approach to parametrizing positive equilibria of biochemical reaction systems*, Bulletin of Mathematical Biology, 81 (2019), pp. 1143–1172.

[85] M. D. Johnston, C. Pantea, and P. Donnell, *A computational approach to persistence, permanence, and endotacticity of biochemical reaction networks*, Journal of Mathematical Biology, 72 (2016), pp. 467–498.

[86] M. D. Johnston, D. Siegel, and G. Szederkényi, *A linear programming approach to weak reversibility and linear conjugacy of chemical reaction networks*, Journal of Mathematical Chemistry, 50 (2012), pp. 274–288, `https://doi.org/10.1007/s10910-011-9911-7`, `http://daedalus-old.scl.sztaki.hu/PCRG/works/publications/Johnston2012.pdf`.

[87] B. Joshi and A. Shiu, *A survey of methods for deciding whether a reaction network is multistationary*, Mathematical Modelling of Natural Phenomena, 10 (2015), pp. 47–67.

[88] B. Joshi and A. Shiu, *Which small reaction networks are multistationary?*, SIAM Journal on Applied Dynamical Systems, 16 (2017), pp. 802–833.

[89] S. A. Kauffman, *The Origins of Order: Self-organization and Selection in Evolution*,

Oxford University Press, 1993.

[90] S. Kondo and T. Miura, *Reaction-diffusion model as a framework for understanding biological pattern formation*, Science, 329 (2010), pp. 1616–1620.

[91] R. Kopelman, *Rate processes on fractals: Theory, simulations, and experiments*, Journal of Statistical Physics, 42 (1986), pp. 185–200.

[92] R. Kopelman, *Fractal reaction kinetics*, Science, 241 (1988), pp. 1620–1626.

[93] G. N. Lewis, *A new principle of equilibrium*, Proceedings of the National Academy of Sciences of the United States of America., 11 (1925), pp. 179–183.

[94] G. Lipták, K. M. Hangos, M. Pituk, and G. Szederkényi, *Semistability of complex balanced kinetic systems with arbitrary time delays*, Systems & Control Letters, 114 (2018), pp. 38–43.

[95] G. Lipták, G. Szederkényi, and K. M. Hangos, *Computing zero deficiency realizations of kinetic systems*, Systems and Control Letters, 81 (2015), pp. 24–30, https://doi.org/10.1016/j.sysconle.2015.05.001, http://daedalus-old.scl.sztaki.hu/PCRG/works/publications/Liptak2015.pdf.

[96] G. Lipták, G. Szederkényi, and K. M. Hangos, *Kinetic feedback design for polynomial systems*, Journal of Process Control, 41 (2016), pp. 56–66, https://doi.org/10.1016/j.jprocont.2016.03.002, http://daedalus-old.scl.sztaki.hu/PCRG/works/publications/Liptak2016.pdf.

[97] A. J. Lotka, *Contribution to the theory of periodic reactions*, Journal of Physical Chemistry, 14 (1910), pp. 271–274.

[98] A. J. Lotka, *Elements of physical biology*, Science Progress in the Twentieth Century (1919-1933), 21 (1926), pp. 341–343.

[99] P. Macheras and A. Iliadis, *Diffusion and Kinetics*, vol. 30 of Interdisciplinary Applied Mathematics, Springer, 2016, pp. 15–36.

[100] T. Malthus, *An Essay on the Principle of Population*, J. Johnson, London, 1798.

[101] M. Manghi and N. Destainville, *Physics of base-pairing dynamics in DNA*, Physics Reports, 631 (2016), pp. 1–41.

[102] L. Michaelis and M. L. Menten, *Die kinetik der invertinwirkung*, Biochemische Zeitschrift, 49 (1913), pp. 333–369.

[103] I. Mirzaev and J. Gunawardena, *Laplacian dynamics on general graphs*, Bulletin of Mathematical Biology, 75 (2013), pp. 2118–2149.

[104] S. Mohan, C. Hsiao, H. VanDeusen, R. Gallagher, E. Krohn, B. Kalahar, R. M. Wartell, and L. D. Williams, *Mechanism of RNA double helix-propagation at atomic resolution*, The Journal of Physical Chemistry B, 113 (2009), pp. 2614–2623.

[105] A. L. Moore, *4 – Production of Fluoroelastomers*, William Andrew Publishing, 2006, pp. 37–76.

[106] S. Müller, J. Hofbauer, and G. Regensburger, *On the bijectivity of families of exponential/generalized polynomial maps*, SIAM Journal on Applied Algebra and Geometry, 3 (2019), pp. 412–438.

[107] S. Müller and G. Regensburger, *Generalized mass action systems: Complex balancing equilibria and sign vectors of the stoichiometric and kinetic-order subspaces*, SIAM Journal on Applied Mathematics, 72 (2012), pp. 1–23.

[108] S. Müller and G. Regensburger, *Generalized mass-action systems and positive solutions of polynomial equations with real and symbolic exponents*, vol. 8660 of Lecture Notes in Computer Science, Springer, 2014, pp. 302–323.

[109] L. Onsager, *Reciprocal relations in irreversible processes I.*, Physical Review, 37 (1931), pp. 405–426.

[110] J. D. Orth, I. Thiele, and B. O. Palsson, *What is flux balance analysis?*, Nat. Biotechnol., 28 (2010), pp. 245–248.

[111] L. Pachter and B. Sturmfels, *Algebraic Statistics for Computational Biology*, vol. 8, Cambridge University Press, 2005.

[112] C. Pantea, *On the persistence and global stability of mass-action systems*, SIAM Journal on Mathematical Analysis, 44 (2012), pp. 1636–1673.

[113] L. Perko, *Differential Equations and Dynamical Systems*, vol. 7 of Texts in Applied Mathematics, Springer-Verlag, 2001.

[114] B. Rauzan, E. McMichael, R. Cave, L. R. Sevcik, K. Ostrosky, E. Whitman, R. Stegemann, A. L. Sinclair, M. J. Serra, and A. A. Deckert, *Kinetics and thermodynamics of dna, rna, and hybrid duplex formation*, Biochemistry, 52 (2013), pp. 765–772.

[115] M. R. Roussel, *The use of delay differential equations in chemical kinetics*, Journal of Physical Chemistry, 100 (1996), pp. 8323–8330.

[116] J. Rudan, G. Szederkényi, K. M. Hangos, and T. Péni, *Polynomial time algorithms to determine weakly reversible realizations of chemical reaction networks*, Journal of Mathematical Chemistry, 52 (2014), pp. 1386–1404, `https://doi.org/10.1007/s10910-014-0318-0`, `http://daedalus-old.scl.sztaki.hu/PCRG/works/publications/Rudan2014a.pdf`.

[117] M. A. Savageau, *Biochemical Systems Analysis: A Study of Function and Design in Molecular Biology*, Addison-Wesley Publishing, 1969.

[118] S. Schnell, *Validity of the Michaelis–Menten equation —- steady-state or reactant*

*stationary assumption: that is the question*, The FEBS Journal, 281 (2014), pp. 464–472.

[119] F. M. Scudo and J. R. Ziegler, *The Golden age of theoretical ecology, 1923–1940: A collection of works by V. Volterra, V.A. Kostitzin, A.J. Lotka, and A.N. Kolmogoroff*, Springer-Verlag, 1978.

[120] E. Sel'kov, *Self-oscillations in glycolysis: 1. A simple kinetic model*, European Journal of Biochemistry, 4 (1967), pp. 79–86.

[121] A. R. Shastri, *Elements of Differential Topology*, CRC Press, 2011.

[122] D. Siegel and M. D. Johnston, *Linearization of complex balanced chemical reaction systems*, unpublished note, (2008). Available at `https://johnstonmd.files.wordpress.com/2015/02/linearization.pdf`.

[123] H. Smith, *An Introduction to Delay Differential Equations with Applications to the Life Sciences*, vol. 57 of Texts in Applied Mathematics, Springer-Verlag, 2011.

[124] H. L. Smith and P. Waltman, *Perturbation of a globally stable steady state*, Proceedings of the American Mathematical Society, 127 (1999), pp. 447–453.

[125] M. Soheilypour and M. R. Mofrad, *Agent-based modeling in molecular systems biology*, BioEssays, 40 (2018).

[126] A. M. Stock, V. L. Robinson, and P. N. Goudreau, *Two-component signal transduction*, Annual Review of Biochemistry, 69 (2000), pp. 183–215.

[127] G. Szederkényi, *Comment on "Identifiability of chemical reaction networks " by G. Craciun and C. Pantea*, Journal of Mathematical Chemistry, 45 (2009), pp. 1172–1174.

[128] G. Szederkényi and K. M. Hangos, *Finding complex balanced and detailed balanced realizations of chemical reaction networks*, Journal of Mathematical Chemistry,

49 (2011), pp. 1163–1179, https://doi.org/10.1007/s10910-011-9804-9, http://daedalus-old.scl.sztaki.hu/PCRG/works/publications/Szederkenyi2011a.pdf.

[129] A. Varma and B. O. Palsson, *Metabolic flux balancing: Basic concepts, scientific and practical use*, Nat. Biotechnol., 12 (1994), pp. 994–998.

[130] P.-F. Verhulst, *Notice sur la loi que la population suit dans son accroissement*, Correspondance mathématique et physique, 10 (1838), pp. 113–121.

[131] E. O. Voit, *Biochemical systems theory: A review*, ISRN Biomathematics, 2013 (2013), https://doi.org/10.1155/2013/897658.

[132] V. Volterra, *Variation and fluctuations of the number of individuals in animal species living together*, ICES Journal of Marine Science, 3 (1928), pp. 3–51.

[133] R. Wegscheider, *über simultane gleichgewichte und die beziehungen zwischen thermodynamik und reactionskinetik homogener systeme*, Monatshefte für Chemie, 32 (1901), pp. 849–906.

[134] D. J. Wilkinson, *Stochastic Modelling for Systems Biology*, Mathematical and Computational Biology, Chapman and Hall/CRC Press, 2 ed., 2011.

[135] T. E. Woolley, R. E. Baker, and P. K. Maini, *Turing's Theory of Morphogenesis: Where We Started, Where We Are and Where We Want to Go*, Springer International Publishing, 2017, pp. 219–235, https://doi.org/10.1007/978-3-319-43669-2_13.

[136] P. Y. Yu and G. Craciun, *Mathematical analysis of chemical reaction systems*, Israel Journal of Chemistry, 58 (2018), pp. 733–741.

# Index

**Bold page numbers** indicate where a recurring term is defined. *Italic page numbers* indicate where it is used in a theorem, proposition, lemma, or corollary.